A PRIMARILY PASSIVE KNEE PROSTHESIS WITH POWERED STANCE AND SWING ASSISTANCE

By

Steven Christopher Culver

Dissertation

Submitted to the Faculty of the

Graduate School of Vanderbilt University

in partial fulfillment of the requirements

for the degree of

DOCTOR OF PHILOSOPHY

in

Mechanical Engineering

December 17, 2022

Nashville, Tennessee

Approved:

Michael Goldfarb, Ph.D.

Eric Barth, Ph.D.

David C. Morgenroth, M.D.

Elliott Rouse, Ph.D.

Karl E. Zelik, Ph.D.

DEDICATION

Dedicated to the Americans, Iraqis, and Cambodians whose lives are marred by war.
Your suffering awoke in me a dedication to the path I walk today.
Towards the end of disability…

ACKNOWLEDGEMENTS

More than anyone, Dr. Michael Goldfarb deserves my gratitude. Your mentorship has transformed me into an effective designer of assistive technology. Your leadership fostered my independence and creativity. Your guidance expanded my understanding and expertise. And your generosity taught me patience and humility. Thank you for everything you have given me, and for putting up with my stubbornness and frequent vacations.

I also want to thank the other committee members: Drs. Eric Barth, David Morgenroth, Elliott Rouse, and Karl Zelik. Your feedback and critique of this work has improved its rigor and ultimately transformed this dissertation into a better contribution to the field. Specifically, I want to thank you for challenging me to convey the motivation for this work, to evaluate it against the state-of-the-art, and to understand from first principles the rationale behind this approach we took.

I want to thank Léo Vailati for his tremendous contributions to this work. The embedded system you designed, your groundbreaking work on passive torque control, and your collaboration on the activity controllers were instrumental in the success of this work. Without your partnership, this project would have crawled in comparison to how quickly it actually evolved. It was a pleasure working with you, troubleshooting with you, formulating ideas with you, and learning from you.

I also want to thank our study participant, who committed to 100 hours of testing over the course of a year to help us build the control systems. Building prostheses of the future would be impossible without putting prototypes to the real test. Your feedback was invaluable for developing and refining this work, and for shaping the approach we take to future designs.

In the spirit of understanding the interconnected nature of my own behavior, I want to thank everyone who has affected my life for the better: a community of researchers who taught me how to design machines; a community of climbers who taught me to cast away my fears; a community of dancers who taught me to cast away my shame; an undergraduate mentor who invested in me; a family that taught me familial love; a family that never gave up on us; a squad of teenagers who became men together; a group of veterans pursuing excellence together; two of the finest Marines I know, and living proof that going to war can drive you bananas; and a woman who challenges me to be the best version of myself. Although you may have never noticed it, your companionship became a part of this project, and for that you deserve recognition.

TABLE OF CONTENTS

LIST OF TABLES

LIST OF FIGURES

CHAPTER I

INTRODUCTION

There are approximately 600 000 people in the U.S. living with a major lower limb amputation, approximately half of whom have transfemoral amputation (TFA) [1]. The worldwide prevalence of TFA is approximately 20-30 times the U.S. prevalence [2]. Individuals with TFA experience ambulation deficiencies such as overuse injuries caused by pathological gait [3], increased frequency of falls [4], and decreased speed of ambulation [5]. Advances in prosthetic limb technology seek to reduce these deficiencies and restore improved ambulatory ability to individuals with TFA. The overall goal of this research is to contribute to the advancement of prosthetic limb technology by investigating the possibility of designing and controlling a powered knee prosthesis to provide the active stance and non-ballistic swing behaviors of currently-available powered knee prostheses without sacrificing the resistive stance and ballistic swing behaviors of currently-available modulated passive knee prostheses.

1. Overview of the Current State of the Art

The essential functions of a prosthetic knee are to provide stance-knee stability during the weight bearing phase of locomotion, and to provide appropriate knee motion during the swing-phase of locomotion, so the user can swing his or her foot forward for the subsequent step. Although many types of knee prostheses have been developed to provide this functionality (e.g., [6]), the current standard of care are energetically passive knee prostheses, which provide high resistance to flexion during stance-phase, and a substantially lower resistance to motion during swing-phase. The latter enables these devices to provide a highly biomimetic facsimile of healthy swing-phase dynamics. Specifically, healthy swing-phase movement has been shown to be the result of inertial coupling between the thigh and shank, combined with passive low-impedance behavior at the knee [7] [8], which effectively becomes a free hinge at low walking speeds. The combination of low-impedance knee resistance and passive inertial mechanics to provide swing-phase motion in healthy individuals has been called “ballistic motion” in the study of human biomechanics. As such, the resistive behavior by which passive prostheses generate swing-phase motion is arguably as close an approximation of the biological knee as possible, and also provides a knee movement that is naturally and fundamentally coordinated with the movement of the user.

The emergence of microprocessor-controlled knees (MPKs) in the late 1990s, which employ microprocessor-modulated resistive behaviors (e.g., an electrically-modulated hydraulic damper), improved further upon ballistic swing-phase emulation by enabling better adaptation to variations in cadence and between users. These energetically-passive MPKs are currently the standard of care in advanced knee prostheses. All current passive MPKs employ hydraulic-fluid-based modulation, either via electrically-controlled flow restriction valves, or via electrically-controlled modulation of fluid viscosity, which enables a range of impedances that spans both the high impedance necessary for knee stability during stance (herein referred to as "resistive stance"), and the relatively much lower impedances (approximately 100 times lower), necessary to facilitate the aforementioned ballistic swing-phase motion.

Despite the efficacy of passive MPKs in providing stance and swing functionality (e.g., [9] [10] [11]), these devices are unable to provide mechanical power generation, as does the biological knee joint when providing stance-knee extension during activities such as step-over stair ascent and steep slope ascent, or during sit-to-stand transitions. In order to restore powered behaviors such as stance-knee extension (herein referred to as "active stance"), several researchers have developed powered knee prostheses (e.g., [12] [13] [14] [15] [16] [17] [18] [19] [20] [21]). Rather than strictly modulate resistance to motion, powered prostheses expand the range of potential knee behaviors to include all four quadrants of the power plane (i.e., both active and resistive torque-speed knee behaviors). These "fully-powered" devices have been shown to offer enhanced functionality in several activities (e.g., [22] [23] [24]).

The additional capabilities of fully-powered prostheses, however, also entail behavioral trade-offs relative to MPKs. One of the most fundamental of these is that powered prostheses are generally unable to achieve the very low output-impedance necessary to provide a strictly-passive ballistic swing-phase. Specifically, in order to achieve the magnitude of knee torque required for stance-phase support from an electric motor, powered knees generally employ drives with large transmission ratios, which typically limit their ability to assume the very low output-impedances provided by MPKs and required for ballistic swing-phase (i.e. large transmission ratios create significant actuator dynamics due to reflected inertia and friction across the transmission). Passively-modulated hydraulic actuators do not use large transmission ratios, and therefore do not entail the same issues with reflected inertia and friction. Therefore, powered prostheses expand the range of behaviors into the powered quadrants of the power plane, while concomitantly narrowing their range of behaviors within the passive quadrants. Since powered prostheses cannot provide ballistic swing-phase, they instead employ other control methods to provide swing-phase motion (e.g., [25]), although these are less biomimetic than strictly-passive means, do not guarantee

coordination with thigh motion, and severely diminish the ability of the user to physically influence the motion of the knee joint. Note that a low output-impedance can be indirectly provided by a powered prosthesis via torque feedback control, but doing so with sufficient bandwidth to perform ballistic swing presents a number of known stability and control challenges, and as such has not yet been demonstrated (see Appendix A for a full discussion of this topic).

To address the swing-phase deficiencies of fully-powered prostheses, some "swing-assist" prostheses have been described (e.g., [26] [27] [28] [29]). These devices use low-ratio electromechanical drives to provide both active and resistive swing-phase behaviors and are capable of providing ballistic swing. However, the electromechanical drives on these devices have low-torque capabilities (relative to stance-knee yielding requirements such as in stair descent), and therefore cannot provide the high-torque, high-power active and/or resistive stance-phase capabilities provided by fully-powered knee prostheses and/or MPKs (i.e., they are capable of limited four-quadrant behavior). Therefore, MPKs are deficient in providing active functionality, fully-powered prostheses are deficient in providing ballistic swing functionality, and swing-assist prostheses are deficient in providing stance-phase functionality.

2. Research Motivation

Replication of healthy knee behavior after amputation requires prosthetic knees to provide active and resistive stance behaviors, as well as ballistic and non-ballistic swing behaviors (note that non-ballistic swing is defined here as a swing-phase motion dominated by active knee torque). While high-ratio and low-ratio PKs have swing and stance phase deficiencies, respectively, a device that is able to assume a high-ratio configuration during stance-phase and a low-ratio configuration during-swing phase can overcome these deficiencies. Arguably, if a PK could achieve a low output impedance similar to what is provided by MPKs in late-stance and throughout swing-phase (e.g., by drastically reducing the gear ratio in late-stance), it would greatly improve upon swing-phase control by providing a knee movement that is naturally and fundamentally coordinated with the movement of the user, which is as close an approximation of the biological knee as possible. Adding ballistic swing functionality to a PK increases the physical capabilities of a PK to provide the four aforementioned essential functions required to replicate healthy knee behavior. While it is theoretically possible to employ feedforward or feedback approaches to provide a sufficiently low output impedance [30] required for ballistic swing, doing so on wearable robots poses a number of control challenges, as discussed in Appendix A of this document.

Presumably as a result of these challenges, employing these methods to reduce the output impedance of a PK to the level required for ballistic swing, as defined herein, has yet to be demonstrated in literature. The challenges of reducing or eliminating friction and inertia via control methods can be circumvented by employing hardware design that provides a low transmission ratio (and therefore low reflected friction and inertia) during portions of the gait cycle that require low torque, high speed, and low output impedance, and a high transmission ratio during portions of the gait cycle that require high torque, relatively lower speed, and during which low output impedance is less important. Such a hardware-based approach has yet to be demonstrated in literature and, if successfully-implemented, would provide to the user the ability to easily move the prosthesis, increasing the functionality of PKs by offering a biomimetic ballistic swing-phase motion and an additional and invaluable form of sensing: user intent.

3. Specific Aims

This research work has four specific aims relative to the design and control of a powered knee prosthesis that can provide active and resistive stance behaviors, as well as ballistic and non-ballistic swing behaviors.

3.1 SA1: Design a powered knee prosthesis capable of assuming a low output impedance in late-stance and throughout swing-phase

The dynamic range of torque and impedance required for resistive stance and ballistic swing requires a large change in transmission ratio between the stance and swing phases, with intra-stride reconfiguration of the transmission, which is a non-trivial endeavor. The design requirements for providing a strictly-passive stance knee-yielding behavior and ballistic swing-phase motion commensurate with commercial MPKs are outlined in Table II-1. A novel actuator (see Fig. II-1) was designed to provide these requirements by the use of an electronically controlled transmission (ECT, see Fig. II-2), which provides a high transmission ratio for stance-phase and a low transmission ratio for swing-phase. Switching between gear ratios is achieved with two clutches (see Fig. II-3 and Fig. II-4), one unidirectional and one bidirectional, which provide four possible transmission configurations (see Fig. II-5), three of which are functional states. Table II-2 shows the conditions for switching between high and low gears, which provides for stance stability (high-gear) and ballistic swing-phase (low-gear). The prosthesis configures the actuator in a slider-crank (see Fig. II-8), which produces non-linear transmission ratios for high and low gears (see Fig. II-9). The range of possible impedances in the high and low gears

was assessed in a benchtop experiment (see Fig. II-10), demonstrating a range of impedances necessary for providing resistive stance and ballistic swing behaviors using motor braking only (see Fig. II-11 and Table II-1). In an experiment with an amputee subject, the prosthesis and control system were shown to switch to a low impedance via reconfiguration of the transmission, enabling ballistic swing-phase motion using motor braking only (see Fig. II-13). Unlike any previously demonstrated PK, the ECT is able to provide strictly-passive functionality in level-ground, up-slope, and down-slope walking similar to a commercial MPK (see Fig. II-14).

3.2 SA2: Design a passive control system for the powered knee of SA1 that provides strictly-passive functionality essentially identical to a state-of-the-art MPK

The goal of SA2 is to design a control system capable of providing: 1) resistive stance behavior adaptive to a range of activities, 2) ballistic swing behavior adaptive to a range of activities and walking speeds, and 3) seamless transitions between activities. The essential design philosophy of the ECT knee is different from conventional PKs. Since (unlike other PKs) the ECT can provide a full suite of strictly-passive functionality (i.e., resistive stance and ballistic swing), the general control approach is to provide a foundational layer of strictly-passive prosthesis behavior, then to subsequently layer active behaviors on top, such that powered behavior is only used for activities that require active stance and non-ballistic swing behaviors. As such, SA2 aims to demonstrate that a PK that can exhibit the same modulated-passive behavior of state-of-the-art MPKs across all standard activities, including level-ground, down-slope, and down-stairs walking, as well as backwards walking and stand-to-sit transitions.

3.3 SA3: Design a powered control system for the powered knee of SA1 that builds upon the passive control system of SA2 by adding powered functionality commensurate with a powered knee

Despite the efficacy of MPKs in providing resistive stance and ballistic swing functionality, these devices are unable to provide active stance and non-ballistic swing functionality, as does the biological knee joint during step-over stair ascent and sit-to-stand transitions. As such, the energetically-passive control system of SA2 suffers the same deficiencies as MPKs. However, because the ECT knee is motor-actuated, it is possible to provide active stance and non-ballistic swing behaviors discrete from the resistive stance and ballistic swing behaviors provided by the control system of SA2. There are three areas of deficiency of MPKs that power-assistance can address: 1) insufficient toe-clearance as caused by reduced knee flexion during slow walking; 2) inability to provide non-ballistic swing behavior during step-over stair ascent; and 3) inability to provide powered knee extension during step-over stair ascent and sit-to-

stand transitions. The goal of SA3 is to explore how to provide power-assistance on top of the energetically-passive control system of SA2 in order to provide power-assisted ballistic swing during slow walking, non-ballistic swing during step-over stair ascent, and active stance behavior during step-over stair ascent and sit-to-stand transitions.

3.4 SA4: Design a control system with seamless transitions between passive and powered functionalities to provide desirable behavior for a range of activities

One value of commercial MPKs is that they are able to seamlessly transition between activities. High-impedance PKs require recognition of user intent because it is difficult for the user to physically influence the motion of the prosthesis. Because the powered knee of SA1 provides a low-impedance in late-stance and throughout swing-phase and also provides a low-impedance to knee extension during the stance-phase, the prosthesis is able to be easily influenced by the user's motion, which provides a valuable control signal of user intent to the control system. This has the potential to allow the prosthesis to provide desirable function for a range of activities without requiring a priori intent recognition; intent can be recognized after the user has initiated motion for the desired activity. The goal of SA4 is to design a control system for the powered knee of SA1 that is able to provide appropriate resistive/active stance and ballistic/non-ballistic swing behaviors for a range of activities without necessitating a priori detection of user intent and with seamless transitions between activities. In other words, the control system of SA4 integrates the control systems of SA2 and SA3 into a unified controller that appropriately responds to user inputs for a range of common activities.

4. Definitions of Generalized Knee Behaviors

Throughout this work, four categories of generalized knee behaviors are used to describe both the behavior of the biological knee joint and the analogous behavior replicated by the prosthetic knee joint. These definitions are relative to the gait phase (stance vs. swing), the mechanical power (positive vs. negative), and the magnitude of knee torque relative to other torque sources that affect knee motion (e.g., inertial torques from gravity and user motion). We have named these four generalized behaviors as resistive stance, active stance, ballistic swing, and non-ballistic swing. These behaviors are depicted in Fig. I-1 and detailed in the following subsections.

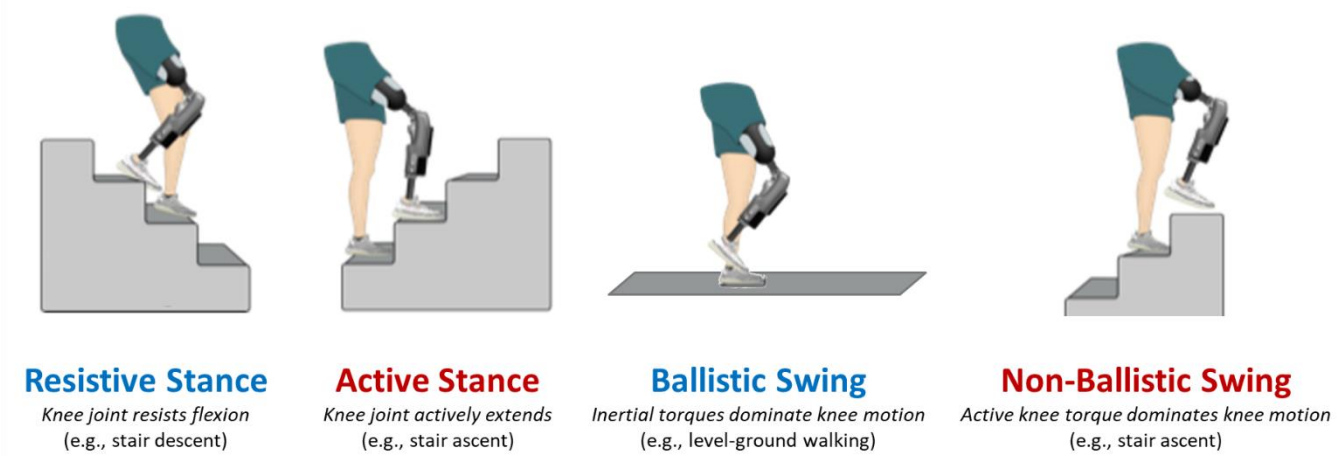

Fig. I-1: Generalized knee behaviors, showing resistive and active stance as well as ballistic and non-ballistic swing. Active and resistive stance are contrasted, wherein the knee joint primarily provides an extensive torque with knee motion either in extension (active stance) or flexion (resistive stance). Ballistic and non-ballistic swing describe the contribution of knee torque to the resultant motion of the lower leg. For ballistic swing, inertial torques (i.e., gravity and thigh acceleration) dominate knee motion, with the knee providing relatively low resistance to control motion; for non-ballistic swing, active knee torque overcomes inertial forces to reposition the lower leg.

4.1 Resistive and Active Stance

Resistive stance is characterized primarily by either negative mechanical power (e.g., extensive torque with flexion velocity) or by a high impedance to motion, such that the knee joint has little or no motion in the presence of externally-applied torques. The converse of resistive stance is active stance, which is characterized by positive mechanical power (e.g., extensive torque with extension velocity). During the stance-phase of most activities, the biological knee joint uses both active and resistive stance behaviors. However, each activity can be generalized by the dominant behavior of the knee joint during that activity. For activities where the knee joint primarily either resists flexion (e.g., level-ground walking) or provides a support moment while flexing and lowering the person's center of mass (e.g., slope descent, stair descent, and stand-to-sit), these activities are generalized by resistive stance. For activities where the knee joint actively extends to elevate the person's center of mass (e.g., slope ascent, stair ascent, and sit-to-stand), these activities are generalized by active stance.

Regarding the replication of resistive and active stance behaviors in prosthetic knee devices, the entire stance-phase behavior need only be characterized by the generalized stance behavior of the biological knee joint to achieve near-biomimetic replication of function. For example, MPKs are capable of providing near-biomimetic resistive stance behavior without providing exactly biomimetic knee kinematics and kinetics during those behaviors. For activities generalized by active stance, this

theoretically also holds true, where a near-biomimetic active stance behavior can sufficiently restore healthy stair ascent and sit-to-stand functions to the knee joint.

4.2 Ballistic and Non-Ballistic Swing

The definitions of ballistic and non-ballistic swing are relative to both the flow of mechanical power (ballistic swing primarily has negative joint power while non-ballistic swing primarily has positive joint power) and the magnitude of joint torque relative to inertial torques (inertial torques dominate motion during ballistic swing, whereas active knee torque dominates motion during non-ballistic swing). Biomechanical data of the swing-phase of the biological knee joint provide clarification on the torque and impedance requirements of the knee joint to provide ballistic swing. During swing-phase, the motion of the lower-leg can be modeled as a pendulum with a forced pivot and torque-control at the pivot. The free body diagram in Fig. I-2 models the lower-leg as a rigid body with its center-of-mass coincident with the line defining the shank angle.

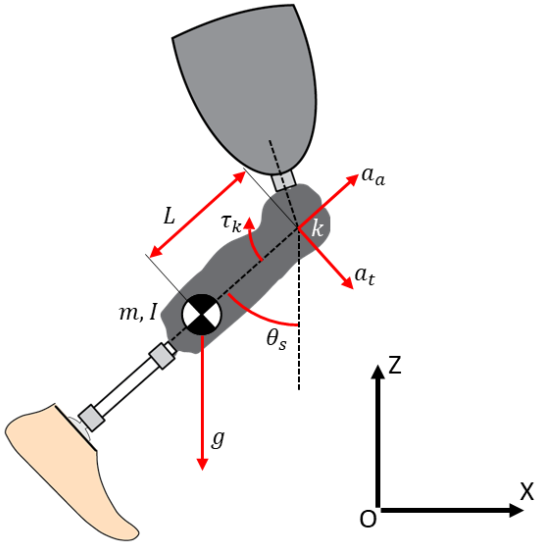

Fig. I-2: Free-body diagram of lower-leg dynamic model

In the lower-leg free body diagram, O is a fixed observer in the global frame, X and Z are the global coordinates in the sagittal plane, k is a revolute joint that defines the knee joint that is accelerating in the global frame, m is the total mass of the lower-leg, L is the distance between the knee joint and the lower leg's center-of-mass, I is the moment-of-inertia of the lower-leg about the knee joint, g is acceleration due to gravity, θ_s is the shank angle in the global frame, a_t and a_a are respectively the tangential and axial acceleration of the knee joint relative to θ_s in the global frame, and τ_k is a torque

produced by the prosthesis at the knee joint. The rotational motion of the lower-leg during swing-phase is determined by the summation of three sources of torque about the knee joint: (1) inertial torque from gravity (τ_g), (2) inertial torque from tangential acceleration of the knee joint in the global frame (τ_t), and (3) internally-generated torques acting at the knee joint (τ_k). The former two torques are mathematically expressed as:

$$\tau_g = mgL \sin \theta_s \tag{I-1}$$

$$\tau_t = mLa_t \tag{I-2}$$

Using this dynamic model and averaged data from [31], Fig. I-3 shows the torque and joint power profiles of these three torque sources during the swing-phase for level-ground walking at five speeds. These data show that both τ_g and τ_t provide generative and dissipative rotational mechanical power, depending on the pose and velocity of the lower-leg throughout swing-phase. But τ_k has a primarily dissipative role, almost always dissipating energy to provide a desirable swing-phase motion. These torques sources affect the swing-phase differently depending on the sub-phase of swing, which in Fig. I-3 is divided into swing-flexion (SF), early swing-extension (SE), and terminal swing-extension (TS). Table I-1 shows the percent contribution to lower-leg motion of each torque source during the three sub-phases, which is calculated from the root mean square of each torque during each sub-phase, averaged over all walking speeds. The data in Table I-1 demonstrates the dominant influence of gravity and inertial-coupling to the motion of the lower-limb during most of swing-phase. The relatively low knee joint torques, the high joint velocities, and the consistently negative joint power of swing-phase imply that the biological knee joint provides a low impedance resistive behavior as the mechanism of ballistic swing. For the prosthetic knee joint, ballistic swing-phase can only be provided if τ_k does not dominate the swing-phase motion, which becomes increasingly challenging as mechanical impedance increases above zero. Additionally, for the small contribution that τ_k has during swing-flexion and early swing-extension, the contribution of resistive torque from prosthetic knee joint impedance should necessarily be small enough to prevent the loss of control authority during the swing-phase (i.e., the mechanical impedance should be less than or equal to the lowest desired joint impedance for the slowest walking speeds with the smallest and/or lightest prosthesis users).

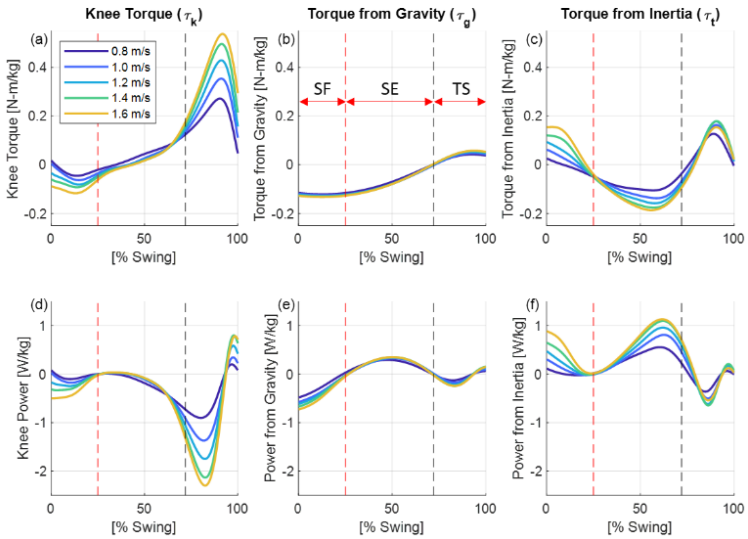

Fig. I-3: Torques that affect knee motion during swing-phase are (a) the knee joint torque, (b) inertial torque from gravity, and (c) inertial torque from tangential acceleration of the knee joint. Positive vertical axis indicates knee flexion torques. Subplots (d)-(g) show the mechanical power of each contributing torque (when compounded with knee joint velocity), where the positive vertical axis indicates positive mechanical work. The swing-phase is subdivided into three sub-phases: (SF) swing-flexion, (SE) early swing-extension, and (TS) terminal swing-extension. Kinematic events that separate the three sub-phases are the knee joint reaching its peak-flexion angle (vertical dashed red line) and the shank aligning with gravity (vertical dashed black line).

Table I-1
Swing-Phase Torques and Their Contributions to Knee Motion

Contributing Torque Source	Percent Contribution to Motion for each Swing Sub-Phase		
	Swing Flexion	Swing Extension	Terminal Swing
τ_k	26%	21%	68%
τ_g	52%	32%	9%
τ_t	22%	47%	23%

Percent contributions of each torque source were calculated from the RMS torque during each swing sub-phase, averaged over all walking speeds.

To contrast with ballistic swing motion that is dominated by inertial torques from gravity and user motion, non-ballistic swing motion is dominated by knee torque. Non-ballistic swing occurs when inertial torques are insufficient to provide desirable motion of the knee joint without also providing positive mechanical power at the knee joint. During activities such as step-over stair ascent, relatively low thigh velocities contribute little to knee motion, and relatively high knee torques dominate knee motion to reposition the knee joint against the force of gravity. For these instances, active knee torque is used to reposition the knee joint.

CHAPTER II

DESIGN OF A POWER-CAPABLE KNEE PROSTHESIS WITH BALLISTIC SWING-PHASE

This chapter proposes a new approach to the design of a power-capable prosthesis; namely, one that expands the behavioral capability of a knee prosthesis into the powered quadrants of the power plane, without sacrificing the range of capable behaviors in the passive quadrants, relative to existing passive microprocessor-controlled knee prostheses (MPKs). It is well-known that swing-phase knee motion during walking in healthy human gait results from the combination of inertial coupling between the thigh and shank, gravitational effects, and passive behavior at the knee. Motor-actuated prostheses with powered stance and swing capabilities have recently emerged, but none have been shown to provide a strictly-passive biomimetic swing-phase. This chapter describes an approach that enables expansion of knee behavior into the powered quadrants of the power plane, without sacrificing the ability to provide a strictly-passive biomimetic swing-phase, or the resistive stance-phase behaviors provided by energetically-passive state-of-the-art MPKs.

1. Introduction

This chapter proposes a new design approach for a powered prosthesis that maintains full coverage of the passive quadrants of the torque-speed plane (relative to existing MPKs) while still offering powered stance and swing functionality. Alternately stated, this chapter presents the design of an electric-motor-actuated knee prosthesis that is capable of providing power, while also providing the strictly-passive ballistic swing-phase functionality offered by MPKs, in addition to the resistive stance functionality also offered by MPKs. In order to achieve the wide range of passive behaviors required of an MPK, the prosthesis employs a unique two-speed transmission which enables two orders of magnitude impedance variation within a stride, in a highly-controllable manner. Although the prosthesis uses a motor to impose these passive controllable impedances, it does so without using electrical power from a battery (other than signal power for control electronics, as do standard MPKs). The design also provides other functional aspects of MPKs, such as unidirectional resistance against flexion during stance-phase and late swing-phase. These fundamental unidirectional behaviors have yet to be demonstrated in any other powered prosthesis.

Key to the device functionality is a unique transmission with three electronically-selectable states: 1) a high-torque, low-speed state that provides unidirectional flexion resistance and extension assistance, with little to no extension resistance, appropriate for the stance-phase of walking; 2) a low-torque, high-speed, low-impedance state that provides bidirectional knee resistance and assistance, appropriate for the swing-flexion phase of walking; and 3) a low-torque, high-speed, low-impedance state that provides unidirectional low-resistance against knee extension or assistance with knee extension, with a simultaneous high-resistance to knee flexion, appropriate for the swing-extension phase of walking. The transmission ratios between the states are different by a factor of 5.4, which combined with motor control (passive or active) enables the two orders of magnitude variation in impedance necessary to sustain the passive biomimetic functionality of an MPK, while also enabling powered assistance in either swing or stance. By utilizing a two-speed transmission, the prosthesis is capable of behaving as a fully-powered prosthesis during stance-phase and as a swing-assist prosthesis during swing-phase. The transmission is able to change between these states under load on the order of milliseconds, which enables the knee to provide essential MPK functionality in an electromechanical device, which is also capable of providing powered behaviors.

Relative to existing hydraulic MPKs, this approach provides the potential to add powered assistance, such as stance knee-extension, to the MPK. Relative to fully-powered knees, this design does not sacrifice passive quadrant behaviors in exchange for access to the powered quadrants, and therefore enables a strictly-passive ballistic swing-phase, and corresponding natural and biomimetic motion and the interaction associated with it. Relative to swing-assist prostheses, this design does not sacrifice stance-phase functionality to achieve ballistic swing. This chapter describes the design approach of the novel knee prosthesis; presents benchtop experimental data characterizing its ability to fully span the passive quadrants of the power plane; demonstrates power generation; demonstrates strictly-passive walking functionality on a subject with TFA; and provides walking data validating the ability of the prosthesis to provide strictly-passive functionality essentially identical to the subject's state-of-the-art daily-use MPK.

2. Design Requirements

2.1 Passive Stance-Phase Resistance

The maximum torque and power requirements of the prosthetic knee joint during stance-phase are a resistive torque of 1.0 N·m/kg body mass and a maximum dissipative power of 3.5 W/kg, both associated

with stair descent, based upon data from [32]. Assuming that the knee joint behaves primarily as a damper during the power-dissipation portions of the stance-phase, knee damping requirements can be estimated from quasi-damping of the biological knee during stair descent [33]. In order to provide similar behavior, a knee prosthesis requires an impedance of approximately 0.55 N·m·s/rad·kg. Therefore, assuming a 100 kg user, the MPK should be designed to provide during stance-phase a maximum resistive torque of 100 N·m, a maximum dissipative power of 350 W, and an achievable impedance of 55 N·m·s/rad.

2.2 Passive Swing-Phase

During swing-phase, the knee is characterized by a low-impedance, which enables user-initiated ballistic swing-phase movement in the manner employed by healthy individuals [7] [8]. Therefore, it is essential that the prosthetic knee be characterized by an appropriately low output-impedance throughout swing-phase; namely, a low reflected inertia from the motor, and low viscous and Coulomb friction coefficients [34]. Based on averaged data from [31], the biological shank and foot has a rotational inertia of approximately 3800 kg·cm^2 about the knee joint. To minimize the effects of an actuator and drivetrain on the swing-phase dynamics, it is desirable to limit the reflected inertia of these elements to less than 10% of this value, or 380 kg·cm^2. Based on the quasi-damping observed at peak knee velocity during the swing-phase across varying ambulatory conditions [31], the biological knee provides a minimum damping constant of approximately 0.02 N·m·s/kg·rad. Due to the reduced inertia of lower-leg prostheses, which can have masses as low as 30% of the intact limb [35], the minimum damping requirements for a prosthesis are even lower. To account for this, the design target was set at 0.005 N·m·s/kg·rad. This low target impedance is substantiated by an investigation of biological knee joint impedance during walking [36]. Other requirements of the prosthetic knee joint during swing-phase are a resistive torque of 0.10 N·m/kg and a dissipative power of 0.4 W/kg, both associated with level-ground walking, based upon data from [37]. Therefore, for a user mass of 100 kg, the prosthesis should provide during the swing-phase a maximum resistive torque of 10 N·m, a maximum dissipative power of 40 W, and a minimum impedance of approximately 0.5 N·m·s/rad of viscous friction and 0.5 N·m of Coulomb friction, preferably lower for slow walking speeds and users with less body mass. Note that the maximum desired stance damping is two orders of magnitude higher than the minimum desired swing damping.

2.3 Powered Swing Assistance

Prior works have demonstrated that powered assistance during swing-phase can offer perturbation robustness in cases of swing-phase perturbations (e.g., stumble), and can potentially facilitate swing-phase

movement during non-ballistic knee movement, such as employed during stair ascent (e.g., [27] [38]). Based on these prior works, requirements for such swing assistance can be approximated by active knee angle trajectory tracking of approximately 60 deg (peak-to-peak) at approximately 1 Hz.

2.4 Powered Stance Knee Extension Assistance

As discussed in [39] and demonstrated in [38], since the stance leg is essentially a closed kinematic chain, power generation at the knee is not strictly required to effect knee-extension during stance-phase, since it can instead be effected via power generation at the hip. As such, there is no clear enabling torque specification in this regard. Nonetheless, powered assistance at the knee reduces hip torque requirements, and therefore aids the user in performing stance knee-extension. Based on prior work (e.g., [38]), a relatively small amount of extension torque provides useful assistance during stance knee-extension events. In order to provide substantial assistance during such events, the powered knee described herein was designed to provide approximately 30 Nm of torque at an extension velocity of 180 deg/s, in order to provide effective assistance during step-over stair ascent and sit-to-stand movements.

2.5 Other Desirable Knee Characteristics

The knee must be able to switch between stance- and swing-phase characteristics in real-time relative to the intra-stride dynamics. Average adult stride times are typically about 1 s, such that one percent of stride would be 10 ms. If one assumes that a “real-time” transition is represented by switching within 2% of the cycle, then the switching needs to occur within approximately 20 ms.

Also, as previously mentioned, it is desirable for a knee prosthesis to provide asymmetric resistance to flexion relative to extension during the swing-extension and early- to mid-stance phases of gait. Specifically, it is desirable to provide a high resistance against flexion during late-swing, which preconfigures the knee for stance-phase loading, regardless of knee angle or detection of heel strike; and it is also desirable to maintain this behavior during stance-phase, so that the knee can be extended (via hip musculature) in stance in the event stance is entered without full knee extension (e.g., in the event of a stumble).

Finally, the knee should be able to change behaviors while under load, since a behavioral change should be determined by the knee controller, unconstrained by the conditions imposed by the environment.

2.6 Load Cell Design Requirements

In order to robustly distinguish between stance and swing states, the proposed prosthesis includes a lightweight force transducer to measure axial load in the shank. Such detection is substantially more robust if the axial load measurement is decoupled from the relatively large lower-limb bending moments associated with ambulation. Based upon biomechanics data of ambulation at various speeds, slopes, and stair angles [31] [33], the load cell located in the prosthesis shank, for a 100 kg user, should be able to sense compressive forces up to 1200 N while minimizing interference from bending moments and torsion associated with locomotion, which can be up to 130 N·m in the sagittal-plane, 20 N·m in the frontal-plane, and 20 N·m in the transverse-plane.

2.7 Size, Mass, and Range of Motion

A survey of four common commercially-available MPKs indicates a mass range of 1.5-2.0 kg, a minimum build height range of 240-310 mm, and a maximum knee range-of-motion **(**RoM**)** of 120-135 deg. A summary of design requirements for the proposed knee prosthesis is given in Table II-1.

Table II-1
MPK Prosthesis Prototype Design Requirements

Design Requirement	Target Values			Actual Values	Units
	Max Above	Max Below	Min Below		
Stance-phase					
-Power dissipation	350			360	W
-Resistive torque	100			100	N·m
-Damping coefficient	55			75	N·m·s/rad
Swing-phase					
-Power dissipation	40			130	W
-Resistive torque	10			19	N·m
-Reflected inertia		380		25	$kg \cdot cm^2$
-Damping coefficient			0.50	0.30	N·m·s/rad
-Coulomb friction		0.50		0.35	N·m
Gear-change time		20		2	ms
Flexion RoM	125			125	deg
Extension RoM	5			5	deg
Build height		310		360	mm
Mass		2.0		1.9	kg
Axial load sensing	1200			900	N

3. Device Design

3.1 Design Strategy

As previously mentioned, current stance-controlled MPKs employ some form of modulated hydraulic resistance to motion. Recent advances in the power density of brushless motors presents the possibility of replacing these hydraulic systems with an electric motor, which clearly can offer access to

the powered quadrants of the power plane, but ideally should not forego the ability to span the passive quadrants of the power plane, relative to existing MPKs. Another desirable property of employing a motor, relative to a hydraulic system, is that knee torque can be controlled directly via control of current, whereas in a hydraulic system, torque cannot be controlled directly; rather, torque results indirectly from modulation of resistance and velocity of fluid flow. Further, resistance is also controlled indirectly, either via modulation of a fluid valve or fluid rheological properties. If designed appropriately, a PWM-controlled brake can modulate resistance without requiring any electrical power (aside from the signal power required to switch MOSFETs), and power regeneration may also be possible. Note that a discussion of the range of passive impedances achievable with a motor, with and without power expenditure, can be found in [40] [41]. As such, the knee torque in a motor-based design is more directly and also more accurately controllable, relative to a hydraulic implementation.

A motor implementation, however, will require a high transmission ratio, which as previously mentioned, introduces significant reflected inertia and/or friction (both proportional to the square of the transmission ratio), relative to passive hydraulic MPKs (which entail much smaller transmission ratios, if any), thus preventing the free-swing behavior required for a ballistic swing-phase. The full dynamic range of stance and swing phases, however, can be accommodated without compromising swing-phase output impedance by implementing a two-speed transmission that can switch in real-time between a high transmission ratio required for stance-phase, and a low transmission ratio that can accommodate swing-phase.

3.2 ECT Actuator Design

The electromechanical modulated-dissipator prototype, shown in Fig. II-1, consists of a DC brushless motor (Maxon EC-4pole 22 90 W), connected to the knee joint through a lead-screw-based (Roton Hi-Lead 60988) slider crank and a novel two-speed electronically-controlled transmission (ECT). The ECT consists of a nominally underdetermined two-stage planetary-gear transmission, wherein the first-stage carrier can be grounded via an electromagnetic clutch (called the carrier clutch), and the common ring-gear can be separately grounded by a unidirectional electromagnetic clutch (called the ring clutch). The two clutches can be engaged or disengaged in various combinations to provide: 1) a high gear ratio appropriate for stance-phase; 2) a low gear ratio appropriate for swing-phase; and 3) a combination that enables a low-gear ratio against extension and high-impedance against flexion.

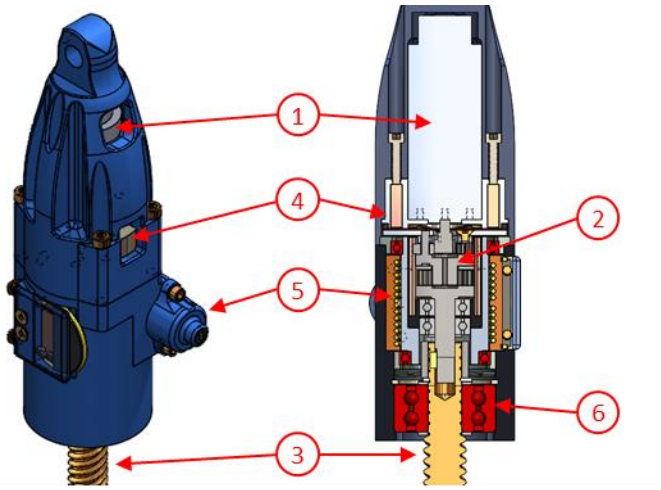

Fig. II-1: Solid model of novel ECT actuator (left) and cross-sectional view (right). The actuator drivetrain includes a brushless DC motor (1), two-stage planetary-gear transmission (2), and lead screw (3). Two solenoid-actuated clutches provide locking of the first-stage carrier (4) and common ring (5) of the transmission. Large axial loads on the lead screw are transferred to the housing through an angular contact bearing (6).

3.2.1 Electronically-Controlled Transmission

Both the high- and low-ratio transmission configurations are shown schematically in Fig. II-2. The transmission is configured in the high-gear ratio when the common ring-gear is grounded while all other components remain free. The transmission is configured in the low-gear ratio when the common ring is allowed to freely spin, while the first-stage carrier and second-stage sun-gear are grounded. The respective high and low transmission ratios are given by:

$$R_H = (1 + N_2/N_1)(1 + N_4/N_3) \tag{II-1}$$

and:

$$R_L = -(N_2/N_1)(1 + N_3/N_4) \tag{II-2}$$

where R_H is the high-gear ratio; R_L is the low-gear ratio; and N_n is the number of teeth on each gear, where n corresponds to the gear number referenced in Fig. II-2. For the transmission employed here, in order to provide the span of ratios that will enable the prosthesis to span the full range of MPK passive quadrant behaviors, the transmission uses $N_1 = N_3 = 10$ and $N_2 = N_4 = 44$, which provides a high-gear ratio of 29:1, and low-gear ratio of 5.4:1 (i.e., a factor of 5.4 between gear ratios). The slider crank and lead screw provide an additional transmission ratio that varies between approximately 9-12:1, depending

on knee angle, such that the total transmission ratio varies between approximately 260-359:1 in the high-gear, and between approximately 50-67:1 in the low-gear. The ECT was constructed using a combination of custom parts, and parts modified from a commercial planetary gearhead (Maxon GP 22 HP 29:1).

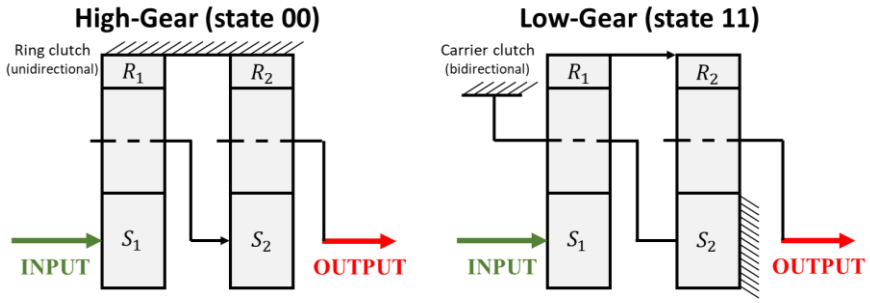

Fig. II-2: Diagrams of transmission configurations for high-gear (left) and low-gear (right). The ECT is an under-determined transmission with two clutches that ground different components and provide different reduction ratios between input and output. During stance-phase, the common ring-gear is grounded, providing a reduction ratio of 29:1. During swing-phase, the first-stage carrier and second-stage sun are grounded, providing a reduction ratio of 5.4:1.

3.2.2 Design of Electromagnetic Clutches

The nominally underdetermined ECT is configured into either a high- or low-ratio by two clutches: a ring and carrier clutch, which act to ground the common ring-gear or first-stage carrier, respectively. The ring clutch, shown in Fig. II-3, grounds the common ring-gear, and is engaged during the stance-phase to provide unidirectional holding against knee-flexion. In order to provide the rated 100 N·m of stance-phase knee torque (Table II-1), the ring clutch must hold against 5 N·m of torque. In order to provide a high holding torque, the ring clutch employs a capstan-type design, which: 1) enables a high holding torque with a low activation force, due to the exponential self-amplification property of a capstan [42]; and 2) provides a unidirectional holding torque, which accommodates the previously described asymmetrical resistance desirable in the stance-phase and late swing-phase (i.e. low-impedance resistance to extension and high-impedance resistance to flexion). As shown in Fig. II-3, the capstan is implemented via a wire rope wrapped around an aluminum sleeve, wherein the one end of the wire rope is grounded to the housing and the other end connected to a small solenoid actuator and held in tension by a spring element. When the solenoid is de-energized (i.e., in the OFF state), the clutch is engaged (which provides unidirectional holding against flexion). When the solenoid is energized (i.e., in the ON state), the clutch is disengaged, and the ring is free to rotate in both directions.

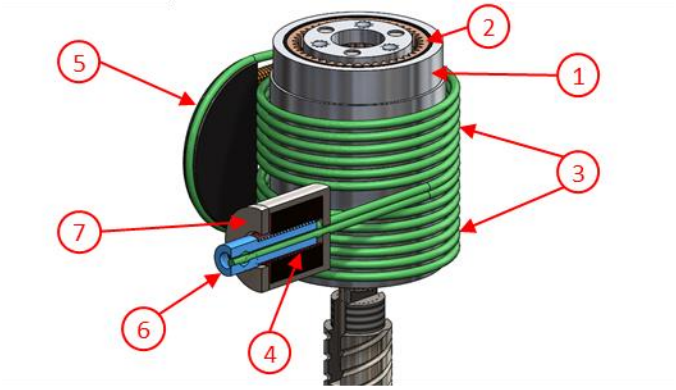

Fig. II-3: Solid model of ring clutch. An aluminum sleeve (1) is pressed onto the ECT common ring-gear (2). A steel wire rope (3) wraps several times around the aluminum sleeve. The stiff wire rope and compliant aluminum sleeve together form a capstan with a high static friction coefficient. A spring element (4) applies tension to one end of the wire rope while the other end is grounded to the housing by an adjustable anchor point (5). A set screw on the anchor point permits adjustment of the spring element's preload tension. The distal ends of the spring element and wire rope are fixed to a solenoid armature (6), which rests inside of the solenoid stator (7). Energizing the solenoid disengages the wire rope from the aluminum sleeve.

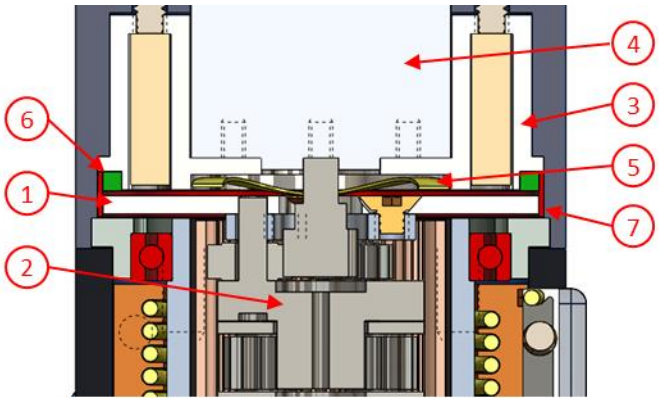

Fig. II-4: Solid model cross section of the carrier clutch. A ferromagnetic disk clutch armature (1) is collinearly fixed to the first-stage carrier (2) of the planetary gear transmission. A custom solenoid clutch stator (3) is collinearly fixed to the drive motor (4). A wave disk spring (5) separates the armature and stator when the clutch is de-energized. A medium durometer square-cross section O-ring (6) is fixed to the stator and becomes compressed by the armature when the clutch is energized. A plain bearing (7) encircles the armature and O-ring. When the clutch is de-energized, rotation and translation of the armature are constrained by the wave spring and plain bearing, respectively.

The second clutch, the carrier clutch, is shown in Fig. II-4. The carrier clutch grounds the first-stage planet-gear carrier and second-stage sun-gear. This clutch is engaged during swing-phase and must hold against 0.5 Nm of torque (i.e., 1/10 of the ring clutch holding requirement). Since the carrier clutch must hold only a modest amount of torque, it is configured as an electromagnetic disc clutch, as shown in Fig. II-4, where a solenoid stator is fixed to the electric motor, and a ferrous disk armature is fixed to the transmission's first-stage carrier. The motor, stator, armature, and transmission are constrained collinearly within the housing. The motor and stator are fixed to the housing, the transmission is simply-supported

by a pair of thin-section bearings so that it is able to freely rotate (when not constrained by the ring clutch), and the armature is constrained with a plain bearing to prevent lateral translation of the first-stage carrier.

When the carrier clutch solenoid is de-energized (i.e., in the OFF state), the spring element keeps the stator and armature separated, and the O-ring is not engaging the armature. When the clutch solenoid is energized (i.e., in the ON state), the armature is pulled to the stator and is engaged by the O-ring, locking the armature to the stator, and preventing rotation of the armature. This prevents rotation of the first-stage carrier and the second-stage sun-gear. For both clutches, using friction-based locking permits locking in any configuration, and using solenoid-actuation permits state changes within several milliseconds, and therefore within a single stride of the gait cycle. Experimental characterization of clutch performance is presented in Section 4.3.

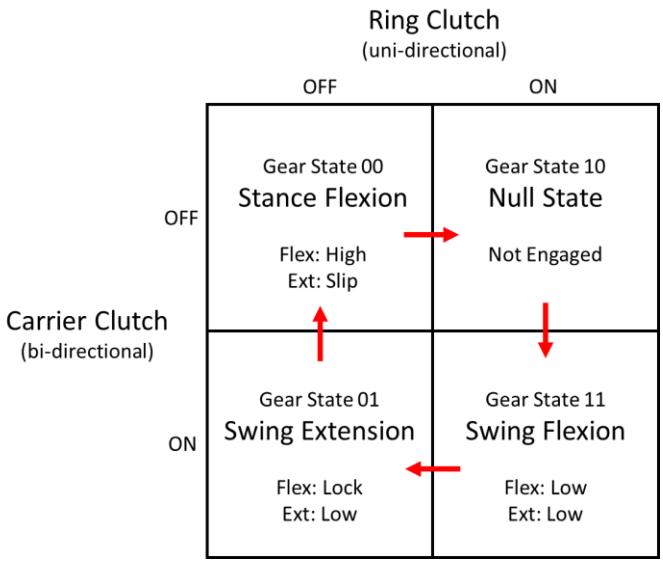

Fig. II-5: ECT configuration state-flow diagram. Axes represent energized state of each electromagnetic clutch (i.e. ON when energized, OFF when de-energized). Arrows show direction of state-flow during the gait cycle. In each state, the configuration of the clutches produces one of four behaviors in each the flexion and extension directions: a low transmission ratio (*low*), a high transmission ratio (*high*), over-determined locking (*lock*), and under-determined motion between input and output (*slip* or *not engaged*).

3.2.3 Clutch and Transmission States

Although there are two defined gear ratios, there are four possible mechanical states of the transmission, described below and outlined in Fig. II-5.

State 00: Both clutches are de-energized. The ring-gear is locked and the transmission provides a high-ratio against flexion, but due to the unidirectional nature of the capstan ring clutch, slips the clutch and provides no resistance against extension. This is the stance-flexion state.

State 10: The carrier clutch is de-energized and the ring clutch is energized. The transmission assumes an under-determined state, which effectively disengages the output shaft from the drive motor. This state is assumed for several milliseconds in order to prevent over-constraining the transmission against flexion before transitioning into the swing-flexion state.

State 11: Both clutches are energized. The first-stage carrier is locked and the ring-gear is unlocked. The transmission provides a low-ratio in both directions. This is the swing-flexion state.

State 01: The carrier clutch is energized and the ring clutch is de-energized. The unidirectional nature of the ring clutch allows the ring-gear to slip against the clutch in the extension direction. The transmission provides a low-ratio when driven in the extension direction, but locks when driven in the flexion direction. This is the swing-extension state. The ECT enters this state in order to preconfigure the prosthesis for the stance-phase in case there is a sudden need to load the prosthesis (e.g. due to stumble). Note that the amount of resistance within each state is controlled by the combination of the transmission ratio, and the PWM duty cycle of passive motor switching.

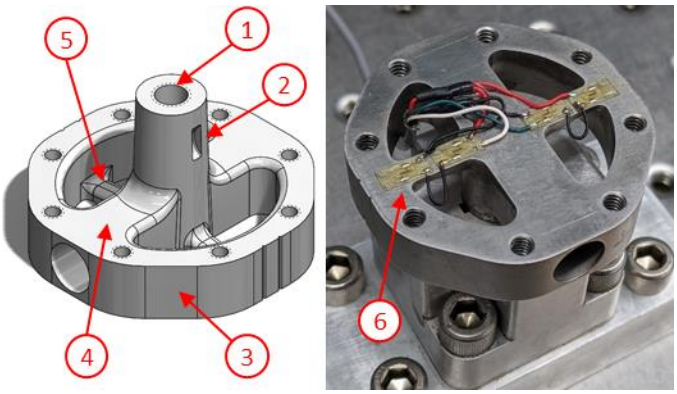

Fig. II-6: Solid model and photo of the load cell. The load cell spring element is fixed to the prosthesis housing via a Morse taper (1) and Woodruff key (2). A rigid outer-ring (3) attaches to the pylon clamp (not pictured) via eight threaded fasteners. The loading-beam (4) and measurement-beam (5) connect the Morse taper to the rigid outer-ring. The loading-beam is the primary load path. Four semiconductor-backed strain gages (6) are mounted to the underside of the measurement beam, which measures the displacement of the loading-beam. The gages are wired in a Wheatstone bridge configuration. Signal processing is achieved with an instrumentation amplifier with a gain of 10.

3.3 Load Cell

A custom load cell, shown in Fig. II-6, was designed and fabricated in order to measure axial loads up to 1200 N in the presence of sagittal, frontal, and torsional moments of 130 N·m, 20 N·m, and 20 N·m, respectively. The authors are unaware of a commercially-available load cell that meets these measurement specifications and remains within the size and weight constraints of the prosthesis. In order to provide

load measurement while rejecting measurements from moments, the authors constructed a strain-gage based transducer with a Maltese-cross spring element similar to those found in [43], [44].

The spring element is fixed to the prosthesis housing via a Morse taper, commonly used in machines to mate components. The center of the taper is tapped in order to secure the spring element via a bolt used as a drawbar. The taper uses a Woodruff key to prevent rotation of the spring element relative to the housing under stance-phase transverse moments. The rigid outer-ring provides grounding of the cross-beams and fixes the spring element to the pylon clamp. The loading-beam is the primary load path between the taper and the rigid outer-ring. A hollow rectangular cross-section was chosen to maximize stiffness-to-weight ratio of the loading-beam. The chosen geometry also provides higher stiffness to torsional moments than bending moments, which provides the necessary compliance under axial load and simultaneously limits torsional displacement under frontal moments. The measurement-beam is placed in parallel with the loading-beam in order to measure its displacement under load while protecting the gages from overload. The measurement-beam is designed with an asymmetrical profile that produces four regions of uniform strain distribution.

The strain gages on the measurement-beam are arranged in a Wheatstone bridge configuration such that forces perpendicular to the beam are transduced as differential bridge outputs, while moments acting in the plane bisecting the length of the measurement beam (in this case, frontal-plane moments) do not produce differential bridge outputs. When subjected to sagittal-plane and transverse-plane moments, the gages lie in the neutral axis of the spring element, and therefore do not theoretically experience a change in resistance under these loading conditions. The spring element was machined from a single stock of 17-4 PH stainless steel, a common high-modulus material in force transducers. Semiconductor gages (Micron Instruments, SS-090-060-1150PB-S4) were chosen for their high gage-factor, small size, and high resistance. The total mass of the load cell, including the transducer spring element and the pylon clamp, is 110 g.

To characterize the ability of the load cell to measure axial load in the presence of moments, a set of known masses was used to apply forces and moments to the load cell in compression. Moments were coupled to forces by placing the weights at a known distance (r) eccentric to the vertical axis of the load cell. Fig. II-7 shows the experimental results for isolated axial loads and coupled moments in the sagittal and frontal planes. Rejection of transverse moments was tested by manually twisting the fixed load cell, which provided no change in output.

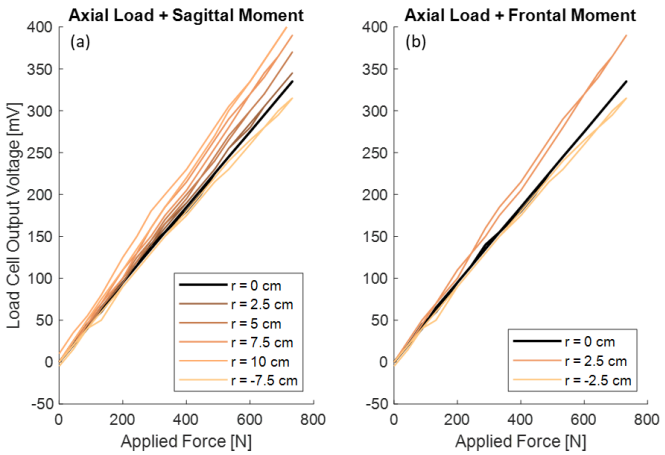

Fig. II-7: Experimental results of load cell validation, showing load cell output for isolated axial loads and coupled moments in the (a) sagittal and (b) frontal planes. Moments were produced by placing known masses at a load-eccentricity distance (r) from the neutral axis of the load cell, where r = 0 cm corresponds to an isolated axial load. Differences in slopes indicates interference between load and moments, and asymmetry between the two directions of load-eccentricity indicates asymmetrical fabrication of the spring element and/or asymmetrical placement of strain gages.

Load cell output was linear with slight hysteresis for all loading conditions, indicating linear response to applied load and moments. Differences in slopes for each load-eccentricity distance (r) is a result of coupling between moments and axial loads. These differences in slopes between the isolated axial load and the coupled moments corresponds to a maximum additional 1.9 N of output reading for every 1 N·m of sagittal moment and 6 N for every 1 N·m of frontal moment. As previously noted, maximum expected axial load, sagittal moment, and frontal moment are 1200 N, 130 N·m, and 20 N·m, respectively. Therefore, the maximum ratios of sagittal and frontal moments in the shank versus axial load are 1:9 and 1:60, respectively, which corresponds to a maximum expected change in load cell output of 20% and 10%, respectively. This interference is unlikely to adversely affect load-sensing for purposes of prosthesis control.

3.4 Prosthesis Housing

The prosthesis housing, shown in Fig. II-8, was designed in two halves with the ECT actuator located between them. The rotational output of the motor is connected to the input of the ECT; the rotation output of the ECT connected to a lead screw; and the lead screw linear motion coupled to the knee via an inverted slider-crank mechanism. Rotational motion of the knee joint is limited by the flexion and extension hard stops, providing a total range of motion of 130° (5° hyperextension to 125° flexion). The actuator reaches a singularity at 107° flexion, as is common practice in linearly actuated MPKs. The length of the crank arm is 25 mm, and the distance between the housing mounting points of the crank arm and

connecting rod is 188 mm. The nonlinear transmission ratio of the slider-crank mechanism in both gear ratios is depicted in Fig. II-9. The length of the prosthesis from the socket mounting location to the base of the pylon clamp measures 360 mm. The total mass of the prosthesis including battery pack, load cell, and embedded system is 1.95 kg.

Fig. II-8: ECT knee prosthesis prototypewith one half of the housing removed (left) displaying the novel actuator (1) and lead screw (2), and fully-assembled prosthesis (right) including absolute encoder (3), battery pack (4), and custom embedded system (5). The range of motion of the crank arm (6) is limited by the hard stops for extension (7) and flexion (8). The load cell (9) is fixed to the bottom of the prosthesis and attaches to the pylon clamp.

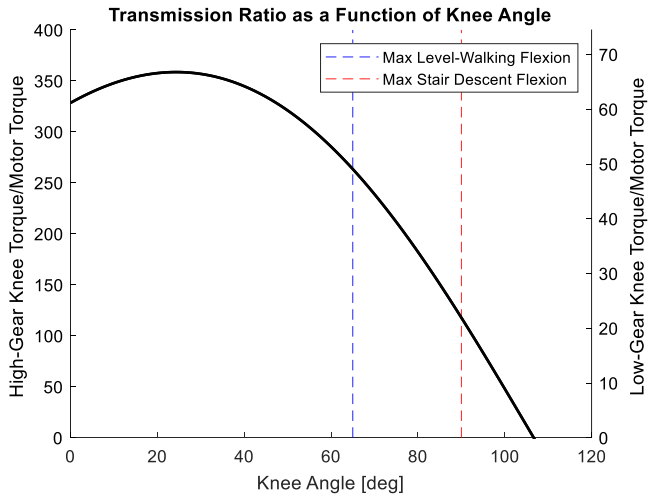

Fig. II-9: Prosthesis transmission ratio between drive motor to knee joint as a function of knee angle. The left and right vertical axes indicate the transmission ratio in the high- and low-gear, respectively. The maximum transmission ratios are 359:1 and 67:1 in the high- and low-gear, respectively. The transmission reaches a singularity at 107° knee flexion. Dashed vertical lines indicate maximum knee flexion for level-ground walking and stair descent.

3.5 Embedded System

A custom embedded system was designed to provide sensing, actuation, and control of the prosthesis actuator. The embedded system includes: 1) a brushless motor drive, which has two separate drive modes to provide motor torque control in either active or passive operation; 2) power electronics to energize the two clutch solenoids; 3) sensing and signal conditioning, including, a high-resolution incremental angle encoder at the drive motor, an absolute angle encoder at the knee joint, axial force load measurement, and a six-axis inertial measurement unit (IMU); 4) two microcontrollers that implement high and low-level control, respectively; 5) SD card for data storage; and 6) Controller Area Network (CAN) communication hardware for interfacing with a host computer. Low-level control is generally provided via a microprocessor optimized for signal processing (Microchip DSPIC 33FJ64GS608-E/PT), which communicates via SPI with a 32-bit general-purpose microcontroller (Microchip PIC32 MZ2048EFM100-I/PF), which runs higher level control functions and interfaces with the IMU sensor, load cell sensor, absolute encoder, SD card, and CAN bus. The output of the load cell is conditioned by an instrumentation amplifier (Texas Instrument INA 331) with a gain of 10, and the resulting voltage is measured by an analog-to-digital converter in the PIC32. The motor and solenoids are switched at a PWM frequency of 45 kHz. In passive mode (i.e., passive motor braking), the three low-side MOSFETs are switched simultaneously, which guarantees smooth and strictly-passive behavior. For purposes of the prototype, the system is powered using four 18650 batteries (INR18650-30Q) in series, providing nominal 16.8 V, 3 A-hrs and 43 W-hrs at full charge, with a maximum continuous current capacity of 15 A. Note that the battery pack was chosen to support eventual operation in the powered quadrants of the power plane. Implementation in a strictly-passive mode, such as demonstrated in this and the following chapters, could be supported with a more compact battery pack with lower energy and power capacities, such as employed in commercial MPKs.

3.6 Passive Motor Control

As previously stated, the motor can be controlled in an active (i.e., power generation) or passive (power dissipation) mode. The passive mode motor control is employed when operating in the passive quadrants of the power plane (i.e., in the strictly-passive mode). In this passive torque control mode, BLDC motor control is achieved by leveraging the intrinsic damping that DC motors exhibit when the leads are shorted, controllable via PWM modulation, where 100% duty cycle corresponds to a maximum amount of damping, and 0% duty cycle to minimum damping (i.e., no motor torque). It is important to

note, however, that the relationship between duty cycle and damping is highly nonlinear, and also dependent on velocity, where most of the actuator dynamic range is achieved in the upper range of duty cycle (see Fig. II-11). In order to achieve fidelity of passive torque control, a combined feedforward-feedback controller architecture was employed which uses current and velocity feedback to control the motor duty cycle. Details regarding the passive motor control approach can be found in [45]. One advantage of this control scheme is that the motor current is entirely induced by the back-EMF voltage, which results in strictly-passive behavior and no battery power consumption by the motor. Note that, when in the powered quadrants, the motor is controlled in the active mode (i.e., it is controlled in a typical BLDC motor torque control mode).

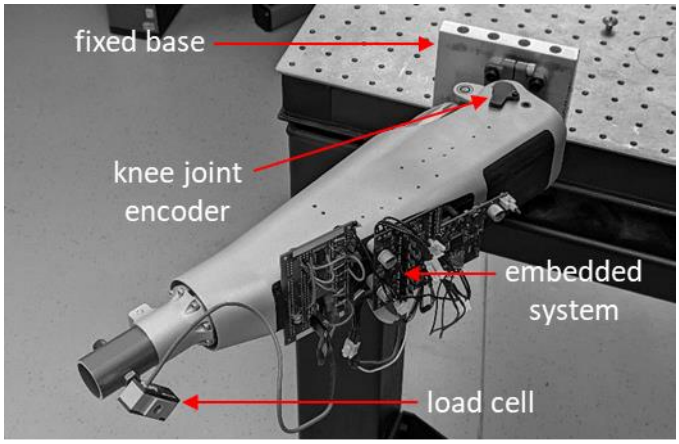

Fig. II-10: Prosthesis impedance characterization test setup with load cell oriented perpendicular to the long axis of the prosthesis. The prosthesis is mounted in the horizontal plane to remove the effects of gravity.

4. Experimental Characterization

4.1 Impedance Characterization

In order to validate that the actuator is able to provide the strictly-passive functionality required for walking, the dynamic range of knee damping (i.e., the span of behavior in the passive quadrants of the power plane) was characterized across both high and low gears. Torque-speed values were collected by measuring knee angle with the absolute encoder at the knee joint, knee angular velocity with the incremental encoder at the motor, and knee torque with a load cell (Transducer Techniques MLP) oriented perpendicular to the long axis of the prosthesis such that applied forces are translated into applied torques (see Fig. II-10). Knee angle, motor angular velocity, and load cell data were collected using the onboard embedded system. The transmission ratio between the knee joint and actuator output was calculated using

the knee angle from the absolute encoder in order to translate values of applied torque into the actuator output space, which produces a linear relationship between applied torque and motor angular velocity.

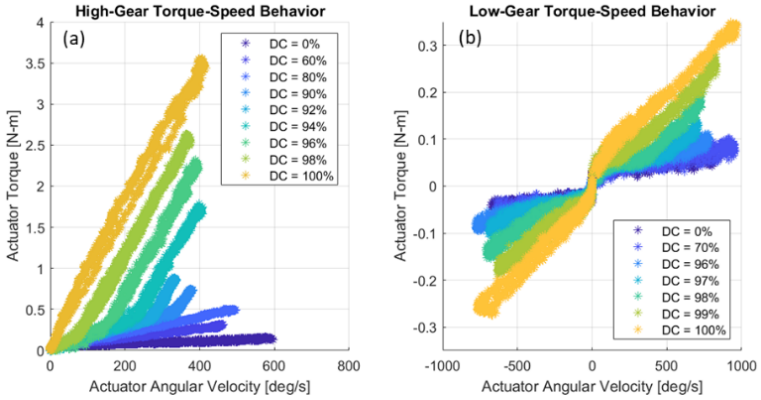

Fig. II-11: Results of impedance characterization experiment, showing applied torque versus angular velocity at the actuator output for a set of motor PWM duty cycles (DC). In the high-gear, the actuator is able to provide high impedance to flexion only, whereas the low-gear is bidirectional. At the knee joint, the actuator damping is able to be varied continuously from 0.30 to 2.75 N·m·s/rad in the low-gear and from 1.5 to 75 N·m·s/rad in the high-gear. The Coulomb friction coefficient, as indicated by the y-intercept of each torque-speed plot, is 0.35 and 0.50 N·m in the low- and high-gear, respectively. Maximum torque demonstrated in the high-gear is 40 N·m when reflected from the actuator output to the knee joint.

Torque-speed relationships were measured for actuator PWM duty cycles between 0% and 100%. The high-gear was characterized in flexion only (i.e., stance resistance is unidirectional); the low-gear was characterized in both flexion and extension. Fig. II-11 shows the experimental results, which demonstrate a maximum damping coefficient of 75 N·m·s/rad in the high-gear, a minimum damping coefficient of 0.30 N·m·s/rad in the low-gear, and a Coulomb friction coefficient of 0.35 N·m in the low-gear. Note that these curves are not linear, due to the nonlinear relationship between velocity, torque, and duty cycle in the passive control of a motor, and note also that this behavior is compensated for by the passive motor torque controller discussed in Section 3.6. The ECT actuator therefore provides a dynamic range of damping (i.e., ratio of maximum to minimum damping) of 250. A maximum resistive torque of 100 N·m in the high-gear is based on the theoretical yielding of the transmission. At a walking speed of 1.2 m/s, the biological knee has a peak velocity of 400 deg/s [46], which corresponds to a maximum resistive torque of 19.2 N·m and maximum power dissipation of 130 W in the low-gear. In the high-gear, the peak power rating is limited by the motor at four-times the continuous current (360 W). Based on the motor data sheet and the maximum transmission ratio in the low-gear, the reflected inertia from the motor and transmission is 25 kg-cm^2 in the low-gear. As a comparison, the reflected inertia in the high-gear is 715

kg-cm^2, which is 200% of the target output inertia – too high to permit a viable user-initiated, ballistic swing-phase motion.

4.2 Powered Stance and Swing Behaviors

Experiments were also conducted to validate the ability of the prosthesis to provide appropriate power generation behaviors. Fig. II-12 demonstrates active trajectory tracking of the prosthesis in the swing-phase configuration, indicating the desired ability to provide swing-phase assistance at approximately 1 Hz. The knee prosthesis was also verified to provide up to approximately 34 Nm of stance knee extension torque at a velocity of approximately 200 deg/s. As such, the prosthesis encompasses a range of powered behaviors that, based on prior works, will provide effective powered assistance during activities that require it.

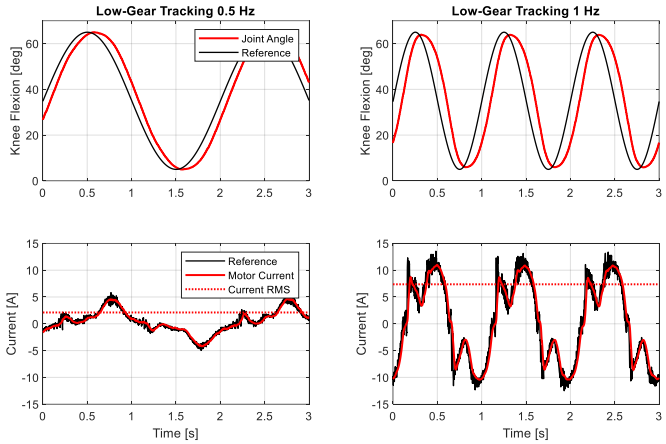

Fig. II-12: Tracking of 0.5 Hz and 1 Hz sine commands in the low-gear, showing knee joint angle and motor current with their respective reference signals.

4.3 Clutch Activation

The ring clutch and carrier clutch were validated to provide holding torques in excess of 5 N·m and 0.5 N·m, respectively, and therefore both meet the holding torque requirements associated with the desired knee torque specifications. Both clutches were also characterized for speed of engagement and disengagement. Specifically, during normal operation, both clutch solenoids are energized using a short spiking period where current is briefly delivered at a PWM duty cycle of 100 percent, followed by a sustained holding period where current is delivered at a much lower PWM duty cycle. When powered by 16 V, the holding period duty cycles needed for robust operation of the ring clutch and carrier clutch were experimentally determined to be 12 percent and 25 percent, respectively. The minimum spiking periods

for the clutches to hold (i.e., the solenoids to latch) were experimentally determined to be 2 ms for each clutch.

Since the holding voltage requires that the respective armatures be in contact with the respective stators, this indicates that the respective armatures have made contact after approximately 2 ms. Note that the spiking periods were subsequently extended to 20 ms to provide a robust factor-of-safety for clutch activation. When transitioning from State 00 to State 11 in late-stance, the knee joint is in hyperextension, and the actuator is not under load, which enables both clutches to be simultaneously actuated without risk of over-constraining or under-constraining the transmission. Therefore, the commanded transition from high-gear to low-gear (i.e. from State 00 to State 11) is approximately 2 milliseconds. Due to the mechanical nature of the ring clutch and the control scheme of clutch state transitions, the transition from low-gear in extension to high-gear in flexion (i.e. from State 01 to State 00) is automatic and essentially instantaneous.

5. Validation of Strictly-Passive Walking Functionality

In order to demonstrate the ability of the ECT knee prosthesis to provide strictly-passive functionality (i.e., stance-knee support and ballistic, biomimetic swing-phase) similar to an MPK, the prosthesis was tested on a user with transfemoral amputation during level, upslope and downslope walking, and the device behavior was compared to the same activities using a state-of-the-art MPK. In order to do so, a unified, strictly-passive walking controller was constructed as follows.

5.1 Walking Controller

A strictly-passive controller, based upon the clutch state-flow diagram shown in Fig. II-5 and passive motor control, was implemented to demonstrate the ability of the ECT knee prosthesis to provide strictly-passive functionality (i.e., stance-knee support and ballistic, biomimetic swing phase) in a device also capable of providing power. The controller enables level and sloped walking by combining the state machine shown in Fig. II-5 with the switching conditions enumerated in Table II-2. State transitions were effected by actuation of clutches (as shown in Fig. II-5); behavioral characteristics in each state are therefore primarily hardware-determined, with the exception of passive modulation of motor current induced within each state, effected by PWM shorting of the motor leads. This structure is in contrast with most conventional finite-state controllers, in which changes in state behavior are generally determined by

feedback control of the motor. Note that the transition from state 00 to 01 is for down-slope walking, which does not require low-impedance swing-flexion motion.

Table II-2
Walking Controller Transmission State Transitions

Transition	Condition
00 to 11	Knee joint is in hyperextension Shank rotating forward Shank forward inclined Rapid decrease in load cell reading
11 to 01	Prosthesis is unloaded Knee joint begins extending
01 to 00	Knee joint velocity is zero, OR Prosthesis becomes loaded
00 to 01	Knee joint is flexed Prosthesis becomes unloaded

5.2 Experimental Protocol

The test participant was a 62-year old male weighing 85 kg. In the experiments, the participant was fit with the ECT knee and walked on a treadmill under three walking conditions while knee angle data was recorded via a motion capture system (Vicon), and ground reaction force was recorded via force plates in the instrumented treadmill (Bertec). The three walking conditions were: 1) level walking at a treadmill speed of 1.1 m/s; 2) upslope walking on an 8-degree ramp at a treadmill speed of 0.6 m/s; and 3) downslope walking on an 8-degree ramp at a treadmill speed of 0.6 m/s. The participant walked at a steady state for approximately 2 min. After walking with the ECT knee, the subject was fit with his daily-use prosthesis, a state-of-the-art passive MPK (Ottobock C-Leg 4), and repeated the same experimental procedures while the knee angle was recorded by the motion capture system. The experimental protocol was approved by the Vanderbilt IRB.

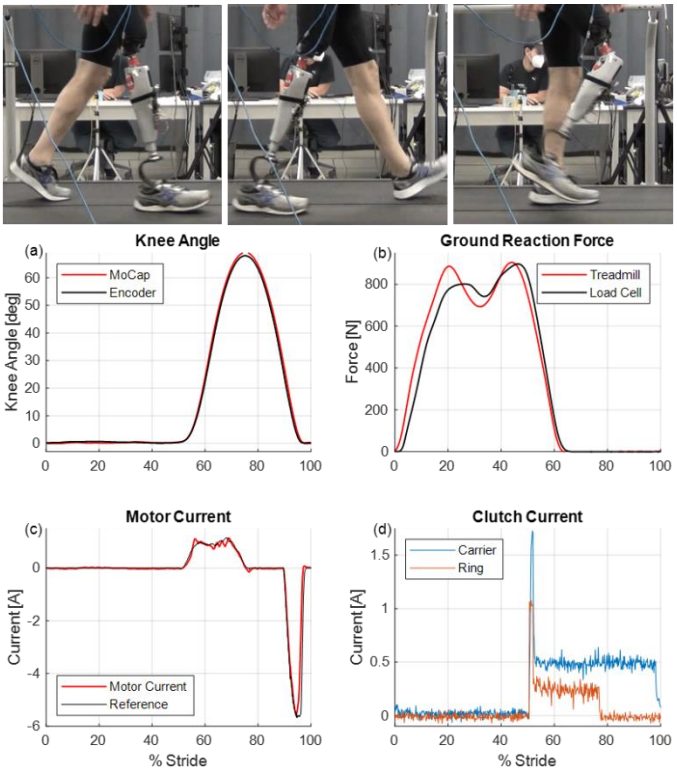

Fig. II-13: Experimental results of treadmill walking validation, showing results for fifteen strides at 1.1 m/s for a single subject with TFA. Gait data were collected using the onboard embedded system and Vicon motion capture and treadmill force data. Plots show: a) 15-stride average knee angle (onboard encoder and Vicon motion capture); b) 15-stride average ground reaction force (onboard load cell and treadmill force plates); c) passive motor current for a single stride; and d) current of both clutches for a single stride.

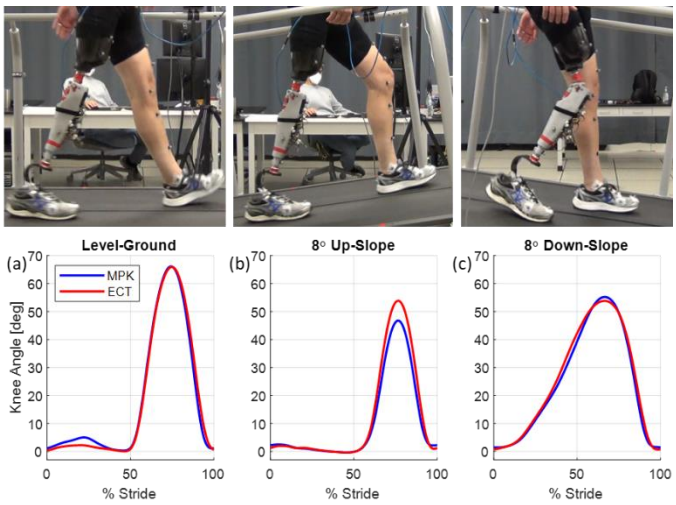

Fig. II-14: Comparison of experimental results between subject's daily-use MPK (blue) and the ECT (red) in three ambulation conditions: (a) level-ground walking at 1.1 m/s, (b) up-slope walking on an 8-degree ramp at 0.6 m/s, and (c) down-slope walking on an 8-degree ramp at 0.6 m/s. Plots show 15-stride average knee angle on subject's prosthesis side.

5.3 Results of Experimental Validation

Fig. II-13 shows data for the ECT during the level walking experiment, which shows the knee joint angle and shank load averaged over fifteen cycles of gait, along with ring and carrier clutch currents for a single stride, and passive motor current (resulting from the passive motor current controller) for a single stride. Average battery power consumption during the walking was 1.5 W, which was required to operate the two clutches and switch the MOSFETs for motor braking, minus energy regenerated. At this rate, a single 18650 onboard battery would be capable of providing 7-8 hours of continuous use, or approximately 45 000 steps of level-ground walking between charges.

Fig. II-14 shows data comparing the behavior of the ECT knee, operated in passive mode, to the daily-use passive MPK for level walking, upslope walking, and downslope walking. As shown in the figure, the ECT offers the same strictly-passive behaviors as the MPK. To the authors' knowledge, this is the first demonstration of a power-capable prosthesis that provides both high-torque stance-knee yielding functionality, along with a strictly-passive ballistic, biomimetic swing-phase motion.

6. Conclusions

This chapter describes a new approach to a powered knee prosthesis design that expands the behavioral capability into the powered quadrants of the power plane, without sacrificing the ability to offer ballistic swing-phase behavior. The prosthesis enables this behavior by employing a specialized electronically-controlled two-speed transmission with selective unidirectional behaviors, in combination with an electric motor used in a strictly-passive braking mode, to provide energetically passive behavior similar to that provided by commercial MPKs (i.e., high-torque, low-speed, high-impedance stance-phase behavior and separately low-torque, high-speed, low-impedance ballistic swing-phase behavior). The authors demonstrated that the proposed motor-actuated device can replicate the passive stance and swing behaviors of an MPK while offering powered stance and swing capabilities. The following chapters describe the passive control system in detail and the powered behaviors layered onto the passive behaviors demonstrated here, namely to provide powered knee extension and to facilitate non-ballistic swing phase in activities that require it, such as step-over stair ascent.

CHAPTER III

AN ENERGETICALLY-PASSIVE UNIFIED WALKING CONTROLLER FOR A TORQUE-CONTROLLABLE KNEE PROSTHESIS

This chapter describes a unified control system for a torque-controllable modulated-passive microprocessor-controlled knee prosthesis (MPK) that provides biomimetic behavior for up-slope, level-ground, down-slope, down-stairs, and backwards walking, as well as stand-to-sit transitions, using minimal battery power consumption and without requiring identification of activity. Energetically-passive behavior was achieved for both stance and swing phase via the combination of transmission ratio modulation and motor-braking using a novel knee prosthesis with an electric motor and electronically-selectable two-speed transmission. The stance-phase controller uses high-impedance, task-invariant resistive torque to provide knee-yielding behavior appropriate for a range of ambulatory activities. The swing-phase controller is based on the observation that energy dissipation in both swing-flexion and swing-extension is linearly-proportional to walking speed, and uses low-impedance resistive torque with a resistive torque appropriate for the user's walking speed, which permits user-initiated ballistic swing-phase motion with appropriate kinematics. Key to the swing-phase controller is a zero-parameter IMU-based walking speed estimation that automatically adjusts swing-phase control parameters. The resultant control system uses only four tunable parameters, each with effects directly-linked to resistive torque and energy dissipation. The device and unified controller were assessed on a single subject with transfemoral amputation during up-slope, level-ground, down-slope, down-stairs, and backwards walking, as well as stand-to-sit transition. Experimental results suggest that the prosthesis and accompanying controller can provide similar or improved behavior relative to commercially-available MPKs using only motor-braking.

1. Introduction

The previous chapter proposed a new hardware design capable of providing a range of energetically-passive controllable impedances commensurate with commercial MPKs, in addition to active behaviors commensurate with powered prostheses. Key to the function of the proposed device is a unique electronically-controlled transmission (ECT) with three selectable mechanical states: 1) a high-torque, low-speed state that provides unidirectional flexion resistance and extension assistance, with little

to no extension resistance, appropriate for the stance-phase of walking; 2) a low-torque, high-speed, low-impedance state that provides bidirectional knee resistance and assistance, appropriate for the swing-flexion phase of walking; and 3) a low-torque, high-speed, low-impedance state that provides unidirectional low-resistance against knee-extension or assistance with knee-extension, with a simultaneous high-resistance to knee-flexion, appropriate for the swing-extension phase of walking. The essential control philosophy of this approach is to provide a foundational layer of strictly-passive prosthesis behavior, then to subsequently layer active behaviors on top. Accordingly, this chapter describes a control system that provides the full range of energetically-passive functionality. Powered behaviors will be layered onto this control structure in the subsequent chapter. The control system described here provides adaptive behavior appropriate for a wide range of ambulatory activities, including level-ground, up-slope, down-slope, and down-stairs walking, backwards walking, and stand-to-sit transitions, all of which are within the range of behaviors achievable by commercial MPKs [25].

Several review articles have provided overviews of control strategies in knee prostheses [12] [25] [47] [48], although these articles mostly describe powered control systems. Some passive control systems for knee prostheses have been described in literature, including those for cadence-adaptive level-ground walking [49] [50] [51] and slope-descent knee-yielding [52]. However, none of these describe a passive control system capable of the all of the aforementioned energetically-passive activities. Additionally, no research prostheses describe passive control systems suitable for backwards walking, although this feature, in addition to all energetically-passive activities, is available on commercial MPKs [25]. As such, there is no publication that fully describes a passive control system capable of replicating an energetically-passive control system appropriate across the range of activities enabled by commercial MPKs.

This chapter presents a control system for an energetically-passive torque-controllable knee prosthesis, capable of the full range of activities previously mentioned. Swing-phase control laws are proposed based upon the observation that energy dissipation in both swing-flexion and swing-extension is linearly-proportional to walking speed. A unified control structure is proposed, and the composite control system is demonstrated in a prosthesis prototype, with performance within each activity compared to a state-of-the-art commercial MPK. This chapter additionally describes all inter-activity transition conditions, and demonstrates the ability of the control system to reliably and seamlessly transition between different locomotion activities. The proposed control structure is applicable to any torque-controllable knee prosthesis capable of providing the dynamic range of passive impedance necessary for both stance-phase knee-yielding and ballistic swing-phase.

2. Unified Walking Control System Design

2.1 Finite State Machine

The unified walking controller is a three-state finite state machine (FSM), diagrammed in Fig. III-1, which provides passive functionality across a wide range of activities. Each state within the FSM has a unique transmission configuration (gear state) and a unique torque control law (see Table III-1). Note that the FSM states and gear states in Fig. III-1 differ such that the FSM states are implemented in software whereas the gear states are related to the hardware implementation (these gear states and their relationship to the torque control laws are discussed in Section 3.1). During each of these states, the resistive torque at the knee joint is governed by a passive control law (discussed in Section 3.2), which guarantees system stability and enables the motor to provide mechanical damping without consuming battery power. Behavior of each FSM state is described below.

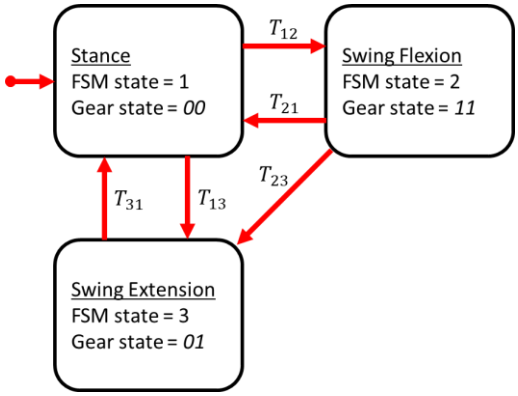

Fig. III-1: Finite state machine for passive walking consisting of three states and the transitions between them. The FSM indicates the corresponding gear states of the hardware on which the control system is implemented (discussed in Section 3.1). Torque control laws and transition conditions are outlined in Table III-1 and Table III-2, respectively.

FSM State 1 (stance): The user is standing on the prosthesis, unilaterally or bilaterally. The transmission is in its high-gear against flexion (gear state 00) and provides support of the user's weight. The motor is in its passive mode so that flexion of the knee joint creates a resistive turbulent damping torque similar to that provided by a hydraulically-actuated MPK, with little to no resistance to knee extension. In this FSM state, the transmission does not consume energy (i.e. the clutches are de-energized and motor current is only produced as a byproduct of back-emf), and energy is only consumed to provide signal power to the motor to modulate passive torque control.

FSM State 2 (swing-flexion): The FSM enters this state in late-stance, when the user is walking forward and has met the necessary conditions for entering the swing-phase. The transition conditions into this state prevent the control system from entering this state unless the user is walking forward with a minimum step length and step frequency. The transmission is in its low-gear (gear state 11), providing for low-impedance free-swinging of the knee joint, which enables user-initiated ballistic swing-phase motion. The motor is in its passive mode and provides a resistive torque that is proportional to the walking speed and the instantaneous knee velocity (discussed in detail in Section 2.4 and Appendix B).

FSM State 3 (swing-extension): The FSM enters this state under one of two conditions: (1) the prosthesis has completed its swing-flexion motion, or (2) the prosthesis is unloaded after it has flexed past a threshold value during stance-phase. The transmission is in its low-gear against extension, but is over-constrained to flexion (gear state 01). The motor is in its passive mode and provides a resistive torque that is proportional to the knee angle and instantaneous knee velocity (i.e. torque modulation is governed by a linear viscous friction coefficient that increases in value as the knee approaches full-extension). The relationship between the damping coefficient and the knee angle is scheduled by the walking speed estimation (discussed in detail in Section 2.5 and Appendix B).

Table III-1
Finite State Torque Control Laws

FSM State	Torque Control Law	
1	$\tau_K = f_1(\dot{\theta}_K)$	$\tau_K = C_1\dot{\theta}_K^2$
2	$\tau_K = f_2(\omega, \dot{\theta}_K)$	$\tau_K = C_2\omega\dot{\theta}_K$
3	$\tau_K = f_3(\omega, \theta_K, \dot{\theta}_K)$	$\tau_K = b_{max}\left[1 - e^{(\theta_K - C_{3\alpha} - C_{3\beta}\omega)/C_{3\gamma}}\right]\dot{\theta}_K$

Within each FSM state, knee torque is governed by a unique control law based upon a combination of sensor inputs: knee angle (θ_K) and velocity ($\dot{\theta}_K$), and walking speed estimation (ω). Each torque control law (f_n) has between one and three tunable parameters (C_n). For f_3, b_{max} indicates the maximum achievable motor braking impedance (i.e., when all motor leads are connected at 100% duty cycle).

FSM state transition conditions are based upon onboard sensing by an IMU, an incremental encoder on the motor, an absolute encoder at the knee joint, and a load cell located in the shank. Collectively, and with the use of real-time differentiating filters, these sensors are able to detect the following kinematic and kinetic states of the prosthesis: knee angle and its derivatives (θ_k), shank angle and its derivatives (θ_s), and axial shank load and its derivatives (F). The FSM state transition conditions are summarized in Table III-2; note that T_{12} was designed to only occur when the user is walking forward, as is done for commercial MPKs.

Table III-2
Finite State Machine Transition Conditions

Transition	Description	Condition
T_{12}	Knee joint is hyperextended, and Prosthesis shank is rotating forward, and Prosthesis shank is inclined forward, and Prosthesis is rapidly unloaded	$\theta_K \approx 0$ $\dot{\theta}_S < \dot{\theta}_{S,th}$ $\theta_S < \theta_{S,th}$ $\dot{F} < \dot{F}_{th}$
T_{23}	Prosthesis is unloaded, and Knee joint is extending	$F \approx 0$ $\dot{\theta}_K > 0$
T_{31}	Knee joint has zero velocity, or Prosthesis is loaded	$\dot{\theta}_K \approx 0$, or $F > F_{th}$
T_{13}	Prosthesis is unloaded, and Knee joint is flexed above threshold	$F \approx 0$ $\theta_K > \theta_{K,th}$
T_{21}	Prosthesis is loaded, and Prosthesis was previously unloaded, or Prosthesis shank is rotating backwards, or Prosthesis shank is not inclined forward	$F > F_{th}, and$ $F^- \approx 0$, or $\dot{\theta}_S > \dot{\theta}_{S,th}$, or $\theta_S > \theta_{S,th}$

Finite state machine transition conditions depend upon measured sensor inputs and several threshold parameters: knee angle ($\theta_{k,th}$), shank angle ($\theta_{S,th}$) and angular velocity ($\dot{\theta}_{S,th}$), shank axial force (F_{th}) and yank ($\dot{F}_{th}$).

2.2 Walking Speed Estimation

In order to provide for swing-phase behavior that adapts to variable walking speeds, it is necessary for the control system to have an accurate estimation of relative walking speed. During the stance-phase of level-ground walking, the biological knee flexes to provide shock absorption at heel-strike and to minimize the motion of the center-of-mass during mid-stance. The range of flexion of the biological knee varies between 0 to 30 degrees (from full extension), depending on the walking speed and individual's gait biomechanics [53]. However, individuals with TFA typically walk on level-ground with less than five degrees of knee flexion during early and mid-stance, only exceeding this small flexion angle in late-stance while transitioning to swing-phase [54]. Because of these typical biomechanics, the prosthesis-side leg is effectively straight during single-support (i.e. the period of gait where the user's weight is supported by only one leg). Thus, the forward translational velocity of the user's pelvis (and by biomechanical constraint, the user's upper body) is proportional to the angular velocity of the stance leg (i.e. the translational velocity of the pelvis (v) is approximately equal to the product of the angular velocity of the leg (ω) and length of the leg (L), and as indicated in Fig. III-2, $v \approx L\omega$). Therefore, a measurement of the prosthetic leg's angular velocity during single-support provides an indirect measurement of the walking speed, such that increases or decreases in the single-support leg angular velocity indicate increases or decreases in the walking speed.

Fig. III-2: Motion of the prosthetic leg during stance-phase.During level-ground walking, the prosthetic leg is straight, implying that the translational velocity of the pelvis (v) is approximately equal to the product of the angular velocity of the leg (ω) and length of the leg (L). A shank-mounted IMU can measure ω, which enables accurate estimation of walking speed when values are averaged over the stance-phase.

Because the knee is straight during single-support, the angular velocity of the shank, as measured by the gyroscope of a shank-mounted IMU, can serve as a proxy for the angular velocity of the whole leg. To estimate the prosthesis user's relative walking speed, the sagittal-plane angular velocity is recorded beginning at heel-strike (the gait event where the prosthesis makes initial contact with the ground, as indicated by a positive reading in the shank-mounted load cell) and ending at knee-break (the gait event in late stance when the user initiates swing-phase by flexing the knee), with recordings averaged each control loop. To provide experimental validation of this walking speed estimation, Fig. III-3 shows the average stance-phase shank angular velocity for a single subject with TFA for nine walking speeds ranging from 0.4 m/s to 1.2 m/s at 0.1 m/s incriments (the mean and standard deviation of average stance-phase shank angular velocity for 15 strides per walking speed are indicated by box-and-whisker plots). These data have low variance, and a line of best fit through the data passes near the origin, indicating the linearity and accuracy of this relative walking speed estimation. As such, the walking speed estimation algorithm is able to provide an accurate estimate of relative walking speed in a single stride using only onboard sensing (in this case, a single IMU and a knee joint encoder).

This relative walking speed estimation has control implications related to swing-phase. Because walking speed is estimated during the early and mid-stance phases, the value returned by the walking speed estimation algortithm can be used by the swing-phase controller for the swing-phase immediately following the current stance-phase. The accuracy of the walking speed estimation removes the need to average estimations over several strides, and the implications of walking speed on the swing-phase dynamics make this estimation valuable for controling the swing-phase motion.

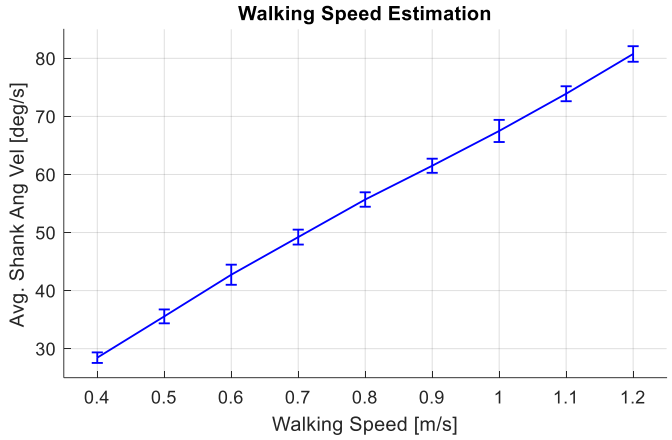

Fig. III-3: Estimated walking speed, as measured by a shank-mounted IMU. Gyroscope readings are recorded and averaged from heel-strike to knee-break. Line plot with error bars indicates fifteeen-stride mean and standard deviaiton for each walking speed for a single subject with TFA. Low variance and linearity indicate the utility of this algorithm for control systems that adapt behavior based upon relative walking speed.

2.3 Stance-Flexion Resistance

To provide stability during the stance-phase, knee prostheses must provide a supportive extension moment. Energetically-passive knee prostheses cannot provide positive power at the knee joint during stance-phase, which limits their ability to provide biomimetic knee-extension behavior when walking up steep slopes and stairs. Despite this limitation, these prostheses are able to provide stance-phase knee-yielding (i.e. a friction-based torque that resists flexion velocity), which permits biomimetic stance-phase behavior during level-ground walking as well as walking down-slope, down-stairs, and up gentle slopes. When descending slopes or stairs using a yielding technique, knee-flexion begins in early stance, shortly after heel strike, and continues throughout the stance-phase, ending when the user unloads the prosthesis and extends the prosthetic knee joint by swinging their thigh forward.

To provide for a comparison of knee-yielding techniques between the proposed control system and a commercial MPK, the constitutive behavior of the knee joint during the stance-phase is governed by the torque control law:

$$\tau_k = C_1 \dot{\theta}_k^2 \tag{III-1}$$

where τ_k is the knee torque, $\dot{\theta}_k$ is the instantaneous knee angular velocity, and C_1 is the stance-phase damping coefficient for a quadratic torque-speed relationship. In this manner, the control system provides the same turbulent damping knee-yielding behavior that is typical of state-of-the-art hydraulic MPKs.

2.4 Swing-Flexion Resistance

During the swing-phase of level-ground walking, the knee joint produces net negative work. Fig. III-4 illustrates the linear relationship between energy dissipation and walking speed, which has implications for control system formulation. During swing-flexion, the knee joint must provide an amount of resistance that: (1) achieves an adequate flexion angle, based on the leg geometry, that provides robust toe-clearance as the thigh swings forward, (2) prevents unnecessary motion of the knee joint by limiting the maximum flexion angle (i.e., too much knee flexion unnecessarily increases the duration of swing-phase), and (3) achieves timing of the peak-flexion knee angle such that the effective length of the leg is shortest when oriented vertically (i.e. the knee is flexed most when the toe is directly under the pelvis). These goals can be realized by formulating a control law based on the dissipation of kinetic energy as a function of the estimated walking speed.

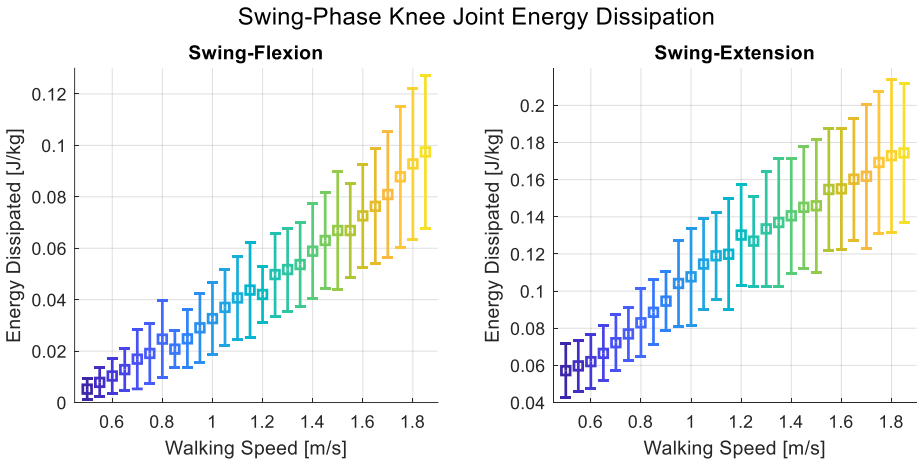

Fig. III-4: Energy dissipation v. walking speed during swing flexion and swing-extension phases of level-ground walking. Box-and-whisker plots indicate mean and standard deviation of 22 subjects from [53]. There is an approximate linear relationship between energy dissipation and walking speed. The knee joint produces net negative work for most walking speeds during swing-flexion and all walking speeds during swing-extension. Implications of this observation on control system formulation are discussed in detail in Appendix B.

Based on observations of the kinematics and energetics of the biological knee joint, the authors propose a swing-flexion torque control law, the formulation of which is described in detail in Appendix B. At the highest level, the control system commands a resistive torque by commanding a desired linear damping coefficient at the knee joint. The torque control equation governing this linear damping behavior is:

$$\tau_k = C_2 \omega \dot{\theta}_k \tag{III-2}$$

where τ_k is the commanded knee torque, $\dot{\theta}_k$ is the instantaneous knee joint velocity, ω is the average shank angular velocity as measured from heel-strike to knee-break (from the walking speed estimation algorithm), and C_2 is a gain constant associated with swing-flexion resistance torque. Note that C_2 has the units of inertia (kg·m^2). The potential benefits of this control law include (1) a smooth torque profile, with minimum discomfort on the socket; (2) stable controller behavior when paired with passive motor behavior (discussed in Section 3.2); (3) user-initiation of swing-phase, due to the absence of a desired swing-phase trajectory or a stiffness term in the impedance control law; (4) a predictable and desirable intrinsic swing-flexion behavior that can be easily learned and adapted to meet the user's needs; and (5) cadence-adaptive swing-flexion behavior is provided by a continuous control law with a single tunable parameter (C_2), simplifying controller implementation.

2.5 Swing-Extension Resistance

During swing-extension, the knee joint must provide an amount of resistance that: (1) is sufficiently in early swing-extension, such that inertial forces can rapidly accelerate the joint velocity, (2) is sufficiently high in terminal swing, such that impact forces at full-extension are negligibly small, and (3) provides a resistive torque profile that minimizes socket reaction forces as the magnitude of resistive torque increases.

Based on observations of the kinematics and energetics of the biological knee joint, the authors propose a swing-extension torque control law, the formulation of which is described in detail in Appendix B. At the highest level, the control system commands a resistive torque by commanding a desired linear damping coefficient at the knee joint as a function of the knee angle. The damping control law begins increasing the linear damping coefficient from zero when the knee angle is less than the terminal-swing initiation angle (θ_k^{TS}), which is determined from the walking speed estimation during stance-phase and is governed by the equation:

$$\theta_k^{TS} = C_{3\alpha} + C_{3\beta}\omega \tag{III-3}$$

where $C_{3\beta}$ is a gain associated with the calculation of θ_k^{TS} for a given estimated walking speed, and $C_{3\alpha}$ is the minimum angle of θ_k^{TS}. From this initiation angle, the desired damping coefficient in the torque control law monotonically increases from zero to its maximum value as governed by the equation:

$$\text{if } \theta_k < \theta_k^{TS}, \quad \tau_k = b_{max}\left[1 - e^{\frac{\theta_k - C_{3\alpha} - C_{3\beta}\omega}{C_{3\gamma}}}\right]\dot{\theta}_k \tag{III-4}$$

where b_{max} is the maximum linear damping coefficient that can be passively delivered by the motor (i.e. when the motor leads are shorted), and $C_{3\gamma}$ is a decay constant that provides shape to the damping profile as a function of knee angle. The exponential decay function acts as a soft saturation of knee damping. Increasing the terminal-swing initiation angle with increasing walking speed permits energy dissipation with the motor alone, the dynamic range of which is limited by the low-gear transmission ratio, the intrinsic properties of the motor (torque constant and phase-to-phase resistance), and the intrinsic mechanical impedance.

3. Hardware Implimentation

To demonstrate the efficacy of the aforementioned control system, passive motor control and model-based control were utilized on the knee prosthesis prototype described in CHAPTER II.

3.1 Two-Speed Powered Knee

The unified passive control system was implimented on a novel knee prosthesis prototype, discussed in CHAPTER II and shown in Fig. II-8. Key to prosthesis functionality is an electromechanical modulated-dissipator prototype (see Fig. II-1), which consists of a DC brushless motor (Maxon EC-4pole 22 90W) connected to the knee joint through a leadscrew-based slider-crank transmission and novel two-speed electronically-controlled transmission (ECT, see Fig. II-2). The ECT provides a high transmission ratio for stance-phase and a low transmission ratio for swing-phase, which produces a range of achievable impedances in the high and low gears (see Fig. II-10) necessary for providing resistive stance and ballistic swing behaviors using motor braking only (see Fig. II-11 and Table II-1). Switching between gear ratios is achieved with two clutches (see Fig. II-3 and Fig. II-4), one unidirectional and one bidirectional, which provide four possible transmission configurations (see Fig. II-5), three of which are functional states appropriate for gait: 1) a high-torque, low-speed state that provides unidirectional flexion resistance, with little to no extension resistance, appropriate for the stance-phase of walking; 2) a low-torque, high-speed, low-impedance state that provides bidirectional knee resistance, appropriate for the swing-flexion phase of walking; and 3) a low-torque, high-speed, low-impedance state that provides unidirectional low-

resistance against knee extension, with a simultaneous high-resistance to knee flexion, appropriate for the swing-extension phase of walking. The amount of resistance within each gear state is determined by the transmission ratio of each gear state and the PWM duty cycle of passive motor switching (discussed in Section 3.2). With this unique actuator, the ECT is able to provide strictly-passive functionality similar to a commercial MPK.

3.2 Passive Motor Control

The torque control laws for stance and swing behavior discussed in the previous sections are implemented in the motor with a passive control approach, where the motor leads are shorted via a PWM control signal, such that the battery cannot provide power to the motor. Even though the battery cannot power the motor in this passive mode of control, the motor is connected to the battery through a set of diodes, such that the motor can regenerate power to the battery during passive operation. Since damping behavior is not emulated like in traditional impedance control approaches, the implementation also guarantees control stability. Note that commanding an impedance greater than the short-circuit limit would require consumption of electric power to sink mechanical power (referred to as plugging reverse current braking) which is not possible with the passive motor control approach. A benefit of this limitation is that energy regeneration is guaranteed, potentially reducing the energy demand of the device. This passive motor control approach is described in detail in [55].

3.3 Model-Based Impedance Control

Using model-based control, the control system compensates for the intrinsic friction and commands an appropriate motor current to achieve the desired passive output torque. To accurately provide the knee joint torque desired by the control system, the mechanical impedance of the actuator was modeled. The intrinsic impedance results from a combination of friction from bearings, gears, and the leadscrew. The intrinsic impedance is a function of the knee angle (i.e. the transmission ratio is a function of knee angle), actuator speed (i.e. increasing actuator speed increases drivetrain losses), and motor current (i.e. increasing motor torque also increases the load on the leadscrew, which increases friction). The torque control laws described in Sections 2.3 through 2.5 each command a motor torque based on the desired output torque and the system impedance, which is governed by the equation:

$$\tau_{cmd} = \tau_{des} - \tau_F(\theta_k, \omega_A, i) \tag{III-5}$$

where τ_{cmd} is the torque commanded to the motor, τ_{des} is the desired knee torque as calculated by the torque control law (from Table II-1), and τ_F is the torque from the modeled mechanical impedance, which is a function of knee joint angle (θ_k), actuator velocity (ω_A), and motor current (i).

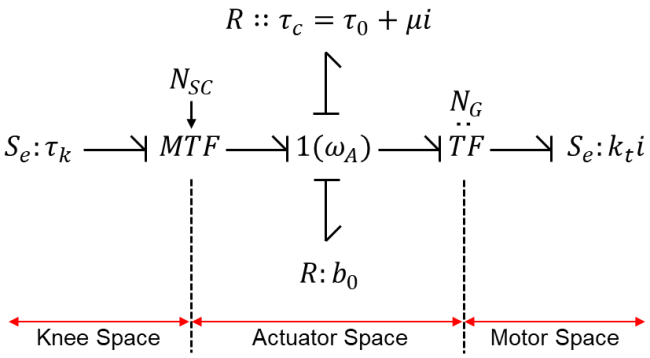

Fig. III-5: Bond graph of impedance model with all impedance terms reflected into the actuator space. With passive motor control, power from an externally-imposed torque (τ_k) flows from the knee joint through the slider-crank transmission (N_{SC}) into the actuator space, where is it dissipated by the combined effects of bearing friction ($b_0\omega_A$), Coulomb friction (τ_C) and motor torque ($N_g k_t i$). Note that Coulomb friction is amplified by motor currents induced by passive motor control due to the lead screw in the drivetrain.

Fig. III-5 shows the bond graph of the impedance model used to estimate system impedance from a set of measured torque-speed relationships. The bond graph is separated into three sections: (1) knee space, which represents the power at the knee joint; (2) actuator space, which represents the power at the output of the planetary transmission (where the transmission mates with the lead screw); and (3) motor space, which represents the power at the motor. For calculating intrinsic friction, effects of inertia were ignored (torque-speed measurement experiments had low accelerations to mitigate the effects of inertia). In the bond graph, τ_k is an externally-imposed knee torque, N_{SC} is the slider-crank transmission ratio, N_G is the planetary gear transmission ratio, ω_A is the actuator angular velocity, k_t is the motor torque constant, i is the motor current, b_0 is the bearing viscous friction, τ_C is the total Coulomb friction torque, τ_0 is the minimum Coulomb friction torque, and μ is the coefficient of additional Coulomb friction torque. The product μi represents an increase in Coulomb friction on the leadscrew due to an increase in motor torque. With passive motor control, power flows in the bond graph such that an externally-imposed torque is dissipated by the combined torques from viscous and Coulomb friction and motor torque, as represented in the equation:

$$\tau_k / N_{SC} = b_0\omega_A + \tau_0 + \mu i + N_G k_t i \qquad \text{(III-6)}$$

The values of τ_k, ω_A, N_{SC}, N_G, and i are known, either a priori or via measurement with onboard sensing. The values of b_0, τ_0, and μ were estimated using linear regression analysis, and their values are reported in Table III-3 for the high and low gears. The resultant model provides accurate estimation of mechanical impedance for any measured motor speed and current.

Table III-3
Impedance Model Experimental Parameter Values

Impedance Parameters		High-gear	Low-gear	Units
Viscous friction coefficient	b_0	9.5	2.2	mN·m·s/rad
Min. Coulomb friction	τ_0	47	33	mN·m
Additional Coulomb friction	μ	275	60	mN·m/A

Fig. III-6 shows a block diagram of the model-based control system. The FSM sends a desired torque (τ_{des}) to the mechanical impedance model, which compensates for the instantaneous mechanical impedance (τ_F) and sends the commanded torque (τ_{cmd}) to the motor damping model. Based upon the current actuator velocity and commanded torque, a model-based feedforward duty cycle (DC_{FF}) is sent to the motor bridge. Additionally, a model-based desired motor current (i_d) is sent to a PI controller, which measures the error between desired current and actual current, and provides a feedback duty cycle (DC_{FB}) to the motor bridge, increasing the accuracy of the control system. The motor then delivers a damping torque (τ_k) to the load (in this case, the knee joint). Such a control scheme allows the ECT to demonstrate the effects of using precise damping at the knee joint, which has implications for the mechanical energy dissipation discussed in Section 5.3.

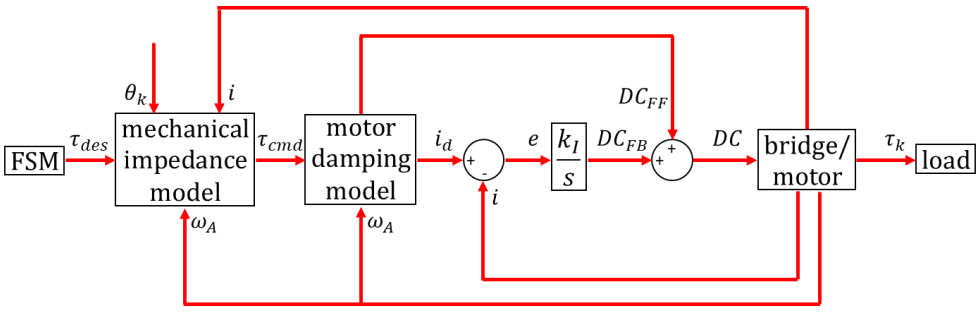

Fig. III-6: Block diagram of model-based control system. The FSM sends a torque command to the mechanical impedance model. The mechanical impedance model compensates for friction and sends a torque command to the motor damping model. The motor damping model measures the instantaneous motor speed and commands a desired motor current and a feed-forward duty cycle to the motor bridge. The result is a precise passive output torque at the knee joint.

4. Experimental Assessment

An experimental assessment was performed to investigate: 1) the ability of the prosthesis and control system to provide strictly-passive functionality essentially identical to a state-of-the-art daily-use MPK; 2) the kinetic energy dissipated by the knee joint during ballistic swing; and 3) the ability of the control system to seamlessly transition between the aforementioned activities. The experimental assessments consisted of three tests: 1) treadmill walking on level-ground and ramps; 2) down-stairs walking on an 8-step staircase; and 3) walking in an over-ground circuit with level-ground, ramps, stairs, and sitting/standing. The assessments were conducted on a single subject with transfemoral amputation – a 62-year old male, weighing 85 kg, who used an Ottobock C-Leg 4 as his daily-use prosthesis. In experiments (1) and (2), the subject first conducted the protocol wearing his daily-use MPK, then followed the same protocol wearing the ECT knee, using the same socket and prosthetic foot (a Fillauer Allpro). Kinematic data were recorded via a motion capture system (Vicon), and ground reaction forces were recorded via force plates integrated into a Bertec instrumented treadmill for experiment (1). Data used by the embedded system to implement the control tasks was also collected and is presented when appropriate.

Experiment (1) had three treadmill walking conditions: 1) level walking at nine treadmill speeds between 0.4 and 1.2 m/s; 2) upslope walking at a slope of 8 deg at three treadmill speeds between 0.5 and 0.7 m/s; and 3) downslope walking at a slope of -8 deg at three treadmill speeds between 0.5 and 0.7 m/s. In the level-ground walking trial, speeds were ramped up from 0.4 to 1.2 m/s, incrementing by 0.2 m/s, then speeds were ramped down from 1.1 to 0.5 m/s, decrementing by 0.2 m/s. The subject was allowed to reach steady-state before motion capture data were recorded, and 15 strides of steady-state walking were recorded for each walking speed. In the up-slope and down-slope trials, speeds were ramped up from 0.5 to 0.7 m/s at 0.1 m/s increments, and data were recorded in the same manner as level-ground trials.

Experiment (2) involved descending an eight-step staircase five times using a step-over gait. Each step was 17 cm (6.5 in) high. The subject was considered to be in steady-state on each step except for the first and last steps, resulting in a total of 15 strides per device. The subject was allowed to use the staircase handrails for balance.

In experiment (3), the subject completed a single loop through a circuit that included level-ground, turns, ramps, stairs, and sitting into a chair. Knee angle and controller state data were recorded using the embedded system. This circuit was only completed once to demonstrate the ability of the control system to adapt to a variety of ambulation conditions, rather than to evaluate the biomechanical efficacy of the controller (which is demonstrated with experiments (1) and (2)). The experimental protocol was approved

by the Vanderbilt Institutional Review Board. The experimental participant provided written informed consent before his participation as required by the approved protocol.

To better control the comparison of energetically-passive behaviors between the ECT and the subject's MPK, the ECT was fitted with the same prosthetic foot, shell, and shoe as the subject's MPK. Prosthesis alignment of the ECT was completed by the same prosthetist who fitted the subject with his daily-use prosthesis. In this manner, if the ECT is able to provide modulated-passive behavior comparable to a commercial MPK, there should be little to no variance in the subject's gait patterns. Total masses of the ECT and subject's MPK, including prosthetic foot, shell, and shoe, were 3.50 kg and 3.25 kg, respectively.

The finite state machine controller was implemented on a laptop using MATLAB Simulink Realtime and communicated with the onboard embedded system via CAN. Controller gains were selected through an iterative process to achieve three kinetic and kinematic goals: (1) tuning of C_1 to provide the same resistance as the subject's MPK, as determined by feedback from the subject; (2) tuning of C_2 to produce a peak-flexion knee angle that is equal to the peak-flexion knee angle of the subject's MPK at 1.2 m/s (to provide an equivalent comparison of cadence-adaptive behavior); and (3) tuning of $C_{3\alpha}$ and $C_{3\beta}$ to produce terminal impact velocities that were approximately equal for walking speeds between 0.4 and 1.2 m/s. It should be noted that the values of $C_{3\alpha}$ and $C_{3\beta}$ were selected to ensure that θ_k^{TS} did not exceed 35° at 1.2 m/s, which would reduce the maximum swing-extension velocities, as discussed in Appendix A. There was no iterative tuning of $C_{3\gamma}$ as this value was chosen before subject testing to produce a torque-angle profile that did not increase more quickly than could be achieved without creating overshoot in the current tracking. Controller gains and their respective units are listed in Table III-4.

Table III-4
Unified Passive Control System Parameters

	Parameter Symbol and Name	Value	Units
C_1	Stance-phase damping coefficient	15	N·m·s^2
C_2	Swing-flexion phase damping coefficient	0.83	kg·m^2
$C_{3\alpha}$	Minimum terminal-swing initiation angle	10	deg
$C_{3\beta}$	Incremental terminal-swing initiation angle	0.3	s
$C_{3\gamma}$	Terminal-swing damping decay constant	10	deg

5. Results

The ability of the ECT and controller to provide walking functionality in a variety of activities was assessed by characterizing the knee joint biomechanics (e.g. joint angles and energy dissipation) and comparing these data to the knee joint biomechanics of a commercial MPK and control data from [53]. Fig. III-7 shows comparisons of knee angle as a function of stride between the ECT and the subject's daily-use MPK in steady-state walking experiments (level-ground, up-slope, down-slope, and down-stairs). Fig. III-8 shows the peak-flexion knee angle of the ECT, commercial MPK, and control data, where the peak-flexion knee angle is calculated as the maximum value of knee angle during the swing-phase. Fig. III-9 shows the terminal-impact knee velocity of the ECT for all treadmill activities and walking speeds, where the terminal-impact knee velocity is the knee joint angular velocity before full-extension and is calculated as the knee velocity in terminal-swing when the knee angle is approximately 2° flexion. All motion capture data were parsed from foot-strike to foot-strike and normalized to percent stride, where foot-strike was identified from treadmill force plate data or foot position/velocity data (for down-stairs walking). Fig. III-7 shows 15-stride average for each walking speed. Box-and-whisker plots show mean and standard deviation for each walking speed. Fig. III-11 shows the energy dissipated during swing-phase, as calculated by the embedded system. Embedded system data were parsed similar to motion capture data, where foot-strike was identified from load cell data. Energy dissipation was calculated as the time integral of knee power, where knee power is the product of knee torque and velocity. Fig. III-11(b) accounts for terminal-impact energy, which is calculated as the product of the rotational inertia of the lower-limb about the knee joint and the squared terminal-impact velocity. Knee velocity was measured with the motor's incrimental encoder, and knee torque was calculated from equation (III-6), using the embedded system measurements of motor velocity and motor current. Fig. III-12 shows the results of the overground walking circuit, showing (a) knee angle and (b) FSM controller state for the whole trial, as recorded by the embedded system. For all data shown, plots in blue are of the ECT, plots in red are of the subject's daily-use MPK, and shaded grey areas are control data from [53].

5.1 Comparison of Walking Kinematics

During level-ground, up-slope, and down-slope treadmill walking, as well as down-stairs walking, the stance and swing phase kinematics are highly similar between the ECT and MPK across activities and speeds, which was one of the design goals. Fig. III-7 shows the knee angle of the ECT and MPK as a

function of stride for a range of walking speeds during level-ground, up-slope, down-slope, and down-stairs walking.

For level-ground and up-slope walking on both prosthetic knees, the knee joint remained extended during the stance-phase and flexed to an angle between 40 and 70 degrees in the swing-phase, depending on walking speed. The swing-phase trajectory of each prosthetic knee has a bell shape of similar duration for each walking speed on level and sloped ground. Because stride times and stance times are similar between prostheses, swing-phase is initiated by the subject at approximately the same time and follows similar spatial-temporal trajectories. Swing-extension occurs at approximately the same time and speed for both prostheses, reaching full-extension at approximately the same percent stride, regardless of prosthesis or walking speed.

Fig. III-8 shows the peak-flexion knee angle of both prostheses across walking speeds during level-ground walking, along with corresponding data from healthy subjects. As shown in the figure, between 0.8 and 1.2 m/s, the peak-flexion knee angles were similar between prosthetic knees; at walking speeds below 0.8 m/s, however, the peak-flexion knee angles of the ECT deviate less from the healthy data, relative to the MPK. For up-slope walking, the ECT exhibited slightly higher peak-flexion knee angles than the MPK, similar to the values in level-ground walking for each walking speed (about 55 degrees).

During down-slope and down-stairs walking, both prosthetic knees showed similar knee trajectories for stance and swing phases. During the stance-phase, the knee joint yielded from heel-strike to toe-off, supporting the subject's weight as the center-of-mass progresses forward and downward. The knee joint flexed to approximately 55 degrees (down-slope) or 75 degrees (down-stairs) during stance-phase for all walking speeds and both activities for both prosthetic knees. The subject initiated swing-phase by swinging the prosthetic thigh forward, lifting the prosthetic foot from the ground. Inertial coupling from thigh acceleration and gravity caused the knee joint to extend. For down-slope and down-stairs walking with both prosthetic knees, the swing-phase had approximately the same spatial-temporal characteristics across all walking speeds.

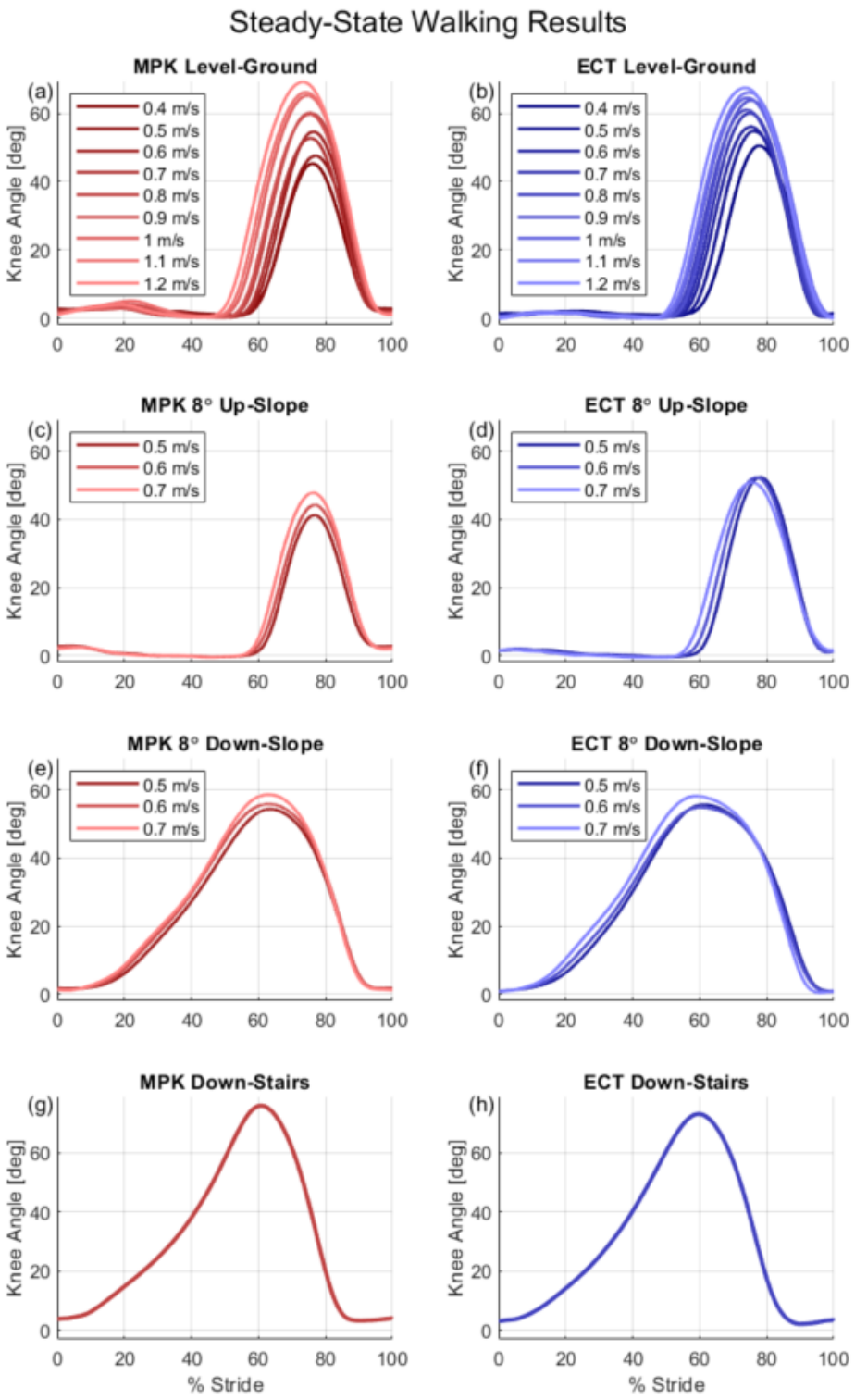

Fig. III-7: Steady-state walking results showing 15-stride average knee angle of (a) commercial MPK and (b) ECT in level-ground walking at walking speeds between 0.4 to 1.2 m/s; (c) commercial MPK and (d) ECT in up-slope walking on an 8-degree ramp at walking speeds between 0.5 to 0.7 m/s; (e) commercial MPK and (f) ECT in down-slope walking on an 8-degree ramp at walking speeds between 0.5 to 0.7 m/s; and (g) commercial MPK and (h) ECT in down-stairs walking on an 8-step staircase with 17cm risers.

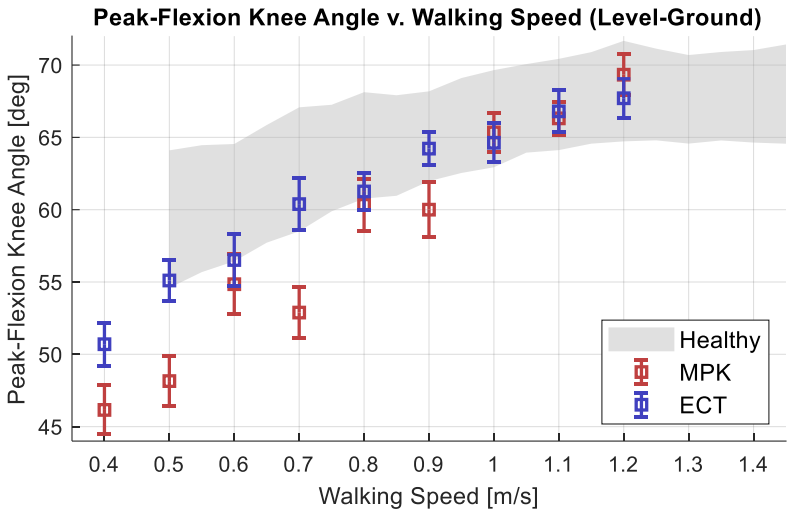

Fig. III-8: Peak-flexion knee angle v. walking speed, comparing ECT (blue) to a commercial MPK (red) and control data from healthy subjects (shaded gray) [53]. Box-and-whisker plots indicate 15-stride mean and standard deviation of the maximum swing-flexion knee angle for each walking speed. Both prostheses show a trend of increasing peak-flexion knee angle with increasing walking speed. The commercial MPK shows more deviation from control data at walking speeds below 0.8 m/s.

5.2 Terminal Impact Velocity

The swing-extension control law was formulated to produce a resistive torque profile that maintained a constant terminal impact velocity across a range of walking speeds and activities. Fig. III-9 shows the terminal-impact knee velocity as a function of walking speed for level-ground, up-slope, and down-slope walking. During level-ground walking, Fig. III-9(a) shows a monotonic increase in terminal-impact velocity with increasing walking speed, which was not the expected result from the control system derivation. During up-slope walking, Fig. III-9(b) shows that the terminal-impact knee velocity is slower than the equivalent walking speed in level-ground walking. Because swing-extension resistance is determined from the walking speed estimation, the reduced terminal-impact velocity is a result of decreased inertial torques on the prosthesis in up-slope walking relative to level-ground walking. However, the reduction in velocity is not so extreme as to prevent the control system from providing a desirable swing-extension behavior (i.e. full-extension in a timely manner). During down-slope walking, Fig. III-9(c) shows a consistent terminal-impact velocity with increasing walking speed, indicating the ability of the swing-extension torque control law to provide consistent swing-extension behavior when descending slopes.

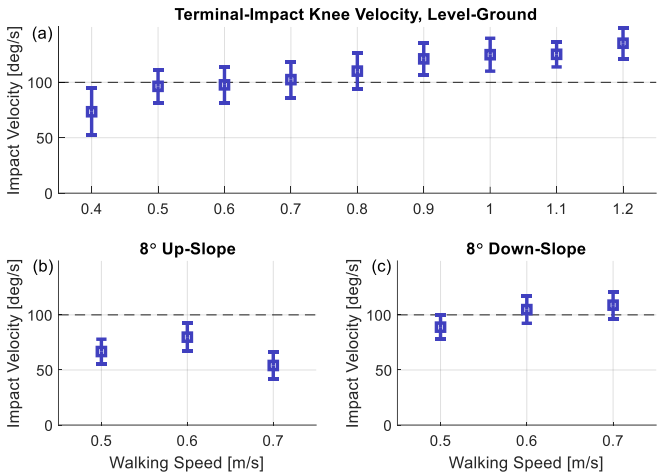

Fig. III-9: Terminal-impact knee velocity during steady-state walking. Experimental results show 15-stride mean and standard deviation of terminal-impact knee velocity of ECT in three activities at variable walking speeds: (a) level-ground walking at walking speeds between 0.4 to 1.2 m/s, (b) up-slope walking on an 8-degree ramp at walking speeds between 0.5 to 0.7 m/s, and (c) down-slope walking on an 8-degree ramp at walking speeds between 0.5 to 0.7 m/s. Horizontal dashed black line at 100 deg/s serves as a visual metric of variability between activities and walking speeds.

5.3 Swing-Phase Energy Dissipation

The ballistic swing control laws in Table III-1 were formualted to dissipate an amount of energy appropriate for the estimated walking speed in both swing-flexion and swing-extension while achieving the kinematic goals oulined in Sections 2.4 and 2.5. Fig. III-11 shows the energy dissipated during swing-phase, as calculated by the embedded system using equation (III-6), and for swing-extension, by adding the terminal impact energy (which is a function of terminal impact veloicty from Fig. III-9). Energy dissipation is linearly proportional to walking speed for both swing-flexion and swing-extension, regardless of the value of C_2. As shown in Fig. III-10, variability in C_2 creates variablility in peak-flexion knee angle as a function of walking speed, where increasing the knee joint resistance decreases the peak-flexion knee angle, and decreasing the knee joint resistance increases the peak-flexion knee angle. This kinematic change has an energetic consequence, where decreasing the peak-flexion knee angle increases the swing-flexion energy dissipation, and increasing the peak-flexion knee angle decreases the swing-flexion energy dissipation. This change in kinetic energy dissipation is related to the change in potential energy stored by gravity. For each walking speed, there is an "energy budget" of lower-limb kineitc energy that must be stored as potential energy or dissipated by the knee joint. In swing-extension, varying C_2, and by consequence varying peak-flexion knee angle, does not affect energy dissipation because most energy is dissipated by the control system in terminal-swing, when knee angles are less than 30 degrees.

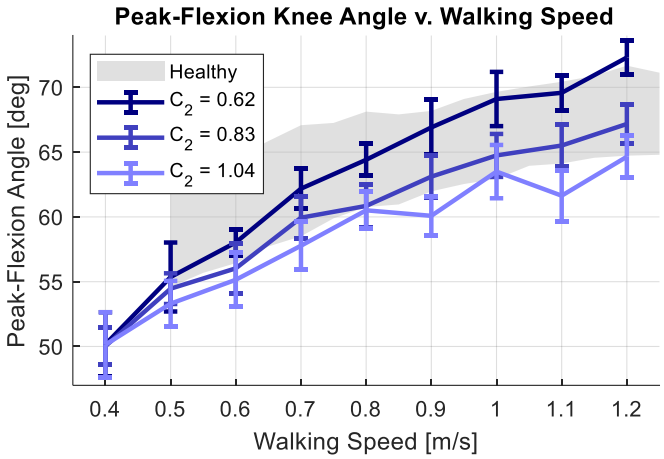

Fig. III-10: Peak-flexion knee angle v. walking speed, comparing three variations of swing-flexion damping coefficient (C_2). Box-and-whisker plots indicate 15-stride mean and standard deviation of the maximum swing-flexion knee angle for each walking speed. As walking speed increases, increasing C_2 decreases peak-flexion knee angle, and decreasing C_2 increases peak-flexion knee angle.

Prosthesis energy dissipation has many similarities to data from [53] (see Fig. III-4). The prosthetis data in Fig. III-11, when overlaid on healthy data, demonstrates similitude except for the slowest walking speeds during swing-flexion. For these cases, the peak-flexion knee angle is less than healthy data, which means that energy normally stored by gravity during swing-flexion was dissipated by knee joint impedance.

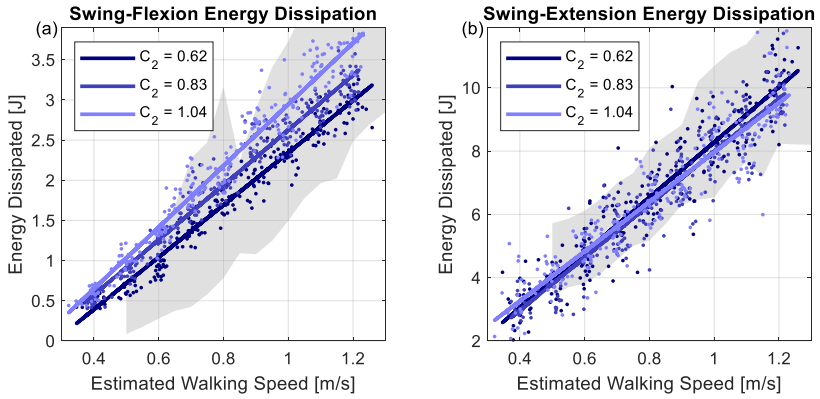

Fig. III-11: Swing-phase energy dissipation v. estimated walking speed in (a) swing-flexion and (b) swing-extension for the three different values of C_2. Shaded grey region indicates healthy subject data from Fig. III-4, scaled by the subject's mass. Energy dissipated is linearly-proportional to walking speed, as discussed in Appendix B. Varying C_2 affects energy dissipation in swing-flexion, but not in swing-extension. In swing-flexion, increased knee joint resistance decreases the peak-flexion knee angle, which reduces the amount of energy stored by gravity. By consequence, more energy is dissipated by knee torque. In swing-extension, varying C_2, and by consequence varying peak-flexion knee angle, does not affect energy dissipation because most energy is dissipated in terminal-swing. For all values of C_2, the energy dissipated in swing-flexion at slow walking speeds is higher than healthy data due to the reduced peak-flexion angles relative to healthy data (i.e. energy that is normally stored as potential energy was dissipated by joint impedance).

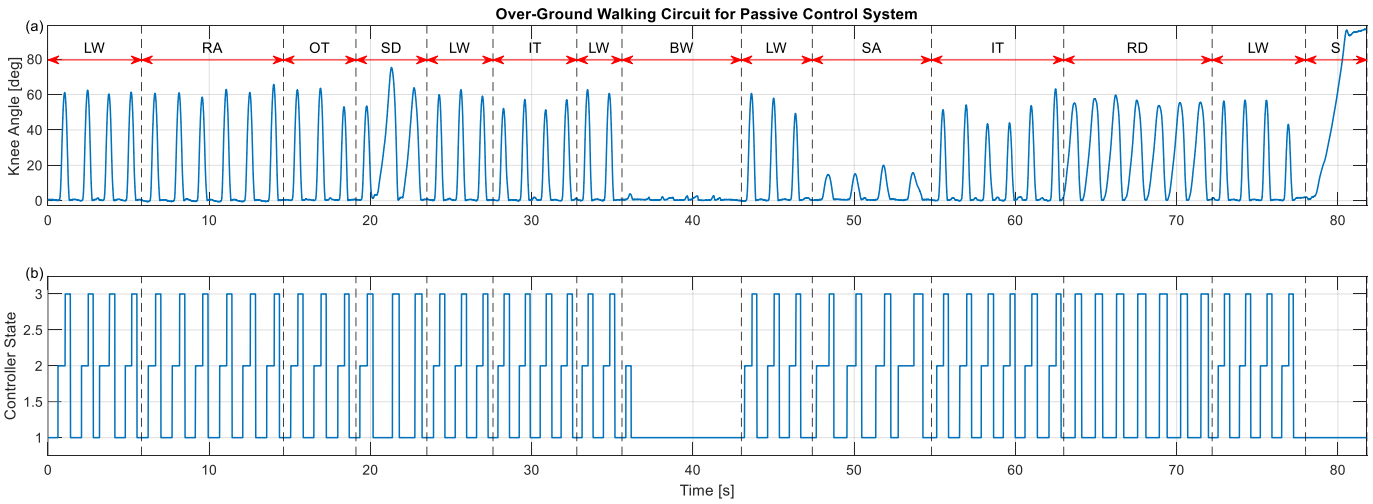

Fig. III-12: Results of over-ground walking circuit showing (a) knee angle and (b) FSM controller state for the entire circuit. For LW, RA, IT, and OT, FSM state-flow is 1-2-3. For RD and SD, FSM state-flow is 1-3. LW = level walking; RA = ramp ascent; RD = ramp descent; SA = stair ascent; SD = stair descent; IT = inside turn; OT = outside turn; S = stand-to-sit. FSM state 1 = stance; FSM state 2 = swing-flexion; FSM state 3 = swing-extension.

5.4 Overground Walking Circuit

Fig. III-12 shows the results of the over-ground walking circuit, where the subject walked with the ECT in a variety of ambulatory conditions using only the passive control system. The figure shows both knee angle and controller state as a function of time to demonstrate the state-flow of the FSM for a variety of ambulatory conditions and the corresponding motion of the knee joint in these conditions. From the figure, the subject began walking on level ground, walked up a ramp, made an outside turn at the top of the ramp, walked down stairs using the knee yielding technique, walked on level ground, made an inside turn, walked on level ground back to the stairs, walked upstairs using the step-to technique, made an inside turn at the top of the stairs, walked down a ramp using the knee-yielding technique, walked on level ground, and sat down. No hesitation nor special movement was required between activities, suggesting that the FSM transition conditions provided for automatic transitions based upon how the user moved the prosthesis. In both stair ascent and descent, the subject used a handrail to assist with balance, as is common for individuals with TFA. The prosthesis has decreased peak-flexion angles for both inside-turns and outside-turns, as consequence of the reduced walking speed when turning. When descending ramps and stairs, the FSM state-flow is 1-3, as low-impedance swing-flexion is not necessary for descent using the knee-yielding technique. To transition to down-slope or down-stairs requires the same user motion as required by the C-leg to utilize stance yielding. When ascending stairs, conditions are met to switch into

FSM state 2. Although it is not necessary to provide a low-impedance swing-phase for step-to stair ascent, there is no detriment to providing this behavior. In all other activities, the FSM state-flow is 1-2-3.

6. Discussion

6.1 Adaptability of Control System

The proposed control system contains only three states, each with distinct constitutive behaviors for the stance, swing-flexion, and swing-extension phases of gait. With no switching between ambulatory controller modes (e.g. separate state machines for level-ground, up-slope, down-slope, up-stairs, and down-stairs walking), the control complexity is greatly reduced. This reduced complexity results in a simpler prosthesis behavior that the user can intuitively learn and adapt to the desired ambulation activity.

In all three states, torque control is provided without designating a desired knee trajectory. Instead, gait phase appropriate resistive torques are provided. In the stance-phase, the prosthesis provides a single constitutive behavior that resists knee-flexion, enabling the user to initiate knee-yielding and adapt the progression of knee-yielding with inputs from the residual thigh. In late-stance, the user is able to switch into the low-impedance swing-phase mode similar to how commercial MPKs switch into their low-impedance swing-phase modes: by walking forward on the prosthesis. By not commanding a swing-phase trajectory, the user is able to initiate swing-phase by thigh inputs alone. And by providing a cadence-appropriate resistive torque, the user does not have to adopt compensatory actions, reducing the cognitive load of walking. The generalized behavior of the torque control laws does not require recognition of specific activities, enabling the three-state FSM to operate in a variety of activities (Fig. III-12), without volitional cues, and able to immediately adapt to these changing activities in a single stride.

6.2 Stance-Phase Controller

In this manuscript, the authors suggested a turbulent damping torque-speed behavior for stance-phase as to provide a controlled comparison between stance knee-yielding behaviors of the ECT and commercial MPK. As a result, the constitutive behavior of the ECT and MPK are similar in all activities at all walking speeds. During level-ground and up-slope walking, the knee joint remains straight with both prostheses (Fig. III-7), illustrating that the prosthesis does not require fine-tuning of knee joint damping to provide desirable kinematic outcomes. In down-slope walking, both prostheses provide knee-yielding behaviors with similar knee kinematics (Fig. III-7), and the results of the over-ground circuit show the

ability of the ECT to provide stance-phase support in stair ambulation (Fig. III-12). These data demonstrate the ability of the ECT to provide strictly-passive stance-phase behavior for a variety of ambulatory activities using a single FSM state and an invariant torque control law. While turbulent damping provided desirable results, controlling stance-yielding electronically allows the control system designer to command any torque-speed relationship that is within the achievable range of strictly-passive motor braking. It is possible that a different generalized stance-yielding behavior could provide better results, yet retain the benefits of providing a single constitutive behavior that the user can easily learn and adapt to a wide range of activities.

6.3 Swing-Phase Controller

The ECT achieves ballistic swing-phase with desirable kinematics in all ambulatory activities and at all walking speeds. In some cases, the ECT achieves a more biomimetic swing-phase motion, such as slow walking speeds on level-ground and all walking speeds up-slope (Fig. III-7). These data demonstrate the ability of the relatively-simple FSM and torque control laws to provide desirable swing-phase behavior across a number of ambulation activities and walking speeds.

The swing-extension torque control law is able to provide rapid extension of the knee joint and cadence-adaptive energy dissipation, which results in biomimetic swing-extension kinematics and energetics. The swing-flexion torque control law is able to provide biomimetic phasing and amplitude of peak-flexion for intermediate and fast walking speeds, which results in biomimetic swing-flexion kinematics and energetics. However, at slower walking speeds, the validity of the swing-flexion torque control law derivation begins to break down, as marked by decreased knee flexion (Fig. III-8). It is likely that a torque control law that provides resistive torques is not appropriate for these slower walking speeds. Although the ECT provides a more biomimetic swing-phase than the commercial MPK at slow walking speeds, the energetically-passive control system provides a less biomimetic swing-phase than has been previously demonstrated on a low-impedance knee prosthesis with swing-assistance [26]. Because the ECT is actuated with an electric motor, and has previously been shown to be capable of active swing-phase behaviors [56], it is possible to switch swing-flexion control strategies from a resistive to an assistive torque at slower walking speeds. This assistive torque can be used to restore biomimetic swing-phase at slower walking speeds without sacrificing the benefits of energetically-passive swing-flexion behavior at faster walking speeds. This approach has the potential to preserve ballistic swing-phase and provide more desirable kinematic outcomes.

In addition to proposing a viable passive swing-phase control system, this investigation quantifies the linear relationship between knee joint energy dissipation and walking speed. In ballistic walking, each walking speed has an associated "kinetic energy budget" for swing-flexion and swing-extension, one that must be dissipated while achieving the kinematic goals of swing-phase (i.e. correct phasing and amplitude of peak-flexion). Because the walking speed can be accurately measured during the stance-phase, this information, combined with a priori information about the linear relationship between walking speed and the kinetic energy budget, can inform the swing-phase torque control law on an appropriate behavior. A special consideration demonstrated in Section 5.3 is that increases/decreases in peak-flexion knee angle at a specific walking speed is associated with decreases/increases in energy dissipation, due to increases/decreases in kinetic energy being stored as potential energy by gravity. This information is valuable for future investigations of ballistic swing-phase control systems.

6.4 Hardware Limitations

Restricting motor control to strictly-passive behavior limits the minimum and maximum torque-speed relationship that the prosthetic knee can provide. One limitation seen in this study is the saturation of torque in terminal-swing. Because the swing-extension torque control equations needed to be limited to providing all resistive torque within the angular range of 0 to 35 degrees of flexion, the total energy that could be dissipated was limited to the maximum torque that could be provided over that angular distance. As a result, the prosthesis could not provide the requisite energy dissipation in terminal-swing to maintain a terminal-impact knee velocity (and consequently a terminal-impact energy) that was invariant to walking speed (Fig. III-9). At walking speeds greater than 0.8 m/s, the terminal-impact energy increases with walking speed, indicative that the motor needs to dissipate more torque than physically possible with the current hardware. Future hardware versions should have a higher maximum achievable motor damping without sacrificing the minimum achievable range of passive impedance.

6.5 Limitations of This Assessment

Because this investigation provides biomechanical assessments, it is inherently limited in the power of these assessments by the participation of a single subject. While more subjects would provide greater confidence in the reported outcomes, probable outcomes on additional subjects can be inferred from the similitude between the ECT and commercial MPK. One advantage of designing a control system that is mimetic to a commercial control system is the extrapolation of widespread usability that can be inferred from successful implementation in a single-subject study. Because the proposed energetically-

passive control system is controlled by the user in a similar manner to a commercial MPK, as demonstrated in this work, it is likely that any MPK user will be able to successfully use the proposed control system on an electromechanical MPK that can assume a low-impedance state during late-stance and swing-phase.

7. Conclusion

This chapter describes an energetically-passive control system for a torque-controllable knee prosthesis. The control system uses a three-state finite state machine with resistive torque control laws for the stance, swing-flexion, and swing-extension phases of gait. In the stance-phase, the controller provides a turbulent damping torque, which is adaptive to level-ground, down-slope, and down-stairs walking, as well as stand-to-sit transitions. In the swing-phase, the controller provides a cadence-adaptive linear damping torque based upon the observation that swing-phase energy dissipation is linearly-proportional to walking speed. The demonstrated control system is able to adapt to a variety of activities and walking speeds, providing passive performance similar to a state-of-the-art MPK. The following chapter describes a powered control system that layers powered behaviors onto the passive behaviors demonstrated here, namely to provide powered knee-extension and to facilitate powered swing-phase motion in activities that require it, such as step-over stair ascent and slow walking.

CHAPTER IV

A CONTROL SYSTEM FOR LAYERING POWERED STANCE AND SWING ASSISTANCE ONTO STRICTLY-PASSIVE BEHAVIOR IN A POWERED KNEE PROSTHESIS

Restoration of healthy knee behavior after amputation requires prosthetic knees to provide active and resistive stance behaviors, as well as ballistic and non-ballistic swing behaviors. Current state-of-the-art prosthetic knees are deficient in providing one or more of these behaviors. This chapter describes a novel approach to the design and control of a powered knee prosthesis that provides a sufficiently low impedance to enable a fully ballistic swing-phase, while also providing sufficiently high torque to offer stance-phase knee-extension during activities such as step-over stair ascent. Restoration of active/resistive stance and ballistic/non-ballistic swing is achieved by employing feedback control, as is conventional in powered knee prostheses, but also by widening the range of behaviors achieved via feedback control by employing mechanical reconfiguration of the transmission between the stance and swing phases of gait. As such, the device can operate in one of two behavioral regimes: 1) a low-impedance, low-torque, high-speed regime with characteristics appropriate for either ballistic swing or for powered swing when appropriate; and 2) a relatively higher-impedance, high-torque, and lower-speed regime appropriate for either resistive stance or active stance depending on the gait situation. The rationale behind this design approach is discussed; the control structure is presented; and experiments with a single study participant with a transfemoral amputation are presented that compare the functionality of the resulting design and control approach with that of a conventional passive microprocessor-controlled knee prosthesis.

1. Introduction

Chapter II of this dissertation described the design of a power-capable prosthesis that could also achieve strictly-passive ballistic swing functionality. Chapter III described a control system that enables a wide array of strictly passive functionality, spanning variable-cadence walking, upslope and downslope walking, and stair descent functionality. The present chapter (IV) describes how powered functionality can be layered on top of the passive functionality described in Chapter III to provide functional improvements in several different activities, including in slow walking, slope ascent, and stair ascent. Specifically, this chapter describes a control system that adds three powered states to the previously

described three passive states, wherein the control system operates in the passive states whenever possible, and moves into the powered states when beneficial. The chapter demonstrates the efficacy of this controller on an individual with transfemoral amputation, and demonstrates measurable benefits of the combined passive/powered controller relative to the passive controller demonstration in Chapter III.

2. Design and Control Approach

The design and control approach presented here is based on categorizing knee joint function during mobility activities into four behaviors: resistive stance behavior, active stance behavior, ballistic swing, and non-ballistic swing. The approach is further premised on the assumption that healthy non-perturbed swing-phase is characterized by a ballistic swing motion, and therefore a replacement of that function should be similarly ballistic (i.e., which requires the knee joint to become essentially a free hinge with very low levels of modulated resistance). Finally, the approach assumes that power generation should only be used for 1) activities requiring net knee extension during stance-phase, such as stair ascent and sit-to-stand; and 2) activities requiring non-ballistic swing, such as swing-phase during stair ascent. When not providing power, the prosthesis should remain strictly-passive. In other words, the device should be passive when possible, and powered only when necessary.

For the approach presented here, activities for which the prosthesis should function in either a passive or powered capacity are depicted in Table IV-1, which categorizes each activity into one of the four stance and swing behaviors described above. Active and resistive stance are analogs, wherein the knee joint primarily provides an extensive torque with knee motion either in extension (active stance) or flexion (resistive stance). Ballistic and non-ballistic swing describe the contribution of knee torque to the resultant motion of the lower leg. For ballistic swing, inertial torques (i.e., gravity and thigh acceleration) dominate knee motion, with the knee providing relatively low resistance to control motion; for non-ballistic swing, active knee torque overcomes inertial forces to reposition the lower leg. Note that resistive stance and ballistic swing are behaviors provided by current commercially-available passive MPKs, while active stance and non-ballistic swing are not, since they require net power generation at the knee. Note that the approach taken here therefore requires that the powered prosthesis be capable of operating both as an MPK (i.e., in a strictly-passive mode that spans both very low variable impedance for cadence-adaptive swing-phase, and also high torque and power dissipation for stance knee flexion in stair and slope descent), and also capable of providing power during non-ballistic swing and stance-knee extension.

Various approaches could potentially be employed for the implementation of such behaviors. For the work presented here, a knee design that incorporates a two-speed transmission in combination with both passive and active motor control is employed in order to broaden the range of achievable impedances and torques. The resulting device is able to match (or exceed) the span of passive behaviors, impedances, and torques provided by current MPKs, and is also able to provide power for non-ballistic swing movements, and stance-knee extension, as subsequently shown.

Table IV-1
Generalized Stance and Swing Behaviors of Different Activities

Functional Activity	Stance-Phase Generalized Behavior	Swing-Phase Generalized Behavior
Level-ground walking	Resistive	Ballistic
Up-slope walking	Active	Ballistic
Down-slope walking	Resistive	Ballistic
Up-stairs walking	Active	Non-ballistic
Down-stairs walking	Resistive	Ballistic
Backwards walking	Resistive	Non-ballistic
Slow walking	Resistive	Non-ballistic
Stand-to-sit transition	Resistive	n/a
Sit-to-stand transition	Active	n/a
Stumble recovery	Resistive	Non-ballistic
Obstacle avoidance	n/a	Non-ballistic

Resistive Stance
Knee joint resists flexion

Active Stance
Knee joint actively extends

Ballistic Swing
Inertial torques dominate knee motion

Non-Ballistic Swing
Active knee torque dominates knee motion

3. Activity Control System

3.1 Finite State Machine

The activity controller is a six-state finite state machine (FSM), diagrammed in Fig. IV-1, which provides full passive and powered functionality across a wide range of activities. Each state within the FSM has a unique transmission configuration and a unique torque control law (see Table IV-2), providing either power dissipation (passive motor control) or generalized active and emulated-passive behaviors (active motor control). Within each state, the knee torque is governed by a torque control law based on sensor inputs and control parameters that produce the following behaviors in each corresponding FSM state: (1) high-torque turbulent damping; (2) low-torque cadence-adaptive viscous damping; (3) low-torque unidirectional cadence-adaptive viscous damping that increases as the knee aproaches full extension; (4) low-torque cadence-adaptive flexion torque pulse; (5) high extension torque that scales with residual hip torque and velocity; (6) low-torque PD controller with a virtual linkage between the thigh and knee joint, adapted from [38]. FSM transitions, shown in Table IV-4, are governed by onboard sensing of knee angle (θ_K), shank angle (θ_S), shank axial force (F), shank axial acceleration (a_a), the walking speed

estimation (ω), and a state timer (t). Depending on the activity, the FSM transitions produce different FSM sequences. Table IV-3 shows the FSM sequences for different activities. Note that the FSM provides appropriate resistive or active stance-phase behavior and appropriate ballisitc or non-ballistic swing-phase behavior, depending on the activity.

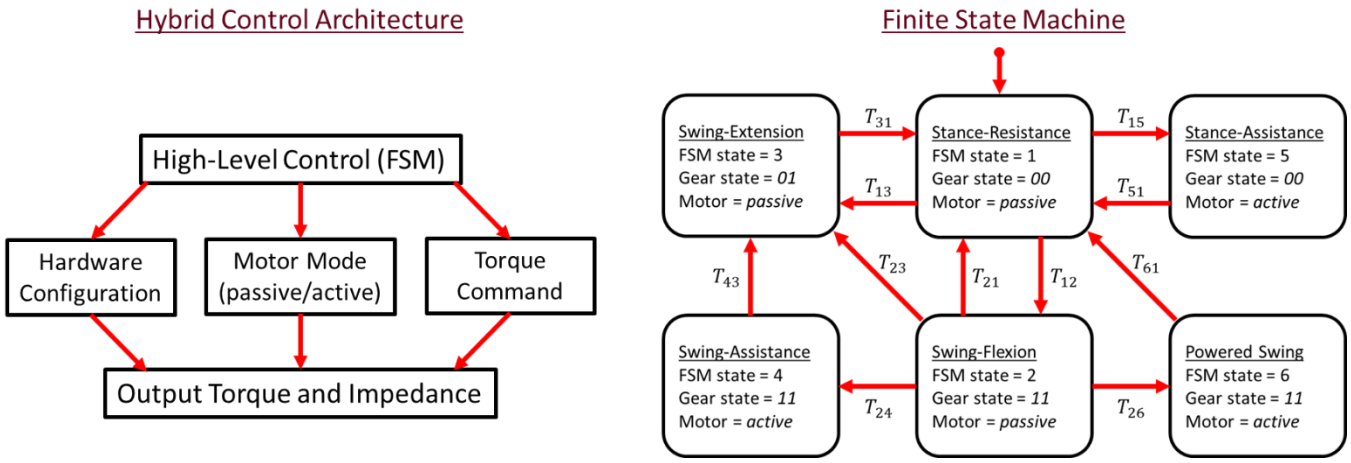

Fig. IV-1: Overview of activity control system. The hybrid control architecture operates by controlling the output torque and impedance via hardware configuration and motor torque commands. Within each state, the motor is commanded to operate passively (i.e., constrained to braking behavior) or actively (i.e., using a standard block-commutation scheme). The finite state machine (FSM) for walking consists of six states and the transitions between them. The FSM diagram indicates the corresponding gear states of the hardware and indicates if the motor is operated actively or strictly passively. Torque control laws within each state are outlined in Table IV-2; transition conditions between states are outlined in Table IV-4.

Table IV-2
Finite State Torque Control Laws

FSM State	Torque Control Law	
1	$\tau_K = f_1(\dot{\theta}_K)$	$\tau_K = C_1\dot{\theta}_K^2$
2	$\tau_K = f_2(\omega, \dot{\theta}_K)$	$\tau_K = C_2[\omega - \omega_0]\dot{\theta}_K$
3	$\tau_K = f_3(\omega, \theta_K, \dot{\theta}_K)$	$\tau_K = b_{max}\left[1 - e^{(\theta_K - C_{3\alpha} - C_{3\beta}\omega)/C_{3\gamma}}\right]\dot{\theta}_K$
4	$\tau_K = f_4(\omega)$	$\tau_K = C_4[1 - \omega/\omega_0]$
5	$\tau_K = f_5(F, \theta_K)$	$\tau_K = C_{5\alpha}F\left[1 - e^{\dot{\theta}_T/C_{5\beta}}\right]\sin\theta_K / [1 - e^{-t/C\_5\gamma}]$
6	$\tau_K = f_6(\theta_K, \dot{\theta}_K, \theta_T)$	$\tau_K = C_{6p}\left[\theta_K - \theta_{EQ}(\theta_T)\right] + C_{6d}\dot{\theta}_K$

Within each FSM state, knee torque is governed by a unique control law based upon a combination of sensor inputs: knee angle (θ_K) and velocity ($\dot{\theta}_K$), thigh angle (θ_T, shank axial force (F), and walking speed estimation (ω). Each torque control law (f_n) has between one and three tunable parameters (C_m). For f_3, b_{max} is a system parameter that indicates the maximum achievable motor braking impedance (i.e., when the motor leads are connected at 100% duty cycle). For f_2 and f_4, ω_0 is a tunable parameter that indicates the crossover walking speed, which is the walking speed where the motor provides neither assistance nor resistance and swing-flexion motion is governed by passive dynamics alone. For f_6, θ_{EQ} is the equilibrium position of the virtual spring, which is a function of the thigh kinematics, as described in [38]. For f_5, t is time as relevant for the filter term.

Table IV-3
Controller Sequences for Different Activities

FSM Sequence	Activities
1	Standing; stand-to-sit; backwards walking
1-2-3	Level-ground and up-slope walking
1-2-4-3	Slow walking (level-ground and up-slope)
1-3	Down-slope and down-stair walking
1-5	Sit-to-stand
1-2-6-1-5	Up-stairs walking

Table IV-4
Finite State Machine Transition Conditions

Transition	Description	Condition
T_{12}	Knee joint is hyperextended, and Prosthesis shank is rotating forward, and Prosthesis shank is inclined forward, and Prosthesis is rapidly unloaded	$\theta_K \approx 0$ $\dot{\theta}_S < \dot{\theta}_{S,th}$ $\theta_S < \theta_{S,th}$ $\dot{F} < \dot{F}_{th}$
T_{23}	Prosthesis is unloaded, and Knee joint is extending	$F \approx 0$ $\dot{\theta}_K > 0$
T_{31}	Knee joint has zero velocity, or Prosthesis is loaded	$\dot{\theta}_K \approx 0$, or $F > F_{th}$
T_{13}	Prosthesis is unloaded, and Knee joint is flexed past threshold	$F \approx 0$ $\theta_K > \theta_{K,th}$
T_{21}	Prosthesis is loaded, and Prosthesis was previously unloaded, or Prosthesis shank rotating backwards, or Prosthesis shank is not inclined forward	$F > F_{th}$, and $F^- \approx 0$, or $\dot{\theta}_S > \dot{\theta}_{S,th}$, or $\theta_S > \theta_{S,th}$
T_{24}	Knee joint begins flexing, and Slow walking speed detected, and Walking speed above threshold	$\theta_K > 0$ $\omega < \omega_0$ $\omega > \omega_{th}$
T_{43}	Prosthesis is unloaded, and Knee joint is extending	$F \approx 0$ $\dot{\theta}_K > 0$
T_{15}	Knee joint is flexed past threshold, and Knee joint is extending	$\theta_K > \theta_{K,th}$ $\dot{\theta}_K < 0$
T_{51}	Knee joint is fully extended, or Knee joint is flexing	$\theta_K \approx 0$, or $\dot{\theta}_K > 0$
T_{26}	Knee joint is hyperextended, and Prosthesis is unloaded, and Shank axial acceleration above threshold	$\theta_K \approx 0$ $F \approx 0$ $a_a > a_{a,th}$
T_{61}	Prosthesis is loaded, or Time in state beyond threshold	$F > F_{th}$, or $t > t_{th}$

Finite state machine transition conditions depend upon measured sensor inputs and several threshold parameters: knee angle ($\theta_{k,th}$), shank angle ($\theta_{S,th}$) and angular velocity ($\dot{\theta}_{S,th}$), shank axial force (F_{th}) and yank ($\dot{F}_{th}$), walking speed estimation (ω_{th}), shank axial acceleration ($a_{a,th}$) and time (t_{th}).

3.2 Resistive and Active Stance

FSM states 1 and 5 provide the necessary mechanical power dissipation and generation during stance-phase to accomplish a variety of activities. Turbulent damping via passive motor control provides knee-yielding akin to a commercial MPK, to provide appropriate knee motion during down-slope and down-stairs walking, as well as stand-to-sit [57]. The novel active stance control law, which uses the motor in active mode, generalizes powered knee extension into a single torque control law that is adaptive across a range of activities that benefit from positive joint power. The control law was developed from observations of the interaction between the biological knee and hip joints during stair ascent. As shown in Fig. IV-2, the torque, velocity, and power of the biological knee joint lag behind those of the hip joint during stair ascent. The torque command in Table IV-2 was designed to input force and motion estimates of the residual hip joint and reproduce the shape and timing of the torque profile of the biological knee joint, but without commanding a desired joint angle, which would otherwise have the prosthesis, rather than the user, control knee motion. During the pull-up phase of stair ascent, the prosthetic ankle constrains

the shank to be approximately vertical; as such, the real-time hip torque is estimated as the product of the load cell force and the sine of the knee angle (see Fig. IV-2(e)). The thigh velocity and knee angle terms in the control law (see Table IV-2) provide for the bell shape of the torque command, and the filtering term provides the phase delay between hip and knee kinetics and kinematics. Ideally, the parameters $C_{5\beta}$ and $C_{5\gamma}$ are invariant between users, providing the torque control law a single parameter ($C_{5\alpha}$) that increases or decreases the magnitude of assistive torque, depending on the user's preference.

The unidirectional high-gear of the ECT enables the prosthesis to provide an extension torque that either passively resists flexion or actively provides extension. Additionally, due to the unidirectional clutch, there is little resistance to user-initiated stance knee-extension (i.e., the user can extend the stance leg via hip musculature without drivetrain resistance). Because the prosthetic foot is frictionally constrained to the ground during stance-phase, the stance leg is a closed kinematic chain, and therefore the prosthesis user has control of knee joint movement during the stance-phase via movement of the hip joint. The user is therefore able to extend the knee joint without power-assistance, albeit with disproportionate hip torque input from the user, as demonstrated in [38]. In the device described here, powered knee extension is activated by the user via hip torque, which initiates a knee extension movement, which in turn is identified by the controller and used to initiate power-assisted knee extension. Because the user is able to volitionally control the activation of powered stance knee-extension, intent recognition algorithms are not necessary for coordinated control; the coordination is inherent because power delivery is solely in reaction to the motion input generated by the user. Additionally, the thigh velocity term in the torque control equation scales torque delivery with estimated thigh power. Just as the biological hip and knee work synergistically to extend the leg when it is in a closed kinetic chain, the prosthetic knee is able to follow motion and force cues from the residual hip (under the user's neuromuscular control) and provide synchronous assistive knee torque. In this manner, the user does not ride the prosthetic knee up the stairs, but rather works with it to extend the leg, similar to the manner in which an electric bicycle coordinates its power delivery with the user's power input. While it is possible to cause controller instability using such a method, since a velocity term is used in the torque control law to add energy, instability is avoided by the combination of making the control law unidirectional, using an exponential decay as a soft saturation on the velocity term, and using the sine of the knee angle to decay the torque as the knee extends. With this control law formulation, if the user stops extending their hip, the user's mass decelerates the knee joint, which reduces the torque and continues the deceleration. When knee velocity inflects, the FSM switches to resistive stance behavior, providing controlled support of the user's weight as the knee flexes.

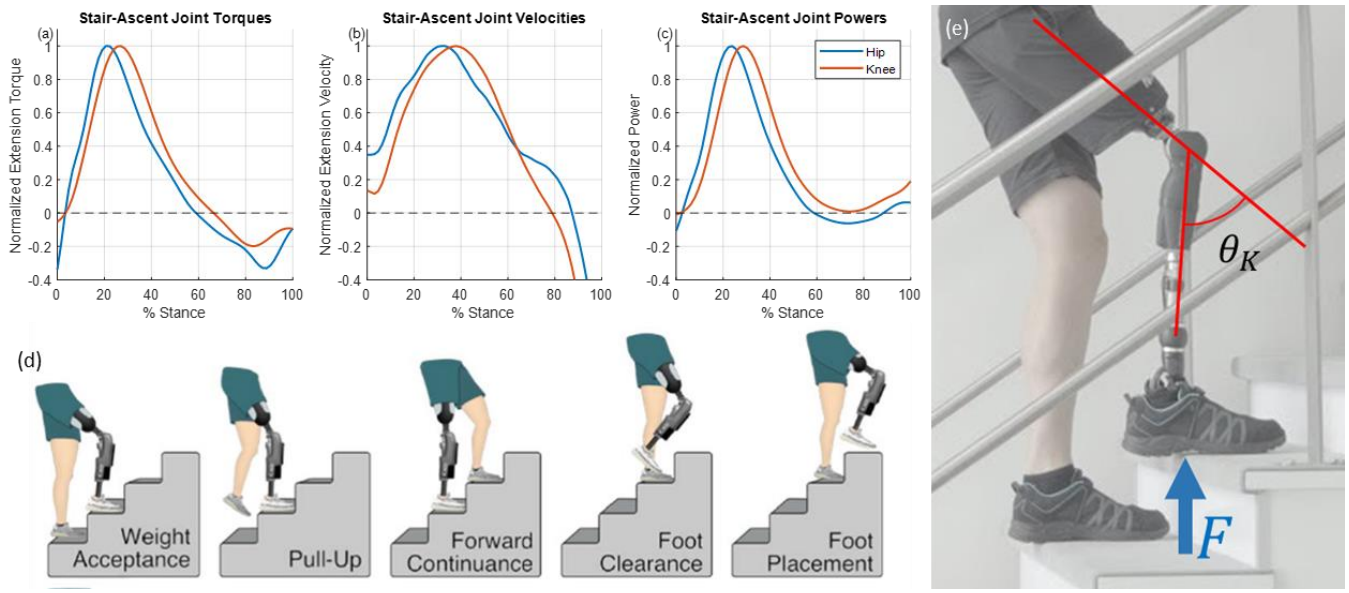

Fig. IV-2: Biomechanical rationale for the active stance control law was based on the stance-phase (a) torque, (b) velocity and (c) power of knee and hip joints during the stance-phase of stair ascent, from [33]. Positive y-axes indicate (a) extension torque, (b) extension velocity, and (c) power generation. Values are normalized to a maximum of unity. These plots demonstrate that the phasing of the knee joint lags the hip joint for most of the stance-phase. (d) The phases of stair-ascent as described in [58], image adapted from [38]. (e) When ascending stairs with a stiff prosthetic foot, the shank is constrained to be approximately vertical. The hip torque can be approximated by onboard sensors as the product of the load cell force (F) and the sine of the knee angle (θ_K). The control system uses this approximation of hip torque to deliver knee torque that is synchronized with the user's motion.

3.3 Ballistic Swing

FSM states 2, 3, and 4 provide walking-speed-adaptive ballistic swing phase behavior (see Fig. IV-3). To estimate walking speed, the shank angular velocity is recorded and averaged from foot contact until the user initiates swing-phase in late-stance. The result is a linear relationship between the value of the average stance-phase shank angular velocity (ω) and the walking speed. As such, ω is a zero-parameter term that measures relative changes in walking speed within a single stride and can be used directly in control equations to provide cadence-adaptive behavior. During swing-flexion, when estimated walking speeds are above the crossover walking speed (i.e., when $\omega > \omega_0$), a damping torque is provided, similar to a commercial MPK. When $\omega < \omega_0$, a feedforward assistive flexion torque is provided, which increases the peak-flexion knee angle to a biomimetic value not achievable with passive dynamics alone. This assistive torque has low amplitude and is provided unidirectionally, without trying to control knee angle directly, which enables a swing-phase motion that is still inertially-coupled (i.e., ballistic swing is preserved because low actuator impedance makes the knee joint receptive to inputs from inertial forces), but with the caveat that the motor is helping the user by "pushing" the lower leg towards flexion.

The magnitude of the swing assistance torque increases linearly with a decrease in walking speed (see Fig. IV-3(a)), which when integrated over the angular range of swing-flexion, which is mostly invarant to walking speed in the biological knee (see Fig. B-4 in Appendix B), provides a predictable linear increase in the mechanical energy of the knee joint during swing-flexion. This linear increase in mechanical energy correlates with the linear decrease in energy dissipated during swing-flexion as walking speed decreases (see Fig. III-4). At the slowest walking speeds, drivetrain impedance dissipates an amount of energy that is linearly proportional to walking speed and greater than the desired amount of energy dissipation (see Fig. III-11). The swing-assistance torque modifies that value by adding an appropriate amount of energy to the knee joint as a function of the walking speed. Effectively, the swing-assistance torque accomplishes impedance compensation indirectly, by compensating for energy dissipation instead.

FSM state 3 provides cadence-adaptive ballistic swing-extension behavior (see Fig. IV-3(c)), which is appropriate for the swing-extension phase of all evaluated walking activities except for stair ascent, which requires non-ballistic swing. For level and up-slope walking, swing-extension behavior is provided immediately after peak-flexion; for down-slope and down-stairs walking, swing-extension behavior is provided when the user lifts the flexed prosthetic knee, allowing inertial and gravitational forces to provide the extensive torque.

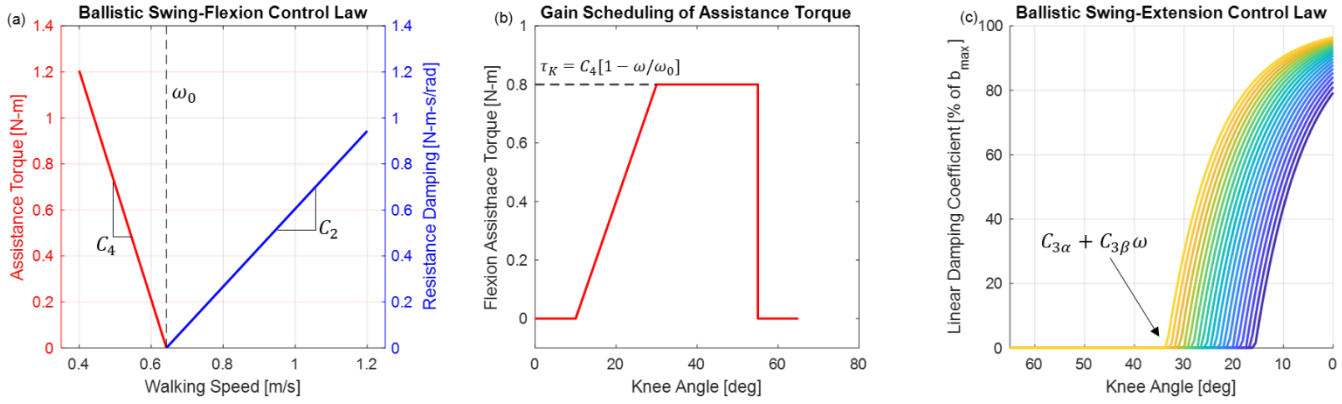

Fig. IV-3: Ballistic swing torque control laws, incorporating both assistive and resistive behaviors. (a) During swing-flexion, for walking speeds below ω_0, an assistive torque is provided; for walking speeds above ω_0, a resistive torque is provided. Both torque control laws are linearly proportional to walking speed, which provides cadence-adaptive behavior. (b) Gain scheduling of swing-flexion assistance torque. After the user has flexed the knee joint past 10 degrees, the assistance torque begins ramping up to the commanded value as a function of knee angle. At 30 degrees of flexion, the assistance torque has reached its commanded value. After 55 degrees of flexion, the commanded torque is zeroed so the knee joint velocity can inflect for swing-extension. (c) The swing-extension torque control law commands a linear damping torque where the linear damping coefficient is a function of the walking speed and the knee angle (walking speeds from slow to fast are graded from blue to yellow). The commanded torque is zero until a predetermined angle that is a function of the walking speed estimation ($C_{3\alpha} + C_{3\beta}\omega$). After this point, the damping coefficient rapidly increases towards the maximum value (b_{max}). An exponential curve serves as a soft saturation of knee damping.

3.4 Non-Ballistic Swing

FSM state 6 provides non-ballistic swing-phase motion appropriate for stair-ascent. The state 6 controller was adapted from [38], albeit with a modification that the FSM must first pass through state 2, ensuring that powered swing is provided as a transition from late-stance similar to other walking conditions. This controller creates a virtual linkage between the thigh and shank, which enables the user to volitionally control the knee joint. To contrast ballistic and non-ballistic swing controllers, the former is controlled through inertial coupling while the latter is controlled through kinematic coupling. Similar control methods have been used by other researchers for obstacle crossing (e.g., [59]).

4. Experimental Assessment

An experimental assessment was performed to investigate: 1) the ability of the prosthesis and control system to provide strictly-passive functionality essentially identical to a state-of-the-art daily-use MPK; 2) the ability of the prosthesis to provide powered functionality for non-ballistic swing and stance-knee extension; and 3) the ability of the control system to seamlessly transition between the aforementioned activities. The experimental assessments consisted of four tests (see Fig. IV-4): 1) treadmill walking on level-ground and ramps; 2) up-stairs and down-stairs walking; 3) sit-to-stand and stand-to-sit transitions; and 4) walking in an over-ground circuit with level-ground, ramps, stairs, and sitting/standing. The assessments were conducted on a single subject with transfemoral amputation – a 62-year old male, weighing 85 kg, who used an Ottobock C-Leg 4 as his daily-use prosthesis. In experiments (1)-(3), the subject first conducted the protocol wearing his daily-use MPK, then followed the same protocol wearing the ECT knee, using the same socket and prosthetic foot (a Fillauer Allpro). Kinematic data were recorded via a motion capture system (Vicon), and ground reaction forces were recorded via force plates integrated into either a Bertec instrumented treadmill for experiment (1), or into the floor (AMTI) for experiment (3). Data used by the embedded system to implement the control tasks was also collected and is presented when appropriate.

Fig. IV-4: Overview of experimental validation. The ECT was evaluated on a subject with transfemoral amputation in several experiments: (a) level-ground, (b) up-slope, and (c) down-slope walking on an instrumented treadmill; (d) upstairs walking; (e) sit-to-stand; and (f) an overground walking circuit with several activities.

Experiment (1) had three treadmill walking conditions: 1) level walking at nine treadmill speeds between 0.4 and 1.2 m/s; 2) upslope walking at a slope of 8 deg at three treadmill speeds between 0.5 and 0.7 m/s; and 3) downslope walking at a slope of -8 deg at three treadmill speeds between 0.5 and 0.7 m/s. In the level-ground walking trial, speeds were ramped up from 0.4 to 1.2 m/s, incrementing by 0.2 m/s, then speeds were ramped down from 1.1 to 0.5 m/s, decrementing by 0.2 m/s. The subject was allowed to reach steady-state before motion capture data were recorded, and 15 strides of steady-state walking were recorded for each walking speed. In the up-slope and down-slope trials, speeds were ramped up from 0.5 to 0.7 m/s at 0.1 m/s increments, and data were recorded in the same manner as level-ground trials.

Experiment (2) involved ascending and descending an eight-step staircase five times using a step-over gait. Each step was 17 cm (6.5 in) high. The subject was considered to be in steady-state on each step except for the first and last steps, resulting in a total of 15 strides per device. The subject was allowed to use the staircase handrails for balance.

Experiment (3) involved standing from and sitting to a chair ten times with each foot placed on separate force plates. The subject did not use his arms to aid standing as to not compromise inverse dynamics. For experiments (1)-(3), the subject rested five minutes between trials, and all data were recorded on the subject's daily-use MPK before the subject was fit with the ECT knee, and repeated the same experimental procedures.

In experiment (4), the subject completed a single loop through a circuit that included level-ground, turns, ramps, stairs, and sitting/standing with a chair. Knee angle and controller state data were recorded

using the embedded system. This circuit was only completed once to demonstrate the ability of the control system to adapt to a variety of ambulation conditions, rather than to evaluate the biomechanical efficacy of the controller (which is demonstrated with experiments (1)-(3)). The experimental protocol was approved by the Vanderbilt Institutional Review Board. The experimental participant provided written informed consent before his participation as required by the approved protocol.

5. Results

This section is organized into four subsections that correspond to the four experiments conducted: 1) treadmill walking on level and sloped ground, 2) stair ascent and descent, 3) sit-to-stand and stand-to-sit transitions, and 4) overground walking with multiple activities. Fig. IV-5 through Fig. IV-7 show data corresponding to experiments (1)-(3) with both the subject's daily-use MPK and the ECT. Specifically, Fig. IV-5 shows the mean knee angle over 15 strides as a function of stride, and corresponding peak-flexion knee angle of peak-flexion as a function of walking speed. Fig. IV-6 shows the fifteen-stride mean values of prosthetic and intact side knee angle, prosthetic side thigh abduction, intact side ankle angle, knee torque, and shank axial load as a function of stride for stair ambulation. Fig. IV-7 shows the mean values across ten sit-to-stand trials of knee angle, knee power, and ground reaction force as a function of time for both the intact and prosthetic sides. Fig. IV-8 shows data corresponding to experiment (4), showing knee angle and controller state for the ECT throughout the walking circuit.

5.1 Treadmill Walking on Level and Sloped Ground

During level and sloped treadmill walking, the stance and swing phase kinematics are highly similar between the ECT and MPK across activities and speeds, which was the design goal. Fig. IV-5(a)-(f) shows the knee angle of the ECT and MPK as a function of stride for a range of walking speeds during level-ground, up-slope, and down-slope walking. For level-ground and up-slope walking on both prosthetic knees, the knee joint remained extended during the stance-phase and flexed to an angle between 40 and 70 degrees in the swing-phase, depending on walking speed. The swing-phase trajectory of each prosthetic knee has a bell shape of similar duration for each walking speed and slope. Fig. IV-5(g) shows the peak-flexion knee angle of both prostheses across walking speeds during level-ground walking, along with corresponding data from healthy subjects. As shown in the figure, between 0.8 and 1.2 m/s, the peak-flexion knee angles were similar between prosthetic knees; at walking speeds below 0.8 m/s, however, the peak-flexion knee angles of the ECT more closely matched the healthy data, relative to the MPK.

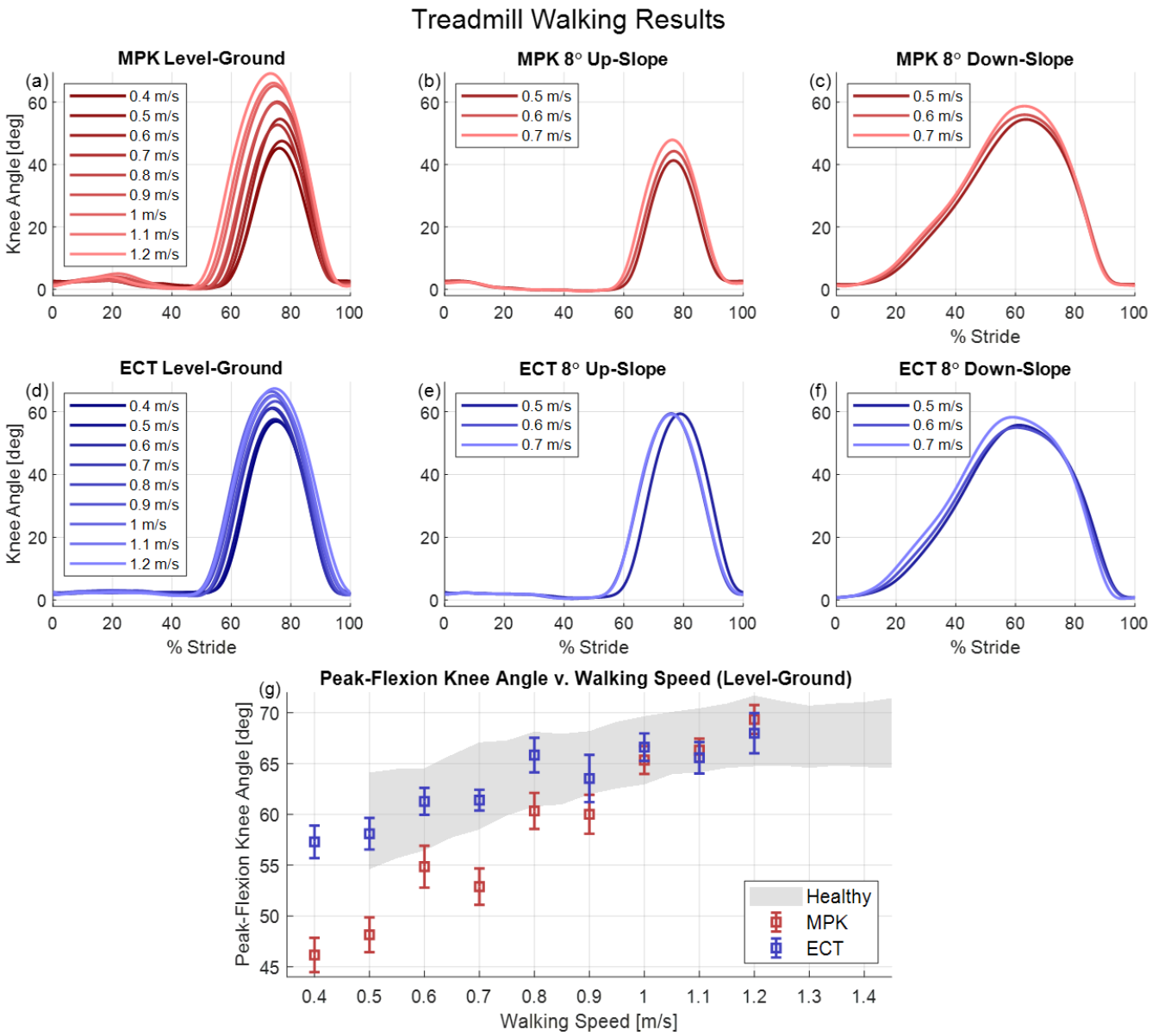

Fig. IV-5: Treadmill walking experimental results, showing 15-stride average knee angle of (a) commercial MPK and (d) ECT in level-ground walking at walking speeds between 0.4 to 1.2 m/s; (b) commercial MPK and (e) ECT in up-slope walking on an 8-degree ramp at walking speeds between 0.5 to 0.7 m/s; and (c) commercial MPK and (f) ECT in down-slope walking on an 8-degree ramp at walking speeds between 0.5 to 0.7 m/s. (g) Peak-flexion knee angle v. walking speed during level-ground walking, comparing ECT (blue) to a commercial MPK (red) and control data from healthy subjects (shaded grey) [53]. Box-and-whisker plots indicate 15-stride mean and standard deviation of the peak swing-flexion knee angle for each walking speed in level-ground walking. Shaded grey areas indicate range of one standard deviation of averaged data from 28 healthy subjects [53]. In plot (g), both prostheses show a trend of increasing peak-flexion knee angle with increasing walking speed. The MPK deviates from healthy data at walking speeds below 0.8 m/s.

For up-slope walking, the ECT exhibited higher peak-flexion knee angles than the MPK, closer to the values in level-ground walking for each walking speed. In both cases (slow level-ground and slow up-slope walking), swing-assistance torque increased the peak-flexion knee angle to biomimetic levels, which

would otherwise not be achievable using passive dynamics alone. This increased knee flexion can potentially reduce the compensatory motion required by the user to avoid catching the toe of the prosthesis during slow walking, since most prosthetic feet cannot actively dorsiflex like the biological ankle does during swing-phase. During down-slope walking, both prosthetic knees showed similar knee trajectories for stance and swing phases. During the stance-phase, the knee joint yielded from heel-strike to toe-off, supporting the subject's weight as the center-of-mass progresses forward and downward. The knee joint flexed to approximately 55 to 60 degrees during stance-phase for all walking speeds for both prosthetic knees. The subject initiated swing-phase by swinging the prosthetic thigh forward, lifting the prosthetic foot from the ground. Inertial coupling from thigh acceleration and gravity caused the knee joint to extend. For downslope walking with both prosthetic knees, the swing-phase had approximately the same spatial-temporal characteristics across all walking speeds.

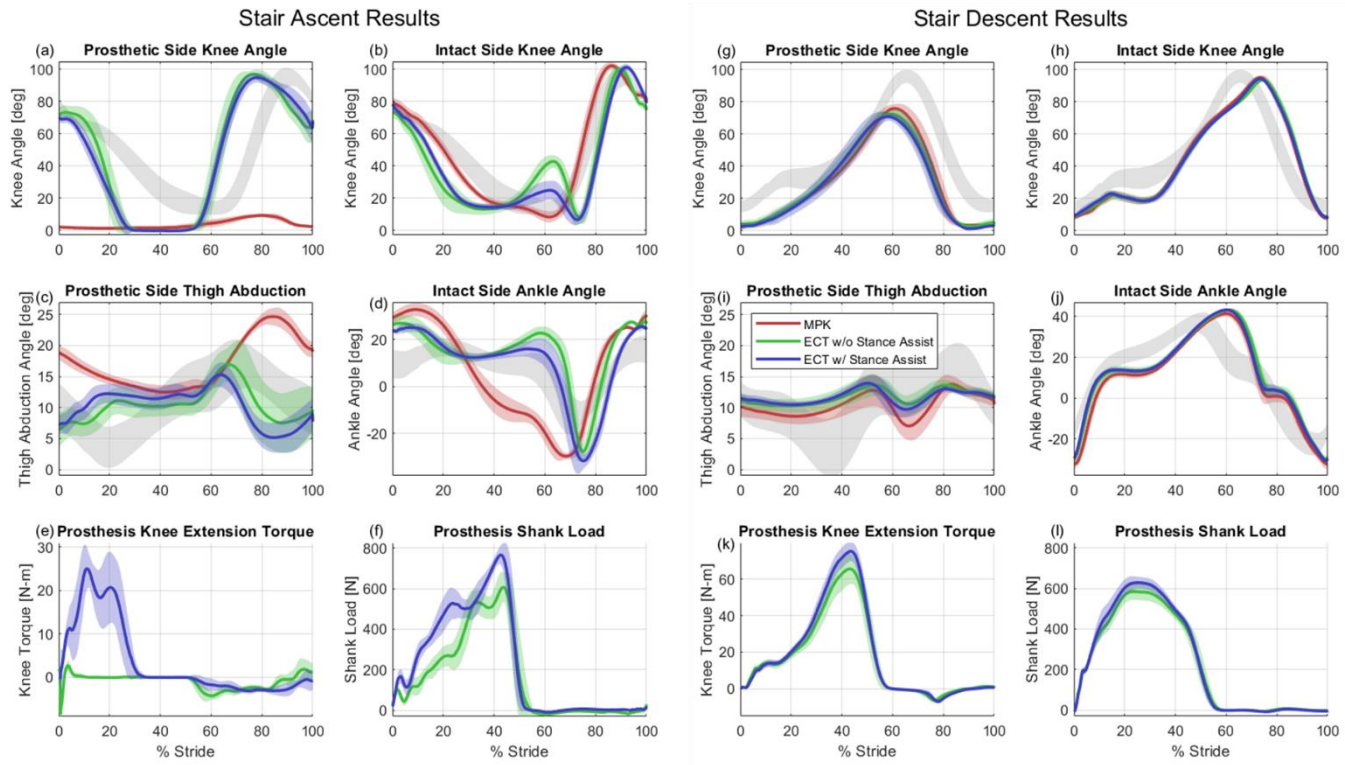

Fig. IV-6: Averaged stair ascent and descent data, showing (a,g) prosthetic side knee angle, (b,h) intact side knee angle, (c,i) prosthetic side thigh abduction angle, (d,j) intact side ankle angle (positive direction is dorsiflexion), (e,k) prosthesis knee extension torque (from embedded system data and actuator model), and (f,l) axial load on prosthetic shank. Most plots compare three prosthesis conditions: subject's daily-use MPK (red), ECT without stance-assistance (green), and ECT with stance-assistance (blue); plots (e,f,k,l) only compare the latter two conditions, since shank load is recorded by the ECT's load cell only and knee torque is calculated from the motor current and actuator friction model. Shaded regions on plots (a)-(d) and (g)-(j) indicate range of one standard deviation of averaged data from 28 healthy subjects [53].

5.2 Stair Ascent and Descent

The subject ascended and descended stairs (with the use of handrails) in a step-over-step manner using both prosthetic knees. As shown in Fig. IV-6(g)-(l), there were no notable differences between prosthetic knees when descending stairs, which was the expected result since the ECT emulates the same turbulent damping as the MPK during resistive stance. As shown in Fig. IV-6(a), during stair ascent the subject was unable to elicit swing-flexion with the MPK, since the kinematics of stair ascent are not amenable to ballistic swing (i.e., the subject would swing the foot into the stair riser). Instead, the subject employed hip circumduction, as indicated by significant thigh abduction in Fig. IV-6(c), with an essentially extended knee in order to ascend stairs in a step-over fashion, similar to the observations reported in [38]. In contrast, the ECT provides a powered swing function (FSM state 6), which produced essentially biomimetic swing kinematics during stair ascent. Fig. IV-6(e-f) shows the knee torque and shank loading for the two cases of ECT stair ascent – one with stance assistance, and one without, showing the increased prosthesis loading during stance-phase when the motor provides stance knee-extension assistance, indicating that the subject is not fully loading the prosthesis until the knee joint is fully extended when there is no assistance. This reduced loading on the prosthetic side must therefore be offloaded to the intact side and/or the handrails. When not providing stance-assistance, the subject vaulted over the prosthetic leg, simultaneously pulling with his arms while extending his hip to straighten the knee joint. As such, the knee joint extended more quickly without stance knee assistance relative to the case with stance assistance, as indicated by the difference in the rate of change of knee angle during early-stance in Fig. IV-6(a).

The subject exhibited compensatory behavior in all three cases while ascending stairs. Fig. IV-6(b) and (d) show that, similar to [60], the subject's intact side knee and ankle joints showed rapid flexion and subsequent extension in late-stance for the two ECT cases. This is likely a compensatory strategy to increase center of mass velocity during the pull-up phase with the prosthetic side. This compensatory motion is more pronounced when not providing any assistive torque, which indicates: 1) a relatively small amount of assistive torque (~25 N-m) is sufficient to reduce compensatory intact side knee and ankle motion by 60% and 65%, respectively (relative to the knee and ankle angles during mid-stance, which are not expected to change in late stance, based on healthy kinematics); and 2) the moderate amount of extension torque provided by the ECT was insufficient to fully reproduce healthy stair ascent behavior, implying that more torque is necessary to do so. However, given that the ECT provides about 30% of the extensive torque of the biological limb (for the subject's mass), a 60-65% reduction in compensatory

motion indicates that it may not be necessary to provide 100% of the torque of the biological limb to improve step-over stair ascent.

To contrast the compensatory strategy used with the ECT, the subject employed a different compensatory strategy with the MPK. During swing-phase on the prosthetic side, the subject abducted his thigh (70-100% of stride, Fig. IV-6 (c)) while simultaneously over-extending his intact side ankle (30-50% of stride, Fig. IV-6(d)), which provided the necessary clearance to place the prosthetic foot on the next step. Once placed, the prosthetic knee was straight, which required the subject to forcefully adduct his prosthetic side thigh (0-30% of stride, Fig. IV-6(c)) while over-extending his intact side knee and ankle (50-65% of stride, Fig. IV-6(b, d)). Of the three methods of stair ascent presented here, the subject indicated that the ECT with powered stance assistance was the most preferable (see Section 6.4), which may indicate that the least amount of compensatory effort was required in that case.

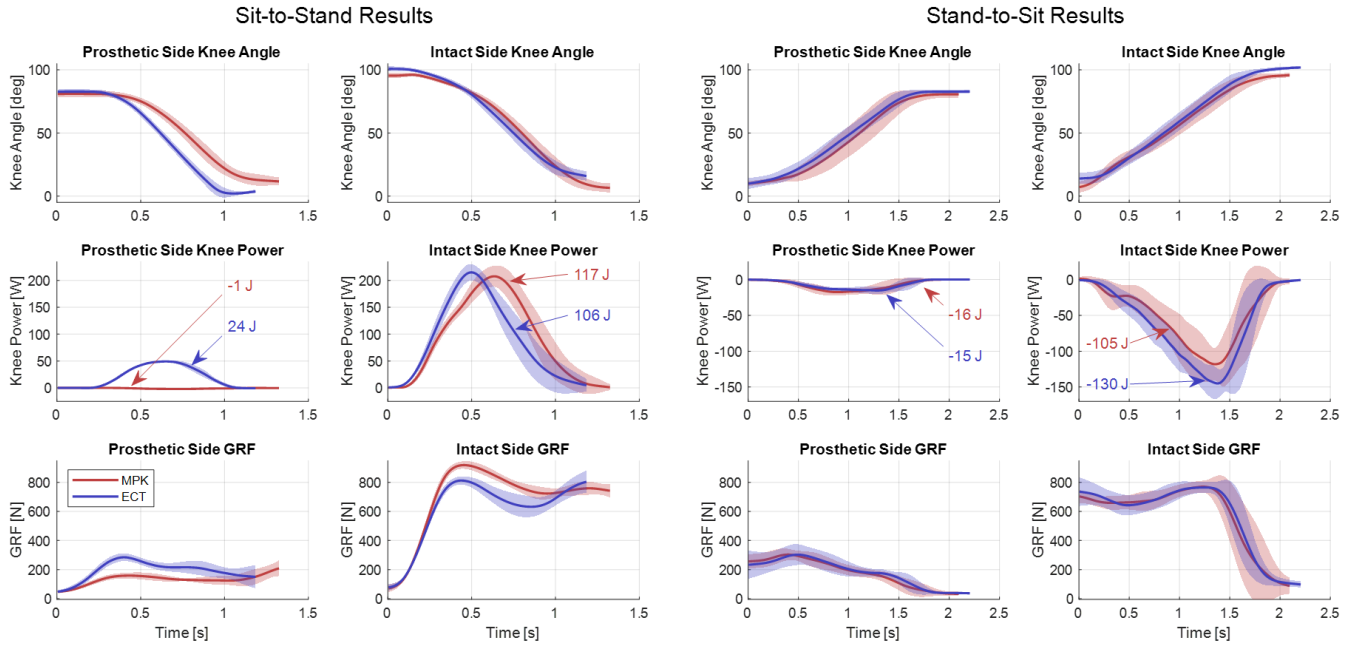

Fig. IV-7: Averaged sit-to-stand and stand-to-sit data, showing knee angle, knee power, and ground reaction force (GRF) on both the prosthetic and intact sides. Each plot compares two prosthesis conditions: subject's daily-use MPK (red), and ECT with stance-assistance (blue). Knee power plots show the total energy generated or dissipated by each side when standing up or sitting down.

5.3 Sit-to-Stand and Stand-to-Sit Transition

The ECT demonstrated similar performance to the MPK during stand-to-sit transitions and superior performance to the MPK during sit-to-stand transitions. Fig. IV-7 shows a comparison between the prosthetic and intact sides while wearing an MPK and the ECT (with stance assistance) during sit-to-stand and stand-to-sit. These data show that providing an assistive knee torque during sit-to-stand reduced

the ground reaction force (100 N/12% reduction in peak force) and knee power (11 J/10% reduction in total positive knee energy) on the subject's intact side, while simutanously increasing those metrics on the prosthetic side (125 N/80% increase in peak force; 25 J increase in total positive knee energy), which are similar results observed in [61].

During stand-to-sit, the expected outcome was that there would be no difference between the MPK and ECT, since it was hypothesized that each prosthesis provides the same turbulent damping resistance to motion. While there are no differences between most biomechanical metrics, the total energy dissipated on the intact side is lower for the MPK than for the ECT, which was an unexpected result. In evaluating the torque-speed behavior of the MPK in the stand-to-sit trials, the authors observed that the control system of the C-Leg 4 increases knee flexion resistance to a very high level before the subject begins sitting. This means that the two prostheses do not have the same constitutive behavior during stand-to-sit, which may be the source of the differences in experimental outcomes. Note that, given the variability in the stand-to-sit data, additional data is necessary to identify significant differences.

5.4 Over-Ground Walking Circuit

Fig. IV-8 shows the results of the over-ground walking circuit, where the subject performed a variety of activities with the ECT. The figure shows both knee angle and controller state as a function of time to demonstrate the state-flow of the FSM within and between each activity and the corresponding knee motion. The figure reflects the following sequence of activities: the subject stood up from a chair, walked on level ground, up a ramp, made an outside turn, down stairs, level ground, made an inside turn, walked on level ground, walked backwards, walked forwards again, ascended stairs step-over-step, made an inside turn, walked down a ramp, walked on level ground, and sat down. No hesitation nor special movement was required between activities, suggesting that the FSM transition conditions provided for automatic transitions based upon how the user moved the prosthesis. To transition to down-slope or down-stairs requires the same user motion as required by the C-leg to utilize stance yielding; to transition to up-stairs, the subject unloads the prosthesis with an extended knee while stepping up with his contralateral leg; to initiate powered sit-to-stand, the user need only begin extending his hip while loading the prosthesis. In addition to providing appropriate gait activity, the FSM permits all transitions between activities to be facilitated through natural user motion.

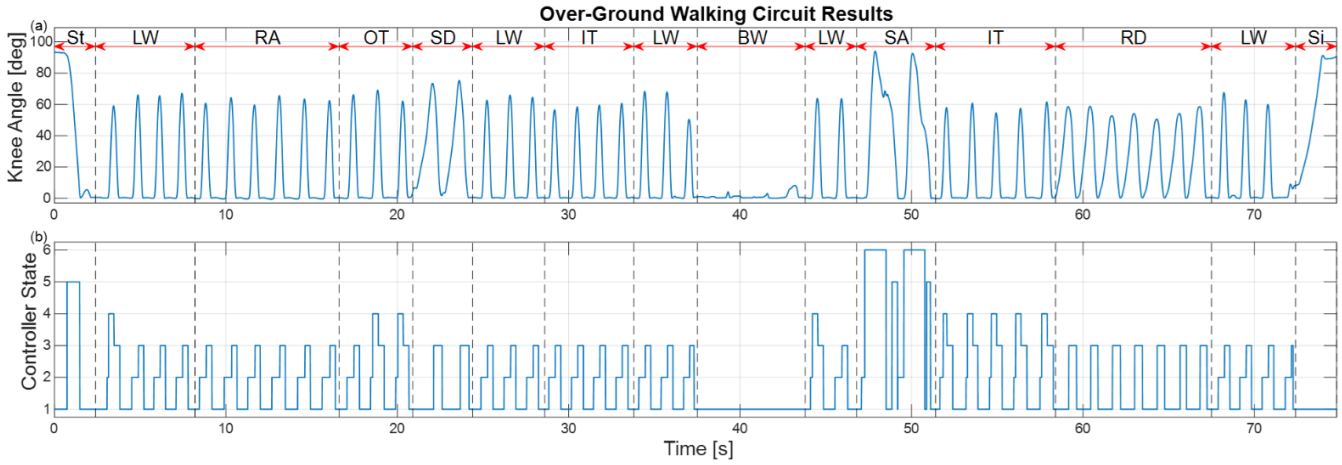

Fig. IV-8: Results of over-ground walking circuit showing (a) knee angle and (b) FSM controller state for the entire circuit. For LW, RA, IT, and OT, FSM state-flow is 1-2-3. For slow walking, FSM state flow is 1-2-4-3. For RD and SD, FSM state-flow is 1-3. For SA, FSM state-flow is 1-2-6-1-5. Activity abbreviations: LW = level; BW = backward walking; RA/RD = ramp ascent/descent; SA/SD = stair ascent/descent; IT/OT = inside/outside turn; St = standing; Si = sitting. FSM controller states as presented in Fig. IV-1: 1 = stance; 2 = swing-flexion; 3 = swing-extension; 4 = swing-assistance; 5 = stance-assistance; 6 = powered swing.

6. Discussion

6.1 Enabling Human-Prosthesis Interaction via Low Impedance

While passive prosthetic knees can only react, PKs can both act and react (i.e., they are capable of producing motion independent of user inputs), thus complicating the human-prosthesis interaction. The controlled interaction between the prosthesis and user therefore becomes substantially more important in PKs. In a low-impedance state, the prosthesis is generally more receptive to user effort, and therefore it is both more controllable by a user, and more sensitive to user input, relative to a high-impedance state. Specifically, impedance is the ratio of (generalized) force to motion (i.e., velocity), meaning that a low impedance will result in increased motion for a given user force input. Therefore, a prosthetic knee capable of assuming a low-impedance state increases: 1) the control the user has over its motion, and 2) the sensitivity of the prosthesis to user input and intent. Strategic implementation of a low-impedance interaction has the potential to enhance the human-prosthesis interaction.

MPKs interact with users by providing an impedance that is both appropriate for the current action (e.g. high-impedance during stance-phase and a low-impedance during swing-phase) and appropriate for detecting the user's intent to act (e.g. low-impedance in late-stance, prior to swing-phase). While PKs use sensing to infer user intent, their relatively higher output impedance reduces their ability to be as receptive to user input as are MPKs. There are several common actions taken by prosthesis users where, in the

opinion of the authors, maintaining a low output impedance behavior such as proposed here, can greatly facilitate inferring intent from a user and providing physical coordination with him or her, including:

Initiation of swing-phase – A low output impedance in late-stance and throughout swing-phase reduces the effort needed by the user to initiate swing-phase and provides for a natural coordination of the user's motion and prosthesis behavior (since it is provided as a reaction to user motion).

Ballistic swing – A biomimetic reproduction of healthy swing-phase dynamics necessitates that the prosthetic knee provides a ballistic swing-phase motion. Additionally, because swing-phase is a net-dissipative knee behavior for most walking speeds, this behavior can be provided entirely by motor braking. The more movements that can be done passively, the lower the power requirements for locomotion.

Non-ballistic swing – Like ballistic swing, a low output impedance enables natural coordination of the intent to initiate a powered non-ballistic swing-phase during late stance. Additionally, a low-impedance non-ballistic swing reduces the actuator torque required to move the knee joint (due to reduced transmission dynamics, resulting in higher overall efficiency), provides a more natural disturbance rejection (due to reduced inertia and Coulomb friction that otherwise act as a low admittance to disturbances, including disturbances that result from swing-phase motion of the user's residual thigh), and may reduce the back EMF when tracking high-velocity trajectories (due to the reduced transmission ratio, as demonstrated in this manuscript).

Initiation of powered knee extension – During the stance-phase, the intent to initiate generalized resistive and active behaviors can be communicated to the prosthesis via flexion or extension of the user's hip musculature (because the stance leg is a closed kinematic chain, this motion is translated to the knee joint). While this intent to flex or extend the knee can be sensed as a torque in a high-impedance device, sensing with motion has the benefit of observing the user's movement and reacting to it. Because stance-phase torques are high with relatively smaller accelerations, it is less important to have low actuator inertia, compared to swing-phase. However, it is important to have low stance-phase friction at low knee velocities, where the direction of motion inflects (i.e. stiction, motor cogging, and Coulomb friction must be low), which otherwise increases the effort required by the user to initiate knee flexion or extension.

User acceptance of powered knees – Prosthesis users are accustomed to interacting with passive devices. Designing PKs with passive dynamics akin to state-of-the-art passive prostheses has the potential to aid with accommodation and ultimate acceptance of PKs. In this case, the replication of MPK-like behavior on the ECT allowed the user to quickly adapt to the function of the new prosthesis.

6.2 Using Power to Assist Motion, Rather than Control Motion

The proposed controller is premised on the idea that, whenever possible, the prosthesis should default to behavior that requires it to react to user inputs, rather than act in anticipation of user motion. While this behavior is inherent when the prosthesis is controlled passively like an MPK, the idea behind this approach can be extended to active behaviors as well. Power can be used to either control the motion of the knee, or to assist the motion of the knee by "pushing" it in the direction that the user is moving it. Utilizing power to do the latter allows the user to initiate motion before the prosthesis provides powered assistance to that motion. Two examples of power assistance are demonstrated in this chapter: (1) During slow walking, inertial forces are insufficient to overcome drivetrain impedance and produce enough knee flexion during swing-phase, even in low-impedance knee prostheses, which leads to compensatory motion to enable ground clearance of the foot. In these cases, power can be used to "push" the knee towards flexion during late-stance and swing-flexion phases. This preserves the inertial coupling of swing-phase (because the increased energy is compensating for the energy dissipated by the drivetrain impedance) without compromising ground clearance. (2) During activities that involve substantial stance knee-extension, the stance leg is a closed kinematic chain, which allows the prosthesis user to control knee joint movement via movement of the hip joint. While possible for the user to extend the knee joint using hip musculature alone (e.g., [38]), this motion can be achieved with less user effort by providing extensive power at the knee. Just as the biological hip and knee work synergistically to extend the leg, the prosthetic knee is able to follow motion and force cues from the residual hip and provide synchronous assistive knee torque. In this manner, the user does not react to the knee's control of motion, but rather works with it to extend the leg, similar to the manner in which an electric bicycle coordinates its power delivery with the user's power input. Although a knee prosthesis is often thought of as a replacement of a joint, as opposed to augmentation of a joint, in the case of stance-knee extension during stair ascent, the knee is essentially in parallel with the hip joint; as such, the knee in stance might better be thought of as a joint that augments hip effort to extend the whole leg, rather than as a joint that acts in series with it.

6.3 Hardware Limitations

The back-drivable lead screw in the ECT's drivetrain has design tradeoffs that benefited passive behavior but degraded active performance. The amount of friction in the leadscrew is torque-dependent. As such, at low actuator torques (e.g., ballistic swing), the amount of friction is very low, while at high actuators torques, the friction is considerably higher. This load-dependent friction creates a benefit for

both resistive stance and ballistic swing by amplifying the resistive motor torque by a factor of two, which increases the range of controllable impedances in the low-gear and protects the planetary gear transmission from overload in the high-gear. However, these benefits come at the cost of decreased efficiency in the forward drive, increasing the electrical energy cost of non-ballistic swing and severely decreasing the maximum stance-phase assistive torque to levels that compromise performance in stair ascent and stand-to-sit activities. For a future version of this design, the designer should consider use of power transmission components that have a better balance of forward-drive and back-drive efficiencies, which will change the ratio of maximum forward-drive and back-drive torques. While necessary to provide high resistive torques in stance (from embedded system data and a model of actuator friction, we calculated the knee torque to be up to 80 N-m during stair descent, which is expected from previous studies [32]), it may not be necessary to provide a biomimetic magnitude of knee extension torque during stair ascent or sit-to-stand to provide benefit to powered knee extension. As demonstrated during stair ascent and sit-to-stand, an assistive torque approximately 30% of the biological limb's for the subject's mass was sufficient to increase prosthetic knee power and ground reaction force, reduce intact limb knee power and ground reaction force, and reduce intact limb compensatory action (e.g., rapid flexion and extension of the intact knee and ankle during late-stance of stair ascent). This is not surprising considering that MPK users average about 75% of the biological knee torque with their prosthesis during stair descent, and transtibial amputees use approximately 25% of the biological knee torque with their prosthetic side knee during stair ascent [32], indicating that they may be unwilling to load the prosthesis to biomimetic levels during stair ambulation. Therefore, it may be unnecessary and perhaps undesirable to provide 100% of the biological knee's extension torque during stair ascent and sit-to-stand.

6.4 Subjective Feedback

When combined with quantitative data, qualitative user feedback provides an important perspective on the assessment of novel design approaches. To give a lens to this new approach to prosthesis design and control, and to provide insight into future developments of this design approach, the study participant was given a follow-up survey to state his preferences for either the C-Leg or ECT Knee in each of the experimental activities. The survey and its results are shown in Table IV-5. For each of the experimental activities, the subject was instructed to select one of the five options below that best describes his preference:

- Greatly prefer the C-Leg

- Somewhat prefer the C-Leg
- No difference in preference
- Somewhat prefer the ECT Knee
- Greatly prefer the ECT Knee

After the survey, an interview was conducted where the subject was asked open-ended questions about his responses to the survey. For experimental activities where the subject preferred the C-Leg over the ECT Knee, the subject was asked the following two questions:

- What about your experience with the C-Leg made it preferable during this activity?
- What about your experience with the ECT Knee made it less preferable during this activity?

For experimental activities where the subject preferred the ECT Knee over the C-Leg, the subject was asked the following two questions:

- What about your experience with the ECT Knee made it preferable during this activity?
- What about your experience with the C-Leg made it less preferable during this activity?

For experimental activities where there was no preference for one over the other, the subject was asked the following question:

- Why was there no preference for either device?

Table IV-5
Post-Study Survey and Interview Responses

Q#	Which prosthesis do you prefer when…	Survey Response
1	…walking at a **slow speed** on a flat treadmill?	**No difference** in preference
	Interview response: Swing assistance makes it easier to walk slowly because I don't have to work as hard to swing the leg. But it is uncomfortable to walk slowly, since I have to spend so much time standing on the prosthesis, so it is difficult to notice the difference that was being made by swing assistance.	
2	…walking at a **comfortable speed** on a flat treadmill?	**No difference** in preference
	Interview response: The ECT did a great job emulating the C-Leg; I had no problem walking with the ECT at these speeds. [The C-Leg and ECT] are very much the same when walking.	
3	…walking at a **fast speed** on a flat treadmill?	**Somewhat** prefer the **C-Leg**
	Interview response: The C-Leg was smoother than the ECT. When the knee extended fully at the end of swing, the ECT was hitting harder than I wanted. But the C-Leg did that more smoothly.	
4	…walking **up-slope** on a treadmill?	**Somewhat** prefer the **ECT Knee**
	Interview response: I liked the swing-assistance for going up-slope. The foot seemed to go into the right place, because the foot extends out further. Like the foot placement was more appropriate for going up a slope. With the C-Leg, my [prosthetic] foot does not get as far out.	
5	…walking **down-slope** on a treadmill?	**Somewhat** prefer the **ECT Knee**
	Interview response: The ECT had more resistance than the C-Leg. The C-Leg feels like it starts to collapse too soon. The ECT held me up better and I was walking smoother. My steps with the C-Leg end too soon.	
6	…walking **up-stairs**?	**Greatly** prefer the **ECT Knee**
	Interview response: With the C-Leg, I have to pole-vault up the stairs. I have to put my leg out to the side and stiff leg it up there. That's not how people climb stairs. With the ECT, I can actually walk up step over step. The motor really helps me climb stairs, to position the foot, with the whole process. I was actually getting pretty good at it. I think with experience and practice I could to it really smoothly. However, the prosthesis takes its time in swing. Getting the foot up there and placing it on the next step was a little slow. I'd like it to go faster than that. Also, it needs more power in stance, probably 50% more power.	
7	…walking **down-stairs**?	**Somewhat** prefer the **ECT Knee**
	Interview response: I felt like I was in control of the ECT. With the ECT, I could go down-stairs without holding the handrail. I can't do that with the C-Leg because it collapses too quickly, and I don't want to injure my knee. The ECT went downstairs smoothly. (note that the subject was instructed to use a handrail during stair descent for safety reasons)	
8	…**standing up** from a chair?	**No difference** in preference
	Interview response: I was able to stand up faster with the ECT, and the assistance does help a bit. But my [intact] leg has to do the bulk of the work, so the difference isn't that much.	
9	…**sitting down** to a chair?	**No difference** in preference
	Interview response: The resistance doesn't matter as much when sitting down because my [intact] leg is doing most of the work. Resistance matters when going down stairs and slopes because I'm putting all my weight on the prosthesis. It might help a little bit, but it's not enough to put even weight on both legs.	
10	Which prosthesis do you prefer **overall**?	**No difference** in preference
	Interview response: The ECT was superior when ascending/descending stairs and slopes. The C-Leg was a bit smoother on level-ground walking. And the C-Leg is quieter.	

Regarding subject preference for the C-Leg in level-ground walking, the terminal impact velocity of the ECT increases at fast walking speeds, relative to slow or comfortable speeds (see Fig. III-9). As discussed in CHAPTER III5.2, at these faster walking speeds the ECT loses control authority of the deceleration of the knee joint. This is due to the saturation of motor braking in the low-gear and the limitation placed on the control system to remain in the motor braking region of the torque-speed plane and to avoid commanding any resistance while the knee joint was still accelerating (i.e., before extending past ~35º of knee flexion during swing-extension). Given these constraints, the maximum amount of energy that can be dissipated in swing extension (before terminal impact) is a function of the motor's physical characteristics, the transmission ratio, and the time integral of the velocity profile (which is constrained by the desirable swing-extension kinematics shown in Fig. B-8(b)). Future designs should increase maximum resistance in terminal swing to avoid this detriment to ballistic swing phase. This can be achieved by changing the transmission ratio, selecting a different motor, or with reverse current braking as discussed in [45], which requires consumption of electrical energy.

Regarding subject preference for the ECT Knee in down-slope and down-stairs walking, this response was surprising, considering that the torque control law for FSM State 1 was designed to emulate the same turbulent damping behavior of the C-Leg and because averaged resistive stance kinematics did not obviously differ between prostheses (see Fig. IV-5 and Fig. IV-6). However, in evaluating the torque-speed behavior of both prostheses during slope-descent and stand-to-sit (note that inverse dynamics were not available for stair-descent), it was noticed that the quasi-damping of the C-Leg is invariant from 0º to about 50º of knee flexion, which means that the C-Leg uses low-bandwidth modulation of flexion resistance (via modulation of the flexion valve angle) to achieve an invariant torque-speed relationship at the knee joint (i.e., the turbulent damping behavior does not change as the slider crank transmission ratio changes). For this range of motion (0º to 50º), the C-Leg and ECT Knee have exactly the same torque-speed behavior). However, at knee angles greater than 50º, the control authority of the C-Leg degrades, and the joint resistance significantly decreases. This degradation in joint resistance modulation is likely a result of the bandwidth limits of the C-Leg's control system and valve motor, the resolution of the restrictive valve, and the rapid rate of change of the transmission ratio at knee angles greater than 50º. The effect of this loss of control authority is that towards the end of stance-phase in slope-descent and stair-descent, where knee angles reach up to 60º and 80º, respectively, the joint resistance rapidly decreases, which is likely the source of feeling unstable for the subject. To contrast with the C-Leg, the quasi-

damping of the ECT is invariant for knee angles up to 80º (the highest in this study), and therefore the knee joint resistance does not decrease at high flexion angles.

7. Conclusion

This chapter describes a new approach to the design and control of a powered knee prosthesis that is capable of strictly-passive functionality, but also capable of layering powered assistance onto the nominally passive functionality when appropriate. Intended features of the control approach include: (1) providing ballistic swing behavior in a powered prosthesis; (2) using knee power only for activities that require knee power; (3) providing assistive power that "pushes" the knee joint in the direction that the user is moving it; and (4) facilitating sensing of user intent by making the prosthesis receptive to user motion (via low impedance states) and providing reactions to that motion. The control system was implemented on a novel powered prosthetic knee that enables low-impedance behaviors associated with ballistic swing, and high torque behaviors associated with passive and powered stance, by employing both passive and active motor control in combination with an electronically switchable two-speed transmission. Experiments comparing the control approach against a strictly-passive MPK demonstrate the ability of the proposed approach to provide essentially identical passive behaviors to the MPK, while also providing powered behaviors to aid stair ascent, slow walking, and sit-to-stand transitions.

CHAPTER V

CONCLUSION

1. Contributions

This dissertation described the design, control, and assessment of a powered knee prosthesis capable of providing the requisite resistive and active stance-phase behaviors as well as the ballistic and non-ballistic swing-phase behaviors necessary to replicate healthy knee behavior. This work makes several contributions to the advancement of prosthetic leg technology, including the introduction of a new class of powered knee prosthesis, the design and full disclosure of a passive control system with performance similar to a commercial MPK, the observation that energy dissipation in swing-phase is linearly proportional to walking speed, and the design of a novel control architecture for a powered knee prosthesis that layers powered behaviors on top of the baseline passive walking controller. Neither this design and control approach nor the resultant behavior and functionality of this approach have been previously demonstrated in literature.

1.1 Powered Knee Design

The mechanical design described in Chapter II is a new approach to the design of a powered knee prosthesis that offers powered capabilities (i.e., active stance and non-ballistic swing) without sacrificing the passive capabilities provided by state-of-the-art MPKs (i.e., resistive stance and ballistic swing). The prosthesis enables these behaviors by employing a specialized electronically-controlled two-speed transmission with selective unidirectional behaviors, in combination with an electric motor. The motor-actuated device can replicate the passive stance and swing behaviors of an MPK while offering powered stance and swing capabilities via the combination of intra-stride reconfiguration of the electromechanical drivetrain and feedback control.

1.2 Passive Control System

The control system described in Chapter III is an energetically-passive control system for a torque-controllable knee prosthesis. The control system is able to adapt to a variety of activities and walking speeds, providing passive performance similar to a state-of-the-art MPK. Such control systems are in common use in commercial MPKs, yet no comparable control system has been demonstrated in literature.

The control system can be used on any torque-controllable knee prosthesis capable of resistive stance and ballistic swing behaviors. The passive control system uses a three-state finite state machine with resistive torque control laws for the stance, swing-flexion, and swing-extension phases of gait. In the stance-phase, the controller provides a turbulent damping torque, which is adaptive to level-ground, down-slope, and down-stairs walking, as well as stand-to-sit. In the swing-phase, the controller provides a cadence-adaptive linear damping torque based upon the observation that swing-phase energy dissipation is linearly-proportional to walking speed. This passive control system is the baseline walking controller onto which powered behaviors are layered to increase prosthesis functionality beyond what is achievable with passive behavior alone.

1.3 Powered Control System

Chapter IV described a new approach to the control of a powered knee prosthesis that is capable of strictly-passive functionality, but also capable of layering powered assistance onto the nominally passive functionality when appropriate. Intended features of the control approach include: (1) providing ballistic swing behavior in a powered prosthesis; (2) using knee power only for activities that require knee power; (3) providing assistive power that "pushes" the knee joint in the direction that the user is moving it; and (4) facilitating sensing of user intent by making the prosthesis receptive to user motion (via low impedance states) and providing reactions to that motion. The control system was implemented on a novel powered prosthetic knee that enables low-impedance behaviors associated with ballistic swing, and high torque behaviors associated with resistive and active stance, by employing both passive and active motor control in combination with an electronically switchable two-speed transmission. This chapter compared the control approach against a strictly-passive MPK, demonstrating the ability of the proposed approach to provide essentially identical passive behaviors to the MPK, while also providing powered behaviors to aid stair ascent, slow walking, and sit-to-stand transitions.

2. Potential Impact

Powered knee prostheses have the potential to improve functional activities for people with transfemoral amputation, particularly ones characterized by substantial positive knee power (e.g. stair ascent, sit-to-stand, stumble recovery). However, the addition of positive mechanical power has generally come at the expense of sacrificing the low impedance behavior that is characteristic of passive knee prostheses, which in turn sacrifices the passively generated swing-phase motion known as ballistic swing. The work presented here is an effort to add powered capabilities to movement only when needed, while

fully preserving ballistic swing-phase motion with the intention of retaining the proven benefits provided by passive prostheses, while also offering the prospective benefits of powered assistance.

REFERENCES

[1] K. Zeigler-Graham, E. J. MacKenzie, P. L. Ephraim, T. G. Vravison and R. Brookmeyer, "Estimating the prevalence of limb loss in the United States: 2005 to 2050," *Archives of physical medicine and rehabilitation,* vol. 89, pp. 422-429, 2008.

[2] R. Renzi, N. Unwin, R. Jubelirer and L. Haag, "An international comparison of lower extremity amputation rates," *Annals of Vascular Surgery,* vol. 20, no. 3, pp. 346-350, 2006.

[3] R. E. Seroussi, A. Gitter, J. M. Czerniecki and K. Weaver, "Mechanical word adaptions of above-knee amputee ambulation," *Arch. Phys. Med. Rehabil.,* vol. 77, no. 11, pp. 209-1214, 1996.

[4] C. Gautheir-Gagnon, M. C. Grise and D. Potvin, "Enabling factors related to prosthetic use by people with transtibial and transfemoral ampuation," *Arch. Phys. Med. Rehabil.,* vol. 80, no. 6, pp. 706-713, 1999.

[5] S. M. Jaegers, J. H. Arendzen and H. J. de Jongh, "Prosthetic gait of unilateral transfemoral amputees: a kinematic study," *Arch. Phys. Med. Rehabil.,* vol. 76, no. 8, pp. 736-743, 1995.

[6] R. E. Stewart and A. Staros, "Selection and application of knee mechanisms," *Bulletin of prosthetics research,* vol. 18, pp. 90-158, 1972.

[7] S. Mochon and T. A. McMahon, "Ballistic walking," *J. Biomechanics,* vol. 13, no. 1, pp. 49-57, 1980.

[8] S. Mochon and T. A. McMahon, "Ballistic walking: an improved model," *Mathematical Biosciences,* vol. 52, no. 3-4, pp. 241-260, 1980.

[9] R. Seymour, B. Engbretson, K. Kott and et al, "Comparison between the C-Leg microprocessor-controlled prosthetic knee and non-microprocessor control prosthetic knees: a preliminary study of energy expenditure, obstacle course performance, and quality of life survey," *Prosthet Orthot,* vol. 31, pp. 51-61, 2007.

[10] J. T. Kahle, M. J. Highsmith and S. L. Hubbard, "Comparison of nonmicroprocessor knee mechanism versus C-Leg on Prosthesis Evaluation Questionnaire, stumbles, falls, walking tests, stair descent, and knee preference," *J Rehabil Res Dev,* vol. 45, pp. 1-14, 2008.

[11] D. J. Bunce and J. W. Breakey, "The impact of C-Leg on the physical and psychological adjustment to transfemoral amputation," *J Prosthet Orthot,* vol. 19, p. 7–14, 2007.

[12] M. Windrich, M. Grimmer, O. Christ, S. Rinderknecht and P. Beckerle, "Active lower limb prosthetics: a systematic review of design issues and solutions," in *Robotics: Science and Systems*, Berlin, Germany, 2013.

[13] D. S. Pieringer, M. Grimmer, M. F. Russold and R. Reiner, "Review of the actuators of active knee prostheses and their target design outputs for activities of daily living," in *Int. Conf. Rehab. Robotics (ICORR)*, London, UK, 2017.

[14] F. Sup, H. A. Varol, J. Mitchel, T. J. Withrow and M. Goldfarb, "Preliminary evaluations of a self-contained anthropomorphic transfemoral prosthesis," *IEEE/ASME Trans. Mechatronics*, vol. 14, no. 6, pp. 667-676, 2009.

[15] M. Lui, P. Datseris and H. H. Huang, "A prototype for smart prosthetic legs - analysis and mechanical design," *Adv. Mater. Res.,* Vols. 403-408, pp. 1999-2006, 2012.

[16] L. Flynn, J. Geeroms, R. Jimenez-Fabian, B. Vanderborgth and D. Lefeber, "CYBERLEGS beta-prosthesis active knee system," in *2015 IEEE-ICORR*, 2015.

[17] A. F. Azocar, L. M. Mooney, L. J. Hargrove and E. J. Rouse, "Design and characterization of an open-source robotic leg prosthesis," in *2017 7th IEEE BioRob*, Enshede, Netherlands, 2018.

[18] T. Elery, S. Rezazadeh, C. Nesler and R. D. Gregg, "Design and validation of a powered knee-ankle prosthesis with high-torque, low-impedance actuators," *IEEE Trans. Robot.*, 2020.

[19] T. Lenzi, M. Cempini, L. Hargrove and T. Kuiken, "Design, development, and testing of a lightweight hybrid robotic knee prosthesis," *Int. J. Robot. Research*, vol. 37, no. 8, pp. 953-976, 2018.

[20] E. C. Martinez-Villalpando, J. Weber, G. Elliott and H. Herr, "Design of an agonist-antagonist active knee prosthesis," in *2nd IEEE RAS EMBS*, 2008.

[21] S. M. Pfeifer, A. Pagel, R. Riener and H. Vallery, "Actuator with angle-dependent elasticity for biomimetic transfemoral prosthesis," *IEEE/ASME Trans. Mech.*, vol. 20, no. 3, pp. 1384-1394, 2015.

[22] B. E. Lawson, J. E. Mitchell, D. Truex, A. Shultz, E. Ledoux and M. Goldfarb, "A robotic leg prostheis: design, control, and implimentation," *IEEE Robot. Automat. Mag.*, pp. 70-81, 2014.

[23] E. D. Ledoux and M. Goldfarb, "Control and evaluation of a powered transfemoral prosthesis for stair ascent," *IEEE Trans. Neural Sys. Rehab. Engr.* , vol. 25, no. 7, pp. 917-924, 2017.

[24] F. Sup, H. A. Varol and M. Goldfarb, "Upslope walking with a powered knee and ankle prosthesis: initial results with an amputee subject," *IEEE Trans. Neural Sys. Rehab. Engr.,* vol. 19, no. 1, pp. 71-78, 2010.

[25] R. Fluit, E. C. Prinsen, S. Wang and H. van der Kooij, "A comparison of control strategies in commercial and research knee prostheses," *IEEE Trans. Biomed. Engr.,* vol. 67, no. 1, pp. 277-290, 2019.

[26] A. Baimyshev, B. Lawson and M. Goldfarb, "Design and preliminary assessment of a lightweight swing-assist prosthesis," in *40th Annual Int. Conf. Engr. Med. Biol. Soc (EMBC),* 2018.

[27] J. T. Lee, H. L. Bartlett and M. Goldfarb, "Design of a Semipowered Stance-Control Swing-Assist Transfemoral Prosthesis," *IEEE Trans. Mech.,* vol. 25, no. 1, pp. 175-184, 2020.

[28] H. Warner, P. Khalaf, H. Richter, D. Simon, E. Hardin and A. J. Van den Bogert, "Early evaluation of a powered transfemoral prosthesis with force-modulated impedance control and energy regeneration," *Med. Eng. Physics,* vol. 100, p. 103744, 2022.

[29] S. Gao, J. Mai, J. Zhu and Q. Wang, "Mechanism and controller design of a transfemoral prosthesis with electrohydraulic knee and motor-driven ankle," *IEEE/ASME Trans. Mech.,* vol. 26, no. 5, pp. 2429-2439, 2021.

[30] N. Hogan, "Impedance control: an approach to manipulation," *J. Dyn. Syst.,* vol. 107, pp. 1-23, 1985.

[31] E. Honert and K. Zelik, "Foot and shoe responsible for majority of soft tissue work in early stance of walking," *Human Move Sci,* vol. 64, pp. 191-202, 2019.

[32] T. Schmalz, S. Blumentritt and B. Marx, "Biomechanical analysis of stair ambulation in lower limb amputees," *Gait & posture,* vol. 25, pp. 267-278, 2007.

[33] R. Riener, M. Rabuffetti and C. Frigo, "Stair ascent and descent at different inclinations," *Gait & posture,* vol. 15, pp. 32-44, 2002.

[34] E. Perreault, L. Hargrove, D. Ludvig, H. Lee and J. Sensinger, "Considering Limb Impedance in the Design and Control of Prosthetic Devices," in *Neuro-Robotics: From brain machine interfaces to rehabilitation robotics*, New York London, Springer Dordrecht Heidelberg, 2014, pp. 59-83.

[35] J. M. Czerniecki, A. Gitter and K. Weaver, "Effect of alterations in prosthetic shank mass on the metabolic costs of ambulation in above knee amputees," *Am. J. Phys. Med. Rehabil.,* vol. 73, pp. 348-352, 1994.

[36] H. Van der Kooij, S. S. Fricke, R. C. Van't Veld, A. V. Prieto, A. Q. Keemink, A. C. Schouten and E. H. Van Asseldonk, "Identification of hip and knee joint impedance during the swing phase of walking," *IEEE Trans. Neural Syst. Rehabil. Eng.*, vol. 30, pp. 1203-1212, 2022.

[37] J. L. Johansson, D. M. Sherrill, P. O. Riley, P. Bonato and H. Herr, "A clinical comparrison of variable-damping and mechanically passive prosthetic knee devices," *Am. J. Phys. Med. Rehabil*, vol. 84, no. 8, pp. 563-575, 2005.

[38] J. T. Lee and M. Goldfarb, "Effect of a swing assist prosthesis on stair ambulation," *IEEE Trans. Neural Sys. Rehab. Engr.*, vol. 29, pp. 2046-2054, 2021.

[39] J. T. Lee and M. Goldfarb, "Swing-assist for enhancing stair ambulation in a primarily-passive knee prosthesis," in *IEEE Int. Conf. Robot Automat. (ICRA)*, 2020.

[40] B. Seth and W. C. Flowers, "Generalized actuator concept for the study of the efficiency of energetic systems," *J. Dyn. Sys. Meas. Control*, vol. 112, no. 3, pp. 233-238, 1990.

[41] R. K. Heinzmann, B. Seth and J. Turi, "Application of a generalized actuator model to the study of energy regeneration control strategies," *J. Dyn. Sys. Meas. Control*, vol. 114, no. 3, pp. 462-467, 1992.

[42] M. Plooij, G. Mathijssen, P. Cherelle, D. Lefeber and B. Vanderborght, "Lock your robot," *IEEE Robot. Automat. Mag.*, vol. March, pp. 106-117, 2015.

[43] V. D. Scheiman, "A preliminary work on implimenting a manipulator force sensing wrist," AI Laboratory Report, Stanford University, Stanford, CA, USA, 1971.

[44] M. Kassi, K. Takeyasu, M. Uno and K. Murakaoka, "Trainable assembly system with an active sensory table possessing six axes," in *11th International Industrial Robots*, Tokyo, Japan, 1981.

[45] L. Vailati and M. Goldfarb, "On using a brushless DC motor as a passive torque-controllable brake," *J. Dyn. Sys., Meas., Control*, vol. 144, p. DOI: 10.1115/1.4054733, 2022.

[46] D. A. Winter, Biomechanics and Motor Control of Human Gait: Normal, Elderly, and Pathological, Waterloo, 1991.

[47] M. R. Tucker, J. Oliver, A. Pagel, H. Bleuler, M. Bouri, O. Lambercy, J. R. Millan, R. Riener, H. Vallery and R. Gassert, "Control strategies for active lower extremity prosthetics and orthotics: a review," *J. Neuro Eng. Rehabil.*, vol. 12, no. 1, pp. 1-29, 2015.

[48] C. Ferreira, L. P. Reis and C. P. Santos, "Review of control strategies for lower limb prostheses," in *Second Iberian Robot. Conf.* , 2016.

[49] H. Herr and A. Wilkenfeld, "User-adaptive control of a magnetorheological prosthetic knee," *Industrial Robot,* vol. 30, no. 1, pp. 42-55, 2003.

[50] J. Kim and J. Oh, "Development of an above knee prosthesis using MR damper and leg simulator," in *IEEE Int. Conf. Robot. Automat.*, Seoul, Korea, 2001.

[51] X. Wang, Q. Meng, H. Lan, Z. Zhewen, C. Chen and H. Yu, "Neural network predictive control of swing phase for a variable-damping knee prosthessi with novel hydraulic valve," *IEEE Access,* vol. 8, 2020.

[52] C. Duraffourg, X. Bonnet, F. Dijan and H. Pillet, "Passive prosthesis control strategy for downhill ambulation," *Comp. Methods Biomech. Biomed. Engr.*, vol. 23, no. 1, pp. S94-S96, 2020.

[53] J. Camargo, A. Ramanathan, W. Flanagan and A. Young, "A comprehensive, open-source dataset of lower limb biomechanics in multiple conditions of stairs, ramps, and level-ground ambulation and transitions," *J. Biomechanics,* vol. 119, p. 110320, 2021.

[54] D. J. Lura, M. M. Wernke, S. L. Carey, J. T. Kahle, R. M. Miro and M. J. Highsmith, "Differences in knee flexion between the Genium and C-Leg microprocessor knees while walking on level ground and ramps," *Clin Biomech,* vol. 30, no. 2, pp. 175-181, 2015.

[55] L. Vailati and M. Goldfarb, "On using a brushless DC motor as a passive torque-controllable brake," *J. Dyn. Sys., Meas., Control,* p. https://doi.org/10.1115/1.4054733, 2022.

[56] S. C. Culver, L. G. Vailati and M. Goldfarb, "A power-capable knee prosthesis with ballistic swing-phase," *IEEE Trans. Med. Robot. Bionics (T-MRB),* 2022.

[57] E. J. Wolf, V. Q. Everding, A. L. Linberg, B. L. Schnall, J. M. Czerniecki and J. M. Gambel, "Assessment of transfemoral amputees using C-Leg and Power Knee for ascending and descending inclines and steps," *J. Rehabil. Research Develop.,* vol. 49, no. 6, pp. 831-842, 2012.

[58] B. J. McFadyen and D. A. Winter, "An integrated biomechanical analysis of normal stair ascent and descent," *J. Biomech.*, vol. 21, no. 9, pp. 733-744, 1988.

[59] J. Mendez, S. Hood, A. Gunnel and T. Lenzi, "Powered knee and ankle prosthesis with indirect volitional swing control enables level-ground walking and crossing over obstacles," *Science Robot.,* vol. 5, no. 44, p. eaba6635, 2020.

[60] H. Hobara, Y. Kobayashi, T. Nakamura, N. Yamasaki, K. Nakazawa, M. Akai and T. Ogata, "Lower extremity joint kinematics of stair ascent in transfemoral amputees," *Prosthetics and Orthotics International,* vol. 35, no. 4, pp. 467-472, 2011.

[61] E. J. Wolf, V. Q. Everding, A. A. Linberg, J. M. Czerniecki and J. M. Gambel, "Comparison of the Power Knee and C-Leg during step-up and sit-to-stand tasks," *Gait Posture,* vol. 38, pp. 397-402, 2012.

[62] R. Ronsse, S. M. De Rossi, N. Vitiello, T. Lenzi, B. Koopman, H. Van der Kooij, M. C. Carrozza and A. J. Ijspeert, "Real-time estimate of period derivatives using adaptive oscillators: application to impedance-based walking assistance," in *IEEE/RSJ Int. Conf. Intel. Robots Syst.*, Vilamoura, Algarve, Portugal, 2012.

[63] W. Huo, Y. Amirat and S. Mohammed, "Impedance reduction control of knee joint human-exoskeleton system," *IEEE Trans. Contol Syst. Tech.*, vol. 27, no. 6, pp. 2541-2556, 2019.

[64] F. Wehbi, W. Huo, Y. Amirat, M. Rafei, M. Khalil and S. Mohammed, "Active impednace control of a knee-joint orthosis during swing phase," in *IEEE Int. Conf. Rehabil. Robot. (ICORR)*, London, UK, 2017.

[65] S. Jannati, A. Yousefi-Koma, M. Ayati and S. Rezaeian, "Impedance control of a knee prosthesis with frictional torque estimation," in *RSI Int. Conf. Robot. Mechatron. (ICRoM),* Tehran, Iran, 2019.

[66] Y. Zhu and E. J. Barth, "Impedance control of a pneumatic actuator for contact tasks," in *IEEE Int. Conf. Robot. Automat.*, Barcelona, Spain, 2005.

[67] W. S. Newman, "Stability and performance limits of interaction controllers," *ASME J. Dynamic Syst. Meas. Control,* vol. 114, no. 4, pp. 563-570, 1992.

[68] Y. Wang and M. Srinivasan, "Stepping the the direction of the fall: the next foot placement can be predicted from current upper body in steady-state walking," *Biol. Lett.,* vol. 10, p. 20140405, 2014.

APPENDIX A: CHALLENGES OF PROVIDING A LOW OUTPUT IMPEDANCE ON A HIGH-IMPEDANCE POWERED PROSTHETIC KNEE JOINT VIA CONTROL METHODS

Variations of impedance control are ubiquitous in the control of powered leg prostheses [25]. In the common implementation of impedance control, the interaction between the desired prosthetic joint trajectory and environmental admittance (i.e., prosthesis user, leg inertia, and ground) is modulated by a commanded impedance [30]. Ideally, the control system is able to modulate the target output impedance via high-bandwidth sensor feedback (e.g., joint and motor encoders, IMUs, and load cells), as described by Hogan. However, the high-torque requirements of knee prostheses during stance-phase necessitate actuators with high reflected inertia and/or friction, which prevents them from providing the very low output-impedances provided by MPKs and required for ballistic swing-phase. If possible, it would be highly advantageous to provide accurate impedance compensation to achieve a low output impedance (i.e. emulated low impedance would enable ballistic swing-phase motion and an increased sensitivity to user intent). Although theoretically possible to reduce actuator impedance to these very low levels with feedforward or feedback control, the near-zero impedance requirement presents a number of stability and control challenges, and as such as not yet been demonstrated.

Several methods of impedance compensation have been described in literature and have been implemented on wearable robots. Impedance compensation methods can be generalized into feedback and feedforward methods, with the former subdivided into kinematic-feedback and force-feedback (or estimated force-feedback) methods. Each of these methods has unique control challenges; the physical basis of these control challenges are described in this appendix.

Kinematic-Feedback Impedance Compensation

Providing impedance compensation with kinematic-feedback control requires both an accurate model of actuator impedance (i.e. inertia and non-linear friction) and high bandwidth sensing of knee joint velocity and acceleration, which are used to compensate for actuator friction and inertia, respectively. Both of these requirements pose significant challenges in PKs.

Inertia Compensation: PKs typically have joint encoders, motor encoders, and shank-mounted IMUs, all of which can theoretically be used to measure actuator acceleration. Measuring actuator acceleration is typically achieved with double differentiation and sensor fusion of the joint and motor

encoders. However, doing so with high bandwidth is challenging due to the tradeoff between signal noise and the frequency response of filtering algorithms. Fig. A-1 shows normative knee joint kinematics from [31], and Fig. A-2 shows a comparison of a feedforward adaptive oscillator estimation, a feedback Kalman filter estimation, and the actual joint kinematics from [62]. This comparison shows that the Kalman filter overestimates peak knee velocity, underestimates peak knee acceleration, and has significant phase lag in the estimation of acceleration, relative to the actual kinematics. Note that knee velocity and acceleration are approximately half the values shown in Fig. A-1. As such, the bandwidth limitation of actuator acceleration estimation will be further exacerbated at walking speeds achievable by knee prosthesis users, requiring a significant phase margin to avoid actuator instability.

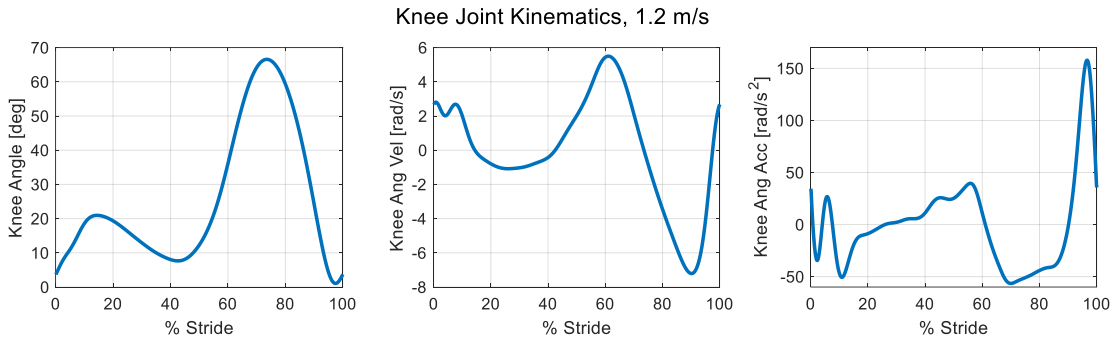

Fig. A-1: Knee kinematics in level-ground walking at 1.2 m/s, averaged from 10 subjects [31]. During swing-phase, the knee joint achieves velocities of 7 rad/s and accelerations of 150 rad/s^2.

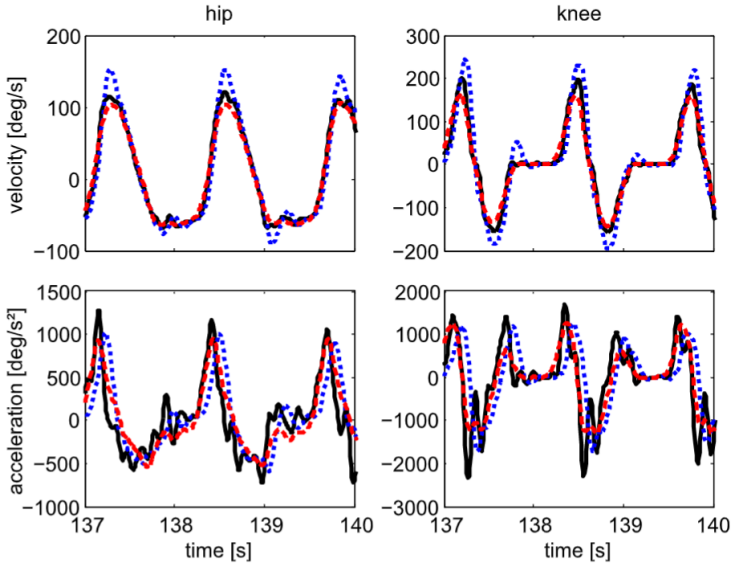

Fig. A-2: Right hip and knee velocity and acceleration during three representative seconds of the "zero-imp" condition (from [62]). Black: actual kinematics; Dotted blue: estimation provided by the Kalman filter; Dashed red: estimation provided by the adaptive oscillator. Note that knee velocity and acceleration are approximately half the values shown in Fig. A-1.

Friction Compensation: Although friction is typically modeled as a linear relationship between torque and speed, with coefficients for Coulomb and viscous friction defining the y-intercept and slope of the frictional torque-speed relationship, friction is highly non-linear in reality. To demonstrate the limitations of feedback friction compensation, the torque-speed characteristics of the Vanderbilt Powered Knee [22] were characterized in the same manner as was done for the ECT (see Fig. A-3 and Section 4.1).

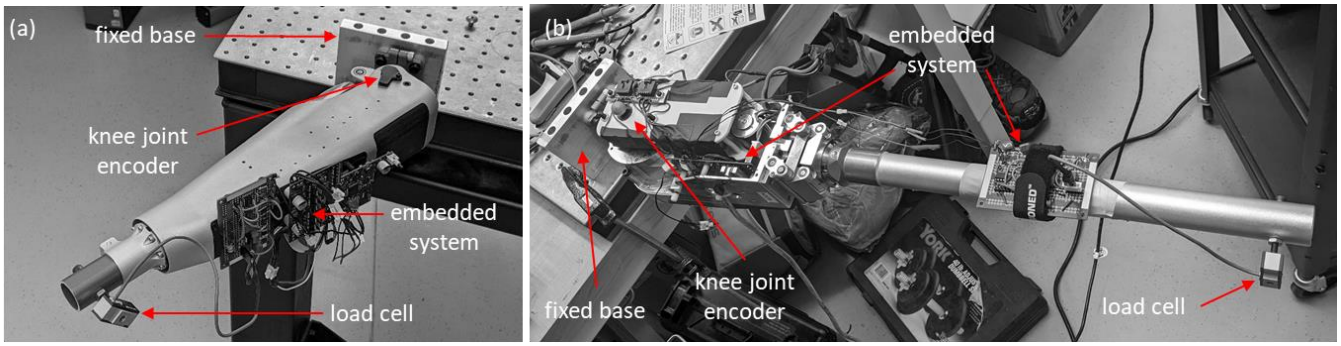

Fig. A-3: Impedance characterization test setup for (a) ECT Knee, and (b) Vanderbilt Powered Knee, with load cell oriented perpendicular to the long axis of the prosthesis. The prosthesis is mounted in the horizontal plane to remove the effects of gravity.

Figure A-4 shows the results of those experiments, comparing the Vanderbilt Powered Knee (with varying forms of friction compensation) to the ECT in the low gear (the latter of which meets the requirements outlined in Table II-1). Figure A-4 demonstrates that friction is not only speed dependent, but on PKs with significant service use, is also dependent on the wear patterns on mechanical components (i.e. friction becomes dependent on direction and position as well). From these data, friction compensation in a high-ratio transmission does not stably provide the same torque-speed characteristics as a low-ratio transmission. While possible to model actuator friction and provide friction compensation based on this nonlinear model, implementation will require a significant phase margin to account for phase lag in the velocity signal and the inevitable changes in friction associated with wear from service use. This naturally limits the amount of actuator friction that can be compensated without risking controller instability.

Fiction is most nonlinear at low velocities, which makes friction compensation more challenging because swing phase dynamics in walking are associated with relatively slow knee joint velocities (less than 7 rad/s), do not involve any steady state velocities, and involve rapid initiation of motion and inflection of output velocity (see Fig. A-1). Additionally, since initiation of swing-flexion and the subsequent inflection of knee velocity after peak-flexion involve low velocities, Coulomb friction will be dominant for these important transition periods, as is the subsequent transition through the non-linearity in friction as velocity increases/decreases. Providing friction compensation to Coulomb friction is

therefore non-trivial for swing-phase, since the control system will still need to recognize user intent to initiate knee-break and the torque generated by the signum term will need to smoothly inflect at peak-flexion. As such, providing real-time compensation of friction is primarily limited by model uncertainty and secondarily by measurement uncertainty (see Fig. A-2).

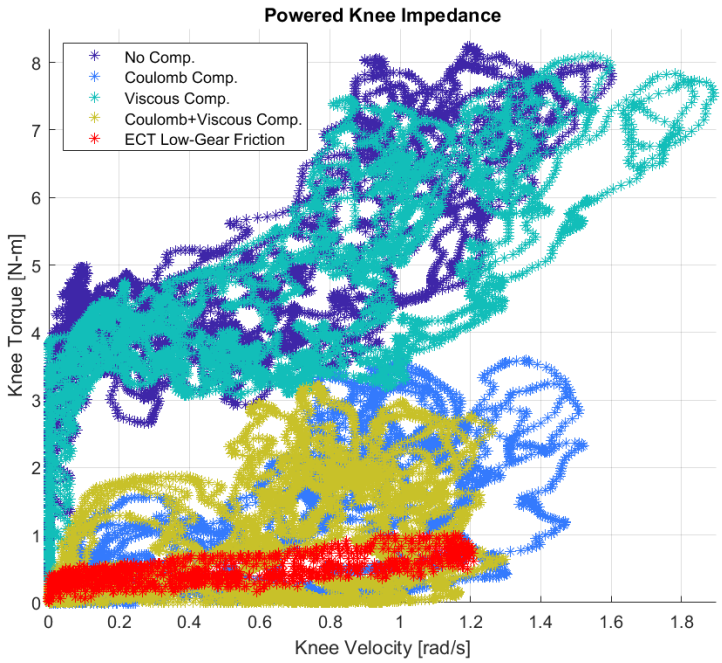

Fig. A-4: Impedance characterization showing applied torque versus angular velocity at the knee joint for two prostheses, the Vanderbilt Powered Knee and the ECT, in five conditions: (1) Powered Knee with no friction compensation; (2) Powered Knee with Coulomb friction compensation; (3) Powered Knee with viscous friction compensation; (4) Powered Knee with Coulomb and viscous friction compensation; and (5) ECT in the low-gear with no friction compensation. In selecting gains for the Powered Knee friction compensation terms, Coulomb friction compensation was selected as the most torque that could be applied without causing the knee to begin flexing on its own, and viscous friction compensation was selected as the highest negative damping that could be applied without causing the knee to accelerate in the absence of an applied force. Condition (4) shows the Powered Knee accelerating on its own at some points, as evidenced by the zero applied torque with non-zero velocity. This unfavorable condition was ignored in favor of letting the friction compensation be higher than would likely be used in a real prosthesis. Additionally, since this experiment was conducted unidirectionally (i.e. force was applied only in flexion from about 0 to 90 degrees of flexion for both prostheses), to benefit the Powered Knee, instead of using the onboard Coulomb friction compensation equation (which filters the torque command to avoid torque discontinuity at near-zero velocities), instead a constant flexion torque was commanded. This eliminates what would inevitably be a high torque spike at near-zero velocities as the control system must "catch up" to the prosthesis. Instead, there is no torque spike in the data, and compensating for Coulomb friction in this open-loop manner reduces torque at near-zero velocities to the same level as the ECT. However, the characteristic increase in friction at speeds between 0.05-0.25 rad/s is not compensated here and therefore causes a sharp increase in torque. While possible to model and compensate for this, doing so in real-time would require a sufficient phase margin to avoid instability, which is already starting to occur as the prosthesis gains velocity due to the viscous friction compensation. Selected gains were 3.8 N-m for Coulomb friction compensation and 0.285 N-m-s/rad for viscous friction compensation.

Due to these limitations, it is typical to find up to 50% model uncertainty in experiments using kinematic-feedback impedance compensation on wearable robots (e.g. [63] [64] [65]). In addition to the aforementioned challenges, providing impedance compensation with kinematic feedback is fundamentally

challenged with the causal relationship of motion and force. In impedance control, actuator motion causes actuator force. Without the use of a load cell to measure externally-applied forces, kinematic-feedback impedance control relies on onboard sensors for measurements of manipulator motion, which informs the controller on what forces to apply to compensate for impedance. For a hypothetical impedance that is much higher than the externally-applied force, little or no motion will be observable by the controller for which to provide impedance compensation (which is the rationale of using a load cell at the output in [30]). In this case, external forces cause motion, which causes force compensation. Before the controller can provide impedance compensation to effectively make the actuator behave as an impedance, the actuator first behaves as an admittance; the causal relationship is reversed. This effectively causes the output port to have high impedance during any acceleration. In other words, feedback impedance compensation using motion sensing will fundamentally be lower than desired during times of increasing velocity and acceleration and higher than desired during times of decreasing velocity and acceleration. As such, the stability margins required for decreasing velocity and acceleration will degrade controller performance during times of increasing velocity and acceleration.

Force-Feedback Impedance Compensation

Providing impedance compensation with force-feedback control requires an accurate measurement of the interaction force between the manipulator and environment (or end-effector, if it is to be considered part of the environment). There are two methods of estimating the interaction force: 1) measurement of strain in the manipulator (e.g., load cell); and 2) measurement of the motion of an elastic element in the manipulator (e.g., series-elastic actuator + encoders or IMUs). Both of these methods pose significant challenges in PKs.

Force Estimation via Motion Sensing of Compliant Actuator: The interaction force can be measured indirectly by utilizing a series elastic actuator to decrease the actuator impedance to a low enough level that enables the environment to easily impose motion on the actuator, which is estimated as a force and used for impedance compensation. This relative motion can be measured as a difference in position across the elastic element or as an acceleration of the end effector inertia. The latter of these is achieved by using a model of actuator inertia and by measuring actuator acceleration using onboard sensing from IMUs (e.g. [66]). However, using this approach on a PK requires two IMUs, one on the shank and one of the thigh, to measure relative acceleration of the two limb segments (see Fig. A-5). For

more accurate measurements, it is ideal to have l_1 and l_2 be as large as possible. However, l_1 is likely to be very small, since knee prostheses typically do not extend far above the knee joint.

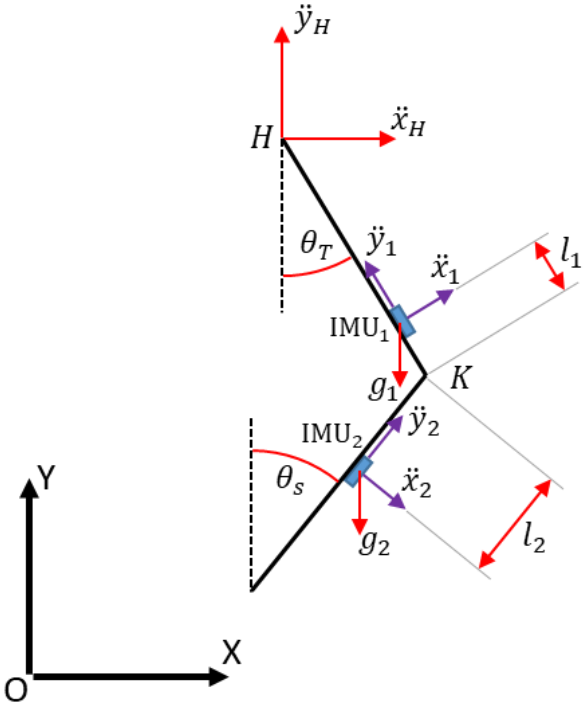

Fig. A-5: Free body diagram of leg during swing-phase, where O is the fixed inertial reference frame with horizontal and vertical coordinates of X and Y in the sagittal plane, H is the hip joint, K is the knee joint, θ_T is the thigh angle, θ_S is the shank angle, IMU_1 is the thigh-mounted IMU, IMU_2 is the shank-mounted IMU, $\ddot{x}_H$ and $\ddot{y}_H$ are the horizontal and vertical accelerations of the hip joint in the sagittal plane with respect to O, $\ddot{x}_1$ and $\ddot{x}_2$ are the tangential accelerations of the thigh and shank as measured by their respective IMUs, $\ddot{y}_1$ and $\ddot{y}_2$ are the axial accelerations of the thigh and shank as measured by their respective IMUs, g_1 and g_2 are the accelerations caused by gravity on their respective IMUs, and l_1 and l_2 are the distances between the knee joint center and their respective thigh and shank IMUs, which is needed for converting resolved measurements of tangential and acceleration into rotational acceleration (i.e. $\ddot{x}_2 = l_2\ddot{\theta}_S$). The knee angle ($\theta_K$) and its derivatives are resolved from the IMU kinematic measurements of the thigh and shank segments from the equation: $\theta_K = \theta_T - \theta_S$.

The real challenge of this approach, however, is that the robot is not grounded to the inertial reference frame and is accelerating in six degrees of freedom. The connection to ground is through the residual thigh and contralateral leg, the latter of which having no kinematic information available, and therefore no precise method of differentiating sources of acceleration in the robot's inertial frame. As such, the robot has no way of discriminating accelerations due to rotation about the knee joint from those caused by translational, centripetal, and Coriolis accelerations of the IMUs (see Fig. A-6). Additionally, in cases where the thigh and shank IMUs are not perfectly aligned in the sagittal plane, some portion of the gravity vector will be projected along the third IMU axis, which would either lead to an inaccurate measurement or would require consideration of all three acceleration axes for estimation of tangential accelerations.

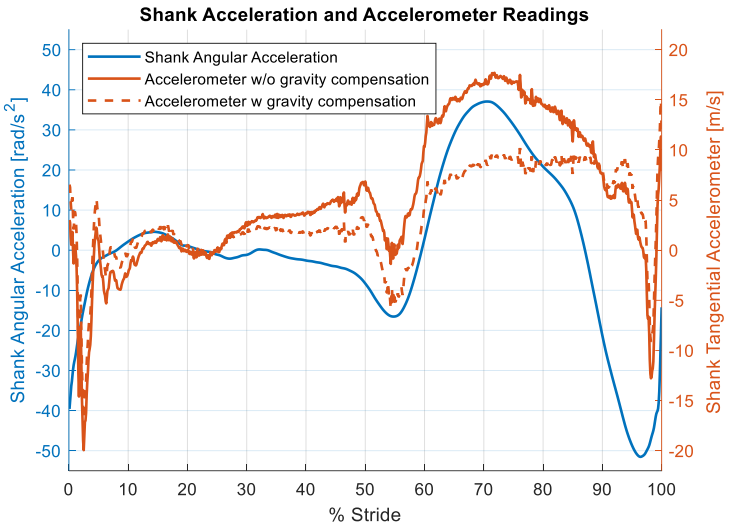

Fig. A-6: Prosthetic shank angular acceleration and shank-mounted accelerometer reading, with and without gravity compensation, while walking at 1.0 m/s on an instrumented treadmill. Shank acceleration data (blue) was derived from motion capture and is averaged over 15 strides. Accelerometer data (orange) for a single stride are taken from the IMU accelerometer that is tangential to the prosthesis shank in the sagittal plane ($\ddot{x}_2$ from Fig. A-5). Even when compensating for gravity (using onboard estimation of shank angle in global frame), there is no correlation between accelerometer reading and shank acceleration. This is because the prosthesis is accelerating in six degrees of freedom, subjecting accelerometer readings to effects of translational, tangential, centripetal, and Coriolis accelerations.

Even if accurate measurements of knee joint acceleration could be made using the IMUs, what matters is not knee joint acceleration, but motor and drivetrain acceleration, as these motions are the sources of the reflected inertial torques at the output. The signal-to-noise ratio shown in Fig. A-6 would become highly problematic when reflected through a high-ratio transmission (e.g. >100:1). Signal noise can be filtered, but at the risk of incurring phase lag, which degrades controller performance. Additionally, because the physical system has backlash (which itself incurs vibrations that degrade IMU measurements), there will always be a difference between knee joint acceleration and actuator acceleration. Therefore, accurate measurement of output acceleration with IMUs does not guarantee controller stability or fidelity.

Furthermore, the experiment in [66] uses a compliant actuator, which facilitates initiation of actuator motion necessary to begin providing compensation of actuator inertia and Coulomb friction. Although some researchers utilize series-elastic actuators in their PKs (e.g., [13]), there is necessarily a tradeoff between the high output impedance required during stance phase support and the low stiffness required for measurement fidelity in the series elasticity.

Similar to the method of using an IMU to measure relative acceleration of the end effector in a compliant actuator, the interaction force can be estimated by measuring the relative displacement of a series-elastic element in a compliant actuator. The major tradeoff of this approach is related to the high torque requirements of stance phase and the low impedance requirements of swing phase, which

necessitates high stiffness for stance-phase support and low stiffness for swing-phase impedance compensation Given this limitation, however, it is theoretically possible to use a hard stop on the elastic element that saturates measurements at levels beyond what is expected in swing-phase. This would increase measurement precision, however, the stance-phase would have considerable backlash coupled to the low compliance series elastic element.

Finally, this method of estimating the interaction force has the same causality problems as using kinematic-feedback: for any acceleration of the end effector, the actuator first has a high-impedance (greater than or equal to the inertia, friction, and compliance of the actuator) to imposed motion. It is only after motion has been imposed can the motor compensate for actuator impedance.

Force Sensing via Load Cell: A load cell is the most direct way to estimate the interaction force in a manipulator's end effector, as the second order dynamics of this measurement technique is characterized by a much higher stiffness than the previous method, which requires the actuator to have significant compliance. While possible to use a load cell to measure forces between the actuator and the end effector (i.e., prosthetic shank and foot), the required force capacity for measuring the actuator-prosthesis interaction force without overloading the load cell during stance-phase would necessitate a less-precise measurement of actuator-prosthesis interaction force during swing-phase, thus leading to the same model uncertainty problems previously stated. Additionally, the six-axis accelerations of prostheses induces significant vibration (as seen in the IMU measurements of Fig. A-6) which must be filtered from the load cell signal, increasing phase-lag in the feedback controller a reduction of controller gains to maintain acceptable stability margins.

While it is possible measure the actuator-prosthesis torque directly with either a load or torque sensor, such an approach cannot discriminate forces generated by internal and external inertial forces. Because the swinging lower limb exerts a force on the actuator, it is not possible to discern prosthesis and actuator inertia. Although actuator inertia is easily modeled and will remain stable over time, measurement of force is not able to discriminate between actuator inertia and whole-leg inertia. Because prosthesis inertia is easily altered by the use of different shoes, different clothing, and whether or not the shoes and/or clothes are wet or dry, there necessarily is uncertainty in the inertia estimation. Furthermore, both linear and rotational accelerations can contribute to forces exerted by external inertial forces, the former of which causes measurements to be compromised when linear force is being measured as a proxy for torque.

Considering the additional complications of estimating the interaction force in knee prostheses, it is expected that the quality of interaction control will be degraded. Considering that interaction controllers

on grounded robots with high resolution load cells and high bandwidth controllers risk instability when inertia is reduced less than 50% [67], it is not surprising that impedance compensation that facilitates a ballistic swing phase has not been demonstrated in literature.

Feedforward Impedance Compensation

Providing impedance compensation with feedforward control requires both an accurate model of actuator impedance (i.e. inertia and non-linear friction) and a priori knowledge of the swing-phase trajectory (i.e. the controller must predict future knee joint velocity and acceleration to accurately compensate for present friction and inertia). Modeling friction and inertia has the same challenges as feedback impedance compensation, and predicting swing-phase trajectory poses significant challenges in PKs.

Predicting swing-phase trajectory is theoretically possible, but has not been demonstrated with high model certainty. One example of this control methodology is demonstrated on an exoskeleton in [62], where an adaptive oscillator was utilized to estimate hip and knee kinematics and provide feedforward torques to compensate for actuator friction and inertia. A comparison of the feedforward adaptive oscillator estimation, a feedback Kalman filter estimation, and the actual joint kinematics is shown in Fig. A-2. This comparison shows that the adaptive oscillator provides velocity and acceleration estimations in-phase with actual kinematics, but with underestimations of peak velocity and acceleration. Additionally, the adaptive oscillator shows signs of bandwidth limitation in acceleration estimations, where the high amplitude rapid oscillations of the knee are filtered to average values. Compared to the feedback estimations provided by the Kalman filter, there is not much improvement in the estimation of knee acceleration, and the experimental results did not indicate differences in outcomes between the two controllers utilizing either feedforward or feedback impedance compensation. Considering that these knee joint kinematics are approximately half the values shown Fig. A-1, it is likely that controller performance will be more negatively affected at walking speeds of 1.2 m/s.

These model inaccuracies in the adaptive oscillator are possibly caused by the inherent variability of walking gait. In ballistic swing, knee joint motion is the result of internal knee torques (as provided by the motor and actuator impedance) and external inertial torques from gravity and acceleration of the knee joint (i.e. user motion) acting on the prosthesis. Therefore, this approach is sensitive to discrepancies between the expected and actual user motion, since actuator impedance must be overcome with motor torque. Because the expected behavior of the prosthesis user is to provide inputs with significant variability

even when walking at steady-state treadmill velocities (e.g., [68]) which cannot be known a priori, an increase in the stability margin of the feedforward controller is necessary to prevent controller instability, which effectively increases the output impedance of the system. Considering that the user is essentially a disturbance to a prosthesis that has its own desired trajectory, it is possible that there can be issues when there is misalignment between user input (i.e. residual thigh acceleration) and expected user input when collaborating on how to provide the ballistic swing-phase motion.

Alternative Approaches to Impedance Control

This appendix outlines the control challenges of providing a low output impedance in a high impedance device using software control methods. Ideally, the control system is able to modulate the target output impedance via high-bandwidth sensor feedback, as described by Hogan [30]. However, Hogan also describes another method of impedance control without feedback, where output impedance is modulated by mechanically reconfiguring the actuator. Although his example uses kinematic redundancies to modulate output impedance, the approach is generalized to any method of mechanically altering the actuator's output impedance. This form of impedance control is appropriate when feedback or feedforward control strategies are insufficient to control the robot's dynamic behavior.

The approach employed in this dissertation modulates the hardware transmission ratio to match the torque, speed, and impedance requirements of the prosthesis during the stance and swing phases. With this approach, the effects of friction and inertia can be reduced to a level where they either do not impede ballistic swing phase or can be further reduced using impedance compensation so that they don't impede ballistic swing phase without the risk of controller instability (i.e., impedance compensation gains are not required to be high because there will always be some nonzero desired output impedance). Unlike many of the previously discussed methods, this method of impedance modulation does not have causality problems; the causal relationship of environmental admittance and actuator impedance is maintained by the physical characteristics of the actuator, which eliminates instability problems from model uncertainty and feedback delay.

In addition to providing a desirable output impedance for swing-phase, this hardware-based approach has the potential to offer higher energy efficiency than software-based approaches using impedance compensation. Rather than spend battery energy to emulate a ballistic swing-phase, energy can be regenerated using motor braking during an actual ballistic swing-phase. If the energetic cost of

transmission reconfiguration (e.g. solenoid-actuated clutches) is less than the energy regenerated by motor braking, it is possible to provide ballistic swing-phase without consuming net battery energy.

APPENDIX B: FORMULATION OF SWING CONTROL LAWS

The swing-phase torque control laws are based on the observation that energy dissipation in both swing-flexion and swing-extension is linearly-proportional to the walking speed. During swing-phase, the motion of the lower-leg can be modeled as a pendulum with a forced pivot and torque-control at the pivot. The free body diagram in Fig. B-1 models the lower-leg as a rigid body with its center-of-mass coincident with the line defining the shank angle.

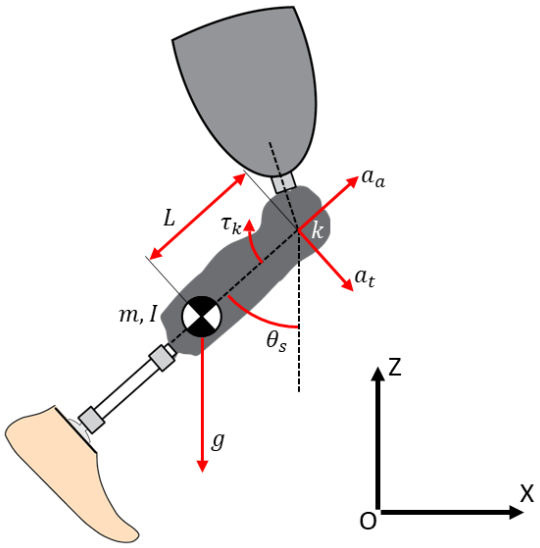

Fig. B-1: Free-body diagram of lower-leg dynamic model

In the lower-leg free body diagram, O is a fixed observer in the global frame, X and Z are the global coordinates in the sagittal plane, k is a revolute joint that defines the knee joint that is accelerating in the global frame, m is the total mass of the lower-leg, L is the distance between the knee joint and the lower leg's center-of-mass, I is the moment-of-inertia of the lower-leg about the knee joint, g is acceleration due to gravity, θ_s is the shank angle in the global frame, a_t and a_a are respectively the tangential and axial acceleration of the knee joint relative to θ_s in the global frame, and τ_k is a torque produced by the prosthesis at the knee joint. The rotational motion of the lower-leg during swing-phase is determined by the summation of three sources of torque about the knee joint: (1) inertial torque from gravity (τ_g), (2) inertial torque from tangential acceleration of the knee joint in the global frame (τ_t), and (3) internally-generated torques acting at the knee joint (τ_k). The former two torques are mathematically expressed as:

$$\tau_g = mgL \sin \theta_s \tag{B-1}$$

$$\tau_t = mLa_t \tag{B-2}$$

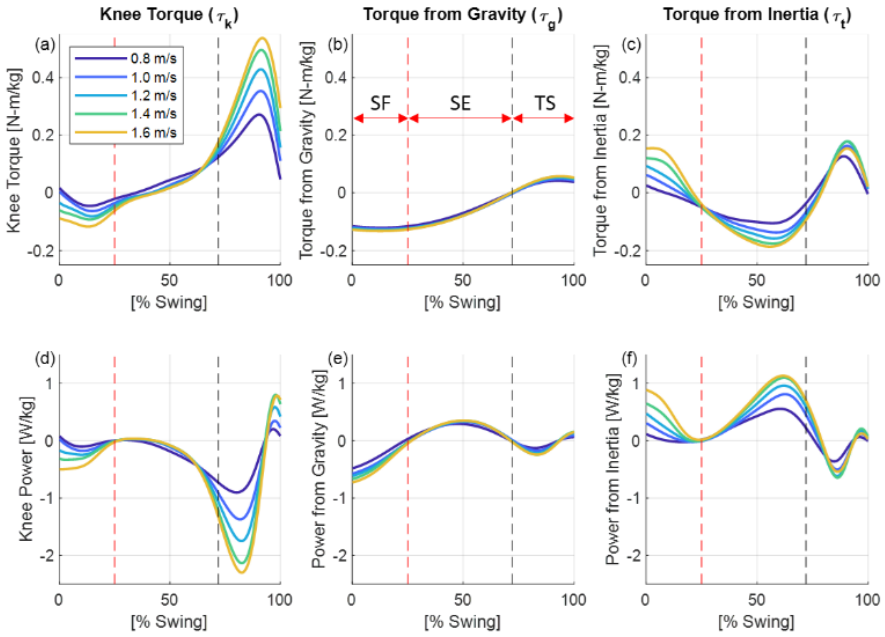

Fig. B-2: The three torques that affect the rotational motion of the lower-limb during swing-phase are (a) the knee joint torque, (b) inertial torque from gravity, and (c) inertial torque from tangential acceleration of the knee joint. Positive vertical axis indicates knee flexion torques. Subplots (d)-(g) show the mechanical power of each contributing torque (when compounded with knee joint velocity), where the positive vertical axis indicates positive mechanical work. The swing-phase is subdivided into three sub-phases: (SF) swing-flexion, (SE) early swing-extension, and (TS) terminal swing-extension. Kinematic events that separate the three sub-phases are the knee joint reaching its peak-flexion angle (vertical dashed red line) and the shank aligning with gravity (vertical dashed black line).

Using this dynamic model and averaged data from [31], Fig. B-2 shows the torque and joint power profiles of these three torque sources during the swing-phase for level-ground walking at five speeds. These data show that both τ_g and τ_t provide generative and dissipative rotational mechanical power, depending on the pose and velocity of the lower-leg throughout swing-phase. But τ_k has a primarily dissipative role, almost always dissipating energy to provide a desirable swing-phase motion. These torques sources affect the swing-phase differently depending on the sub-phase of swing, which in Fig. B-2 is divided into swing-flexion (SF), early swing-extension (SE), and terminal swing-extension (TS). Table B-1 shows the percent contribution to lower-leg motion of each torque source during the three sub-phases, which is calculated from the root mean square of each torque during each sub-phase, averaged over all walking speeds. The data in Table B-1 demonstrates the dominant influence of gravity and inertial-

coupling to the motion of the lower-limb during most of swing-phase. For the prosthetic knee joint, ballistic swing-phase can only be provided if τ_k does not dominate the swing-phase motion, which becomes increasingly challenging as mechanical impedance increases above zero. For that reason, providing biomimetic ballistic swing-phase motion with a high-impedance powered knee prosthesis requires high-fidelity impedance compensation, which has yet to be demonstrated in literature.

Table B-1
Swing-Phase Torques and Their Contributions to Knee Motion

Contributing Torque Source	Percent Contribution to Motion for each Swing Sub-Phase		
	Swing Flexion	Swing Extension	Terminal Swing
τ_k	26%	21%	68%
τ_g	52%	32%	9%
τ_t	22%	47%	23%

Percent contributions of each torque source were calculated from the RMS torque during each swing sub-phase, averaged over all walking speeds.

Swing-Flexion Resistance

During the swing-flexion phase of level-ground walking, acceleration of the knee joint generates rotational kinetic energy of the lower-limb, which increases the kinetic energy of the lower-limb after toe-off. This kinetic energy is either stored as potential energy by gravity or is passively absorbed by the viscoelastic properties of the thigh muscles (i.e. energy is dissipated by damping and stored by stiffness). However, given the net-dissipative nature of τ_k during swing-flexion, it is not necessary to use energy-storage or energy-generative mechanisms to provide a desirable swing-flexion motion, as indicated by MPKs that provide biomimetic swing-phase motion for a range of activities using energetically-passive actuation elements (e.g. hydraulic flow restriction). Rather, it is only necessary to dissipate the kinetic energy of the lower-limb to inflect the knee velocity (which is driven into extension by gravity and centripetal acceleration of the knee joint).

Figure B-3 shows the net energy dissipation by the knee joint in swing-flexion as a function of the walking speed, based on an analysis of data from [53], which demonstrates that the knee joint produces net-negative work in swing-flexion for most walking speeds. This plot also suggests an approximate linear relationship between knee energy dissipation and walking speed, with an energy-neutral walking speed (i.e. the walking speed at which net swing-flexion energy is neither dissipated or generated) between approximately 0.5 m/s (for first-degree polynomial regression) and 0.35 m/s (for second-degree polynomial regression), significantly slower than most individuals' self-selected walking speed. As walking speed increases, the knee joint must dissipate more energy to limit peak knee flexion (see Fig. B-

2) by providing higher extension torques, which reduces the total range of motion and reduces the duration of swing-phase. As walking speed decreases, the energy dissipated also decreases. If the knee joint is not able to assume a joint impedance below a certain level, as is the case for MPKs, there is a range of walking speeds where the inertial torques generated by the knee joint acceleration are insufficient to overcome the minimum impedance of the prosthesis, resulting in peak knee flexion angles lower than ideal (i.e. less than necessary to prevent the use of compensatory behaviors like hip elevation during swing-phase). Within that context, the trend demonstrated in Fig. B-3 serves as a "kinetic energy budget" for swing-flexion during any specific walking speed; biomimetic ballistic walking can only be accomplished if the intrinsic friction of the knee joint causes an energy loss less than the energy budget for the desired range of motion.

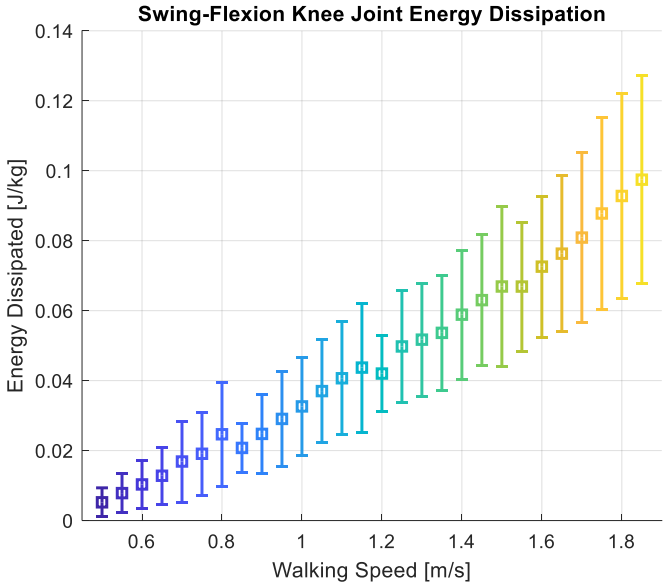

Fig. B-3: Energy dissipation v. walking speed during the swing-flexion phase of level-ground walking. Box-and-whisker plots indicate mean and standard deviation of 22 subjects. There is an approximate linear relationship between energy dissipation and walking speed. The knee joint produces net negative work for most walking speeds.

Figure B-3 suggests that desirable swing-flexion knee behavior can be provided by a torque control law that dissipates kinetic energy at a rate proportional to walking speed. With a precise and linear method of measuring relative walking speed, and a linear relationship between energy dissipated and walking speed, the values generated by the walking speed estimation can be used as a control variable that does not require tuning. To develop a control system for a low-impedance motor-actuated knee prosthesis, the total energy dissipated at the knee joint can be expressed as:

$$E_k^{SF} = \int_{\theta_k^{TO}}^{\theta_k^{PF}} \tau_k \, d\theta_k \tag{B-3}$$

where E_k^{SF} is the total energy dissipated at the knee joint during swing-flexion, τ_k is the instantaneous knee torque, and θ_k^{TO} and θ_k^{PF} are the angles of the knee joint at toe-off and peak-flexion, respectively. In the biological knee, the profile of resistive torque as the swing-flexion phase progresses is nonlinear with respect to time, angle, and velocity; it is also highly variant between individuals. However, it is not necessary to provide a biomimetic torque profile to achieve a biomimetic swing-flexion motion. In terms of gait biomechanics, the resistive torque profile must provide a knee motion profile that: (1) achieves an adequate flexion angle, based on the leg geometry, that provides robust toe-clearance as the thigh swings forward, (2) prevents unnecessary motion of the knee joint by limiting the maximum flexion angle, and (3) achieves timing of the peak-flexion knee angle such that the effective length of the leg is shortest when oriented vertically (i.e. the knee is flexed most when the toe is directly under the pelvis).

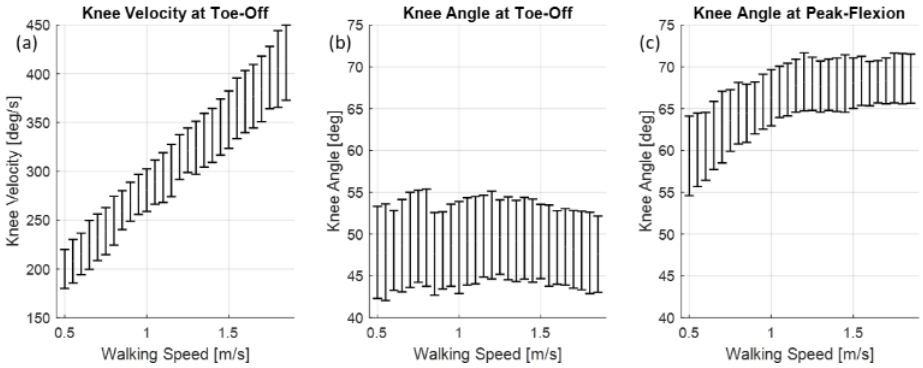

Fig. B-4: Three kinematic trends in swing-flexion: (a) toe-off knee velocity increases linearly with walking speed, (b) toe-off knee angle is invariant with walking speed, and (c) peak-flexion knee angle gradually increases with walking speed, then remains invariant at speeds above 1 m/s.

Figure B-4 shows three kinematic trends from [53]: (1) a toe-off knee velocity that increases linearly with walking speed; (2) a toe-off knee angle that is invariant with walking speed (because toe-off limb-configuration is a function of limb geometry); and (3) a maximum swing-flexion knee angle that gradually increases with walking speed, up to about 1 m/s, and then remains invariant. The knee angle at peak-flexion provides toe-clearance during swing-phase, the phasing of which is more difficult to coordinate as walking speed increases, which leads to higher peak-flexion angles to account for variability in peak-flexion timing and provide robust toe-clearance. For future control system designers, the implications of (1) are that toe-off velocity has a relationship to lower-limb kinetic energy that must be

dissipated by the knee joint; and the implications of (2) and (3) are that the range of motion over which the knee torque must dissipate the lower-limb's kinetic energy is largely invariant, except for the slowest walking speeds.

The amplitude and phasing of peak-flexion provide the kinematic constraints on the knee motion that must be provided by the knee joint kinetics (i.e. the resistive torque profile). In determining an effective resistive torque profile for swing-flexion, several considerations are taken: (1) as the swing-flexion phase progresses, the knee velocity has an approximately linear monotonic decrease, reaching zero at the moment of peak-flexion; (2) fast changes in applied torques creates discomfort in the user's socket, which necessitates a control system that gradually and smoothly changes the amplitude of resistive torque; (3) the linear relationship between swing-flexion energy dissipation and walking speed can be exploited by the walking speed estimation; and (4) the purpose of this resistive torque is to control the motion of the lower-limb such that it provides robust toe-clearance (i.e. produces desirable amplitude and phasing of peak-flexion). Assuming a control law that produces an instantaneous knee torque that is linearly proportional to the knee angular velocity (i.e. linear damping), the energy dissipation equation becomes:

$$E_k^{SF} = \int_{\theta_k^{TO}}^{\theta_k^{PF}} b\dot{\theta}_k \, d\theta_k \tag{B-4}$$

where b is the linear damping coefficient and $\dot{\theta}_k$ is the instantaneous knee angular velocity. If, for a given walking speed, the value of b is constant for the duration of swing-flexion, the equation can be rewritten as:

$$E_k^{SF} = b \int_{\theta_k^{TO}}^{\theta_k^{PF}} \dot{\theta}_k \, d\theta_k \tag{B-5}$$

where the integral of the velocity profile over the angular range of motion is the kinematic integral. The damping coefficient and the kinematic integral can be considered separately. Figure B-5 shows (a) the swing-flexion kinematic phase plane from [53], where normative knee velocity is plotted against normative knee angle for level-ground walking at 28 walking speeds, and (b) a candidate control law where b is linearly-proportional to the walking speed, (i.e. $b = C \cdot WS$, where C is a gain constant and

WS is the walking speed). For this control law derivation, kinematics are assumed a priori to be normative. This assumption is made because the velocity only decreases in swing-flexion, which makes it reasonable to use a control law that is resistive only, provided that the resultant energy dissipation is equal to the normative data (i.e. energetic inequality in the derivation implies kinematic inequality in the physical system).

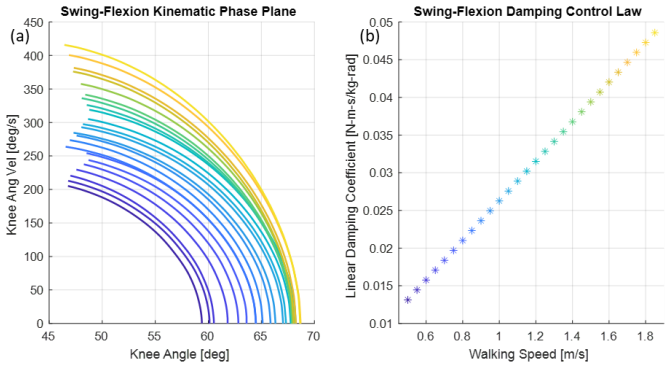

Fig. B-5: Plots showing (a) normative knee velocity v. normative knee angle during the swing-flexion phase of level ground walking for 28 walking speeds, configured in a kinematic phase plane, and (b) proposed swing-flexion control law, where the linear damping coefficient is linearly proportional to the walking speed.

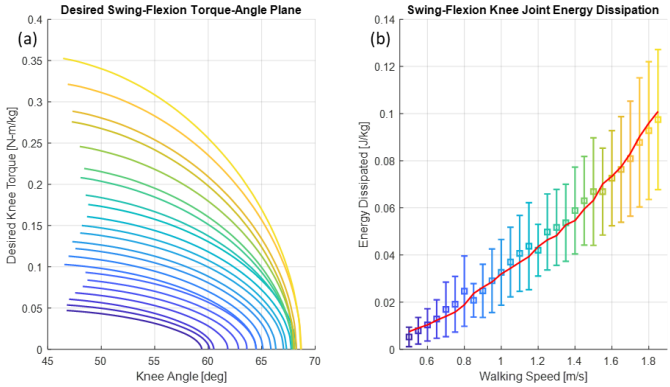

Fig. B-6: Plots showing (a) desired torque-angle plane for the swing-flexion control law, and (b) energy dissipation v. walking speed during the swing-flexion phase of level-ground walking. The red line overlaid on (b) indicates the total energy dissipated by the proposed control law from Fig. B-5(b), where the total energy dissipated is equal to the integral of (a) for each walking speed. The approximate equality between normative energy dissipation and derived energy dissipation implies that the candidate control law may produce desired kinematics.

If, for each walking speed, the damping control law is applied to the velocity profile, there is a resultant torque-angle relationship for each walking speed, shown in Fig. B-6(a). The integral of this torque-angle relationship is the total energy dissipated at each walking speed, shown in Fig. B-6(b), that when plotted on top of the previously shown plot of swing-flexion energy dissipation v. walking speed (red line), the result is a control law that provides approximately equivalent energy dissipation as the normative values observed. This implies that a control law that provides a torque profile that is linearly

proportional to both instantaneous knee velocity and estimated walking speed can provide the necessary knee joint energy dissipation with a kinematic profile approximately equal to that of normative kinematics.

At the highest level, the control system commands a resistive torque by commanding a desired linear damping coefficient at the knee joint. The equation governing this damping behavior is:

$$b_{des} = C_2 \omega \tag{B-6}$$

where b_{des} is the desired linear damping coefficient, ω is the average shank angular velocity as measured from heel-strike to knee-break (from the walking speed estimation algorithm), and C_2 is a gain constant associated with swing-flexion resistance torque. The torque control law for FSM state 2 is therefore:

$$\tau_k = C_2 \omega \dot{\theta}_k \tag{B-7}$$

The potential benefits of this control law include (1) a smooth torque profile, with minimum discomfort on the socket; (2) stable controller behavior when paired with passive motor control; (3) user-initiation of swing-phase, due to the absence of a desired swing-phase trajectory or a stiffness term in the impedance control law; (4) a predictable and desirable intrinsic swing-flexion behavior that can be easily learned and adapted to meet the user's needs; and (5) cadence-adaptive swing-flexion behavior is provided by a continuous control law with a single tunable parameter (C_2), simplifying controller implementation.

Swing-Extension Resistance

Similar to swing-flexion, the motion of the lower-limb in swing-extension is largely driven by inertial forces and, for the biological limb in early swing-extension, by an extension torque at the knee joint. Despite a small net-positive knee power at the initiation of swing-extension, which in the biological limb is likely the result of the passive stretch-reflex of the thigh tendons in swing-flexion, the knee joint always produces net-negative work during the swing-extension phase. Figure B-7 shows the net energy dissipation by the knee joint in swing-extension as a function of walking speed [53].

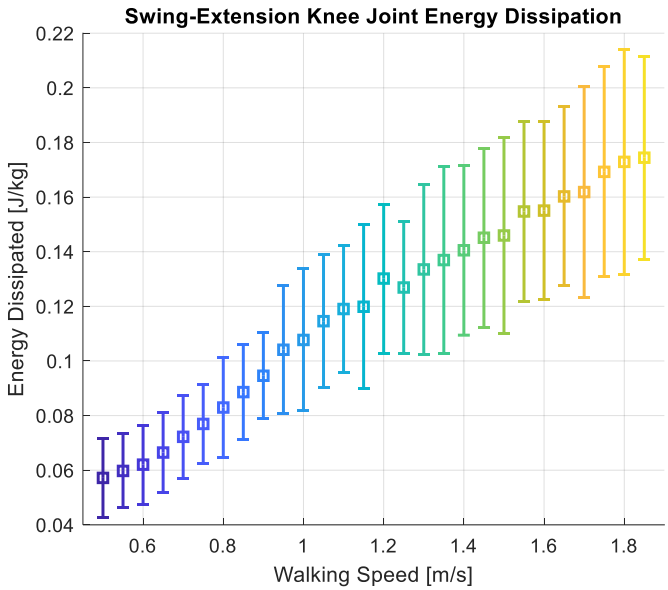

Fig. B-7: Energy dissipation v. walking speed during the swing-extension phase of level-ground walking. Box-and-whisker plots indicate mean and standard deviation of 22 subjects. There is an approximate linear relationship between energy dissipation and walking speed. The knee joint produces net negative work for all walking speeds.

Figure B-7 suggests three conclusions: (1) the magnitude of the energy dissipated in swing-extension is higher than the energy dissipated in swing-flexion for each walking speed; (2) there is a linear relationship between knee energy dissipation and walking speed; and (3) the energy-neutral walking speed in swing-extension is approximately 0 m/s, meaning that energy is dissipated for all walking speeds. These conclusions imply that a knee joint with a zero-impedance would have significant terminal impact energy for all walking speeds, which necessitates a dissipative torque during swing-extension with a magnitude and/or duration that is a function of the walking speed (to provide increasing energy dissipation with increasing walking speed). For a knee prosthesis with a low intrinsic mechanical impedance, especially one with a passive extension aid (i.e. a spring placed in parallel to the actuator with an equilibrium angle in hyperextension), biomimetic swing-extension behavior can be achieved with dissipation alone (i.e. without consuming battery power). It should be noted that applying dissipative torques in early-to-mid swing-extension is undesirable as this prevents user-controlled rapid extension of the knee joint, significantly reducing the extension velocity, and increasing the time it takes to rotate the knee joint from peak-flexion to full-extension. Therefore, it is desirable to have a low-impedance during most of swing-extension and a high resistance moment during the final portion of the swing-phase (i.e. terminal-swing) that rapidly decreases the velocity of the knee joint. This terminal-swing resistance moment should be gradually increased from a minimum level to avoid inducing high reaction torques in the user's socket.

The swing-extension control law begins with zero motor braking impedance and then gradually and monotonically increases to a maximum impedance. To develop the passive control law, the swing-extension controller has three control objectives: (1) provide an impedance behavior that permits full swing-extension motion (from peak-flexion to full-extension) that is synchronized with the phasing of the user's motion (i.e. full-extension is reached in a timely manner); (2) dissipate a quantity of energy appropriate for the individual user and the walking speed that limits the terminal impact energy; and (3) provide resistive torque profiles that produce minimal socket reaction forces. To develop a control system for swing-extension, the total energy dissipated at the knee joint can be mathematically expressed as:

$$E_k^{SE} = \int_{\theta_k^{PF}}^{\theta_k^{FE}} \tau_k \, d\theta_k \tag{B-8}$$

where E_k^{SE} is the total energy dissipated at the knee joint during swing-extension, τ_k is the instantaneous knee torque, θ_k^{PF} is the angle of the knee joint at peak flexion, and θ_k^{FE} is the angle of the knee joint at full-extension (for prosthesis users, it is desirable to achieve $\theta_k^{FE} \approx 0$). If we assume a control law that produces an instantaneous knee torque that is linearly proportional to the knee angular velocity (i.e. linear damping), the energy dissipation equation becomes:

$$E_k^{SE} = \int_{\theta_k^{PF}}^{\theta_k^{FE}} b\dot{\theta}_k \, d\theta_k \tag{B-9}$$

where b is the linear damping coefficient and $\dot{\theta}_k$ is the instantaneous knee angular velocity. For the swing-extension control law, the value of b is a function of the instantaneous knee angle and estimated walking speed. As with swing-flexion, the total energy dissipated during swing-extension can be approximated with normative gait data configured in a kinematic phase plane. One limitation of this derivation is that all applied torques must be constrained to the portion of swing-extension after the maximum knee velocity. As with the swing-flexion control law derivation, using a damping-only control law necessitates only applying the control law to portions of the kinematic phase plane with negative acceleration. Figure B-8 shows (a) the swing-extension kinematic phase plane from [53], where normative knee velocity is plotted against normative knee angle for level-ground walking at 28 walking speeds, and (b) the desired kinematic

phase plane for a prosthetic knee, based on normative kinematics, but with a target knee angle of zero at the termination of swing-phase, which is desirable for prosthetic knee control. Terminating swing-phase at full-extension permits the dissipation of energy during terminal impact, which provides proprioceptive feedback to the prosthesis user that the prosthesis has completed swing-phase and it is now safe to load the prosthesis with the user's weight.

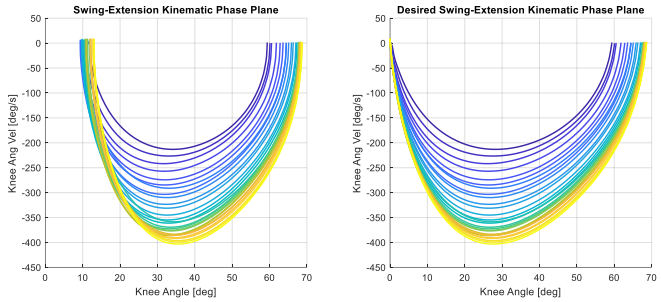

Fig. B-8: Plots showing (a) normative knee velocity v. normative knee angle during the swing-flexion phase of level ground walking for 28 walking speeds, configured in a kinematic phase plane, and (b) desired kinematic phase plane with final knee angle adjusted to zero, which is desirable for prosthetic knee control.

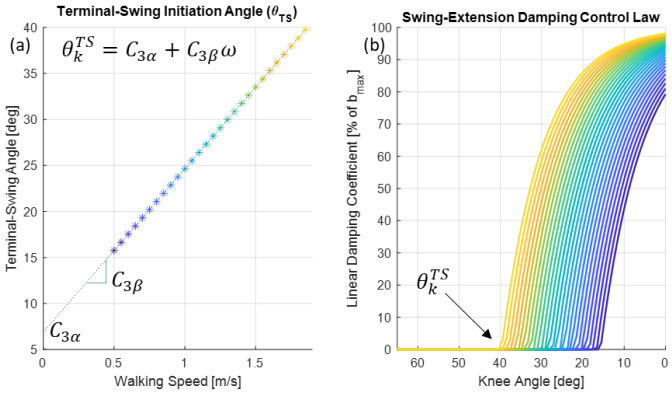

Fig. B-9: Plots showing (a) terminal-swing initiation angle (θ_k^{TS}) as a function of the walking speed estimation (ω), and (b) proposed swing-extension control law, where the linear damping coefficient is a function of the walking speed and the knee angle. The damping coefficient remains zero for most of swing-extension, then rapidly increases towards the maximum value (b_{max}). An exponential decay serves as a soft saturation of knee damping.

From the desired kinematic phase plane in Fig. B-8(b), a torque-angle plane can be generated by assigning a value of torque as a function of knee velocity, knee angle, and the estimated walking speed. The damping control law begins increasing the linear damping coefficient from zero when the knee angle is less than the terminal-swing initiation angle (θ_k^{TS}), which is determined from the walking speed estimation during stance-phase. Figure B-9(a) shows θ_k^{TS} as a function of the walking speed estimation (ω), which is governed by the equation:

$$\theta_k^{TS} = C_{3\alpha} + C_{3\beta}\omega \tag{B-10}$$

where $C_{3\beta}$ is a gain associated with the calculation of θ_k^{TS} for a given estimated walking speed, and $C_{3\alpha}$ is the minimum angle of θ_k^{TS}. From this initiation angle, the desired damping coefficient (b_{des}) monotonically increases from zero to its maximum value (shown in Fig. B-9(b)) as governed by the equation:

$$\text{if } \theta_k < \theta_k^{TS}, \quad b_{des} = b_{max}\left[1 - e^{\frac{\theta_k - C_{3\alpha} - C_{3\beta}\omega}{C_{3\gamma}}}\right] \tag{B-11}$$

where b_{max} is the maximum linear damping coefficient that can be passively delivered by the motor (i.e. when the motor leads are shorted), and $C_{3\gamma}$ is a decay constant that provides shape to the damping profile as a function of knee angle. The exponential decay function acts as a soft saturation of knee damping. Increasing the terminal-swing initiation angle with increasing walking speed permits energy dissipation with the motor alone, the dynamic range of which is limited by the low-gear transmission ratio, the intrinsic properties of the motor (torque constant and phase-to-phase resistance), and the intrinsic mechanical impedance.

If, for each walking speed, the damping control law is applied to the velocity profile, there is a resultant torque-angle relationship for each walking speed, shown in Fig. B-10(a). The integral of this torque-angle relationship is the total energy dissipated at each walking speed, shown in Fig. B-10(b), that when plotted on top of the previously shown plot of swing-flexion energy dissipation v. walking speed (solid red line), the result is a control law that provides energy dissipation that is less than the total energy normally dissipated by approximately the same quantity for any given walking speed. This implies that the proposed control law is capable of dissipating most of the kinetic energy of the lower leg while leaving some kinetic energy to be dissipated upon terminal impact, with the total terminal impact energy being invariant for any walking speed. By formulating a control law with terminal impact energy invariant to walking speed, the terminal impact energy serves as proprioception for the user that the prosthesis has completed swing-phase, socket discomfort does not increase at fast walking speeds, and the prosthesis is able to complete swing-extension at slower walking speeds.

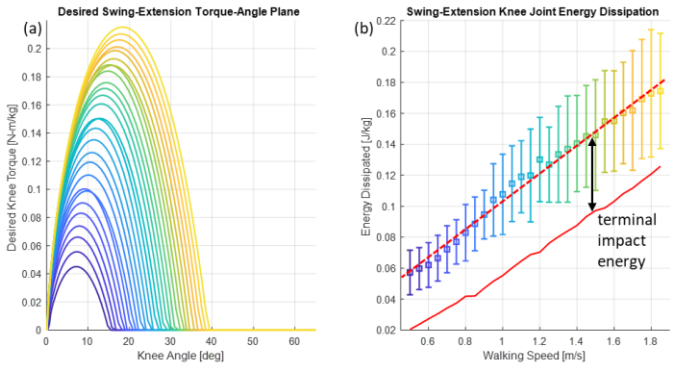

Fig. B-10: Plots showing (a) desired torque-angle plane for the swing-extension control law, and (b) energy dissipation v. walking speed during the swing-extension phase of level-ground walking. The solid red line overlaid on (b) indicates the total energy dissipated by the proposed control law from Fig. B-9(b), where the total energy dissipated is equal to the integral of (a) for each walking speed. The difference between the dashed and solid red lines is the terminal impact energy (i.e. the kinetic energy remaining at full-extension which serves as proprioception to the user that the knee has completed swing-phase).